1. INTRODUCTION

As the construction projects become larger in scope, and more sophisticated in terms of technical challenges, there are even further smaller urban areas fit for such projects in turn. Ground improvement techniques carried out under specific steps gains even more importance in such an environment.

Geotechnical engineering is concerned with virtually all aspects of environmental control, including water resources, water pollution control, waste disposal and containment, and the mitigation of such natural disasters as floods, earthquakes, landslides. The behavior of soil mass and rock at the location of any project has a major influence on the success, economy and safety of the work. Soil mass is almost always treated as a continuum for analysis and design. Nonetheless, the values of properties such as strength, permeability, and compressibility are determined directly by the size and the shape of the particles, their arrangements and the forces between them. (Mitchell, 1992)

Fiber reinforcement as a soil improvement technique is neither new nor rarely researched. It has been the subject of many thesis, and academic publications. However, using paper as an inorganic material for soil improvement is a relatively new, and less researched area. Usage of straw paper in modification of clay, change the geotechnical properties of clay like hydraulic conductivity, workability, shear strength parameters and compressibility. All these parameters are within the scope of this project and are covered with respect to different points of view.

In this study direct shear tests, unconfined compression, linear shrinkage, split tensile, hydraulic conductivity and plasticity of reinforced clay tests were conducted. The effect of paper cut fibers and paper pulp in different amount of inclusion ratios by weight has been investigated. Samples were prepared at maximum unit weight and optimum water content. The main parameters of soil like hydraulic conductivity, shrinkage, compressibility, Atterberg parameters like plastic limit, liquid limit, plasticity index, shear strength parameters were tested, and investigated on paper-pulp added kaolinite , paper cut fiber added kaolinite. The main objective of this study was to improve the geotechnical properties and workability of clay.

Partly because this is a relatively new area in the field of soil improvement techniques, and partly because there is promising potential for using straw paper in improving multiple properties of clay simultaneously, it is believed that this project can be broadened in many ways in terms of applications, it proposes in paper usage as a soil improvement technique, and the study, both in academic sense, and practical applicability vise, can be a part of long term efficient, and fruitful efforts.

2. LITERATURE REVIEW

2.1. Ground Modification

There are mainly four steps to be methodologically completed in order to come to the conclusion that ground improvement is essential for the sake of the current project. These are control steps in nature, and have to be exhausted one by one before proceeding with ground improvement. These steps for decision follow each other and rejoin, work with economical parameters. The first of these steps is avoiding a particular construction site, relocating a planned project development site from the original planned site to a site with more favorable soil, and ground characteristics. Second step is designing the planned structure accordingly. Some of the many possible approaches are to use a raft foundation supported by piles, to design a very stiff structure which is not damaged by settlement, or to choose a very flexible construction which accommodates differential movement or allows for compensation. The solution selected will essentially depend on the geotechnical performance criteria related to stability, deformation, and seepage. Third step is removing and replacing unsuitable soils from the site. Removing organic topsoil, which is soft, compressible, and volumetrically unsuitable, is a standard precautionary practice commonly observed in road or foundation construction projects. The last and the fourth step are to attempt to modify the existing ground as a last resort. The ground improvement technique chosen should be selected in a manner that it will be both suitable for the particular conditions of the construction site, and also will be economical, practical, and reliable (Hausmann, 1990). The general modification techniques, which have subcategories, are classified into four groups;

- **Mechanical Modification:** Short term external mechanical forces are applied to soil with a lower than average density. The methods for this type of modification include compaction of the surface layers by static, vibratory, or impact rollers and plate vibrators; and deep compaction by heavy tamping at the surface or vibration at depth.

- **Hydraulic Modification:** Free-pore water is forced out the soil via drains or

wells.

- **Physical and Chemical Modification:** Mixing additives to surface layers, and columns of soil at deeper levels is covered under physical modifications. This method is also called modification by admixtures.

- **Modification by Inclusions and Confinement:** Reinforcement by fibers, strips, bars, meshes and the fabrics imparts tensile strength to a constructed soil mass.

2.1.1. Concept of Soil Reinforcement

Soil reinforcement is concerned with reinforcing a soil mass to improve its stability, increase its bearing capacity, and reduce settlements and lateral deformations. The meaning of soil reinforcement was broadened its definition, also includes methods of erosion control and stress transfer via anchors and piles. Soil reinforcement can be achieved by relatively flexible, extendable, and sometimes compressible materials, such as non-woven fabrics or large quantities of individual fibers. Also, the actual strengthening of a soil mass may be a secondary effect, e.g., as achieved through accelerated consolidation (Hausmann, 1990).

2.1.2. Reinforced Soil as a Homogeneous Composite Material

Although having their merits, there are basically two approaches to the analytical modeling of reinforced soil: representation as a homogeneous composite material or representation by discrete structural elements like soil, reinforcement, and boundary elements. Treating reinforced soil as a homogeneous composite material improves the mathematical efficiency of some methods of determining load-deformation behavior using finite elements; in addition, it has value in the interpretation of laboratory tests and has conceptual appeal in evaluating reinforced soil behavior in practical applications.

It must be realized that even plain concrete, made up of mortar and aggregate, is a composite material. Its strength and elastic modulus are generally evaluated on a macroscopic scale. In other words, for the purpose of analysis and design, plain concrete is

considered a homogeneous material and its properties are studied taking a phenomenological approach. The same applies to steel, which can be considered macroscopically homogeneous, although microscopically it is made up of crystalline constituents.

On the other hand, steel reinforced concrete is generally treated as a homogeneous composite material and its properties investigated at a micromechanical level. Strength of materials approach to the design of beams, plates, and shells, certain simplifying assumptions are made regarding the mechanical behavior of the composite material; e.g. it is generally assumed that the strains in the reinforcement are the same as in the surrounding concrete mix. In reinforced soil, this assumption may or may not be appropriate, dependent on the stress level and relative moduli of the materials involved. If one considers how the mechanical properties of composite materials can be explained and described, three classes of theoretical problems can be distinguished. (Spencer, 1972)

- Interface problems involving the local interactions between the fiber and the matrix
- Problems which concerns the relation of the properties of the composite to the individual properties of the fiber and matrix
- The macroscopic behavior of the composite as a whole under specified loading

2.2. Soil Fabric and Its Measurement

The term fabric refers to the arrangement of particles, particle groups, and pore spaces in a soil. The term structure is sometimes used interchangeably with fabric. Although soils are composed of discrete soil particles and particle groups, a soil mass is almost always treated as a continuum for analysis and design. Nonetheless, the values of properties such as strength, hydraulic conductivity, and compressibility are determined directly by the size and the shape of the particles, their arrangements, and the forces between them. To understand a property requires knowledge of these factors. With some theories of particulate mechanics and computational method, such as the discrete element method, are now becoming available.

The particle arrangements in soils remained largely unknown until development of suitable optical, X-ray diffraction, and electron microscope techniques made direct observations possible starting in the mid-1950s. Interest then centered mainly on clay particle arrangements and their relationships to mechanical properties. In the late 1960s, knowledge expanded rapidly, sparked by improved techniques of the sample preparation and the development of the scanning electron microscope. In the 1970s attention was directed also at particle arrangements in cohesionless soil.

2.2.1. Particle Associations in Clay Suspensions

Particle associations in clay suspensions can be described as follows and as illustrated in figure 2.1. (van Olphen, 1977).

1. Dispersed: No face-to-face association of clay particles;
2. Aggregated: Face-to-face association (FF) of several clay particles;
3. Flocculated: Edge-to-edge (EE) or edge-to-face (EF) association of aggregates;
4. Deflocculated: No association between aggregates.

Thicker and larger particles result from FF association. EF and EE association can produce cardhouse structures that are quite voluminous until compressed.

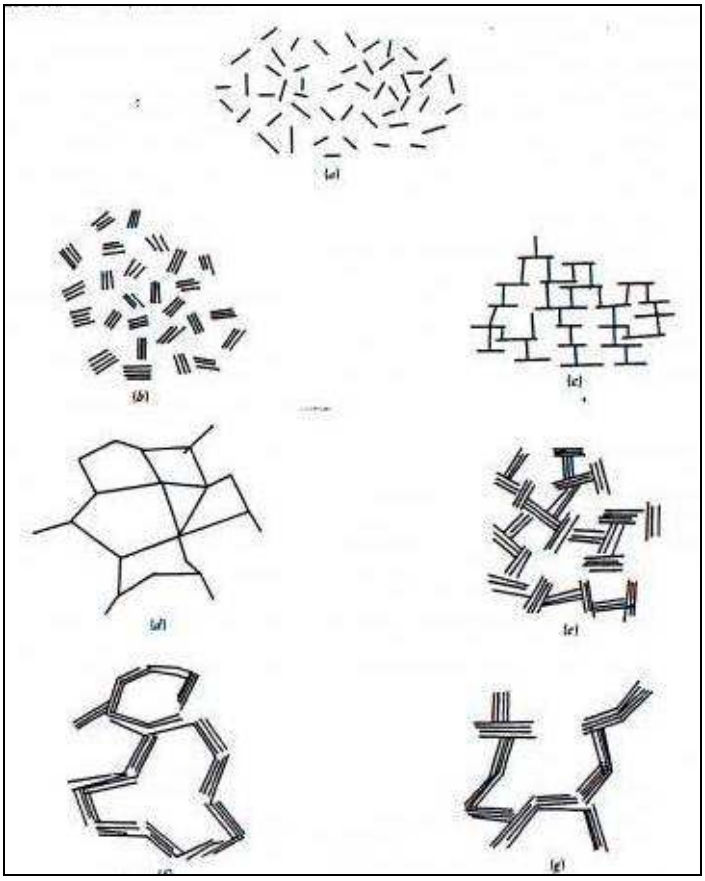

Figure 2.1. Modes of particle associations in clay suspensions and terminology. (a) *Dispersed* and *deflocculated*. (b) *Aggregated* but *deflocculated* (face to face association, or parallel or oriented aggregation). (c) Edge-to-face flocculated but *dispersed*. (d) Edge-to-edge flocculated but *dispersed*. (e) Edge-to-face flocculated and *aggregated.* (f) Edge-to-edge flocculated and *aggregated.* (g) Edge-to-face and edge-to-edge flocculated and *aggregated.*(van Olphen, 1977).

2.2.2. Particle Associations in Soils

Particle associations in sediments, residual soils, and compacted clays assume a variety of forms; however, most of them are related to the combinations of the configurations shown in figure 2.1 and reflect the difference in water content between a suspension and a denser soil mass. Whereas single grain fabrics are found in cohesion less soils, fine-grained soils are almost always composed of multiparticle aggregates.

1. Elementary particle arrangements: Single forms of particle interaction at the level of individual clay, silt, or sand particles.
2. Particle assemblages : Units of particle organization having definable physical boundaries and a specific mechanical function, and which consist of one or more forms of the elementary particle arrangements
3. Pore spaces.

Schematic illustrations of each of the fabric features in these three classes are shown in figure 2.2. Figures show the overall fabric of undisturbed Tuscan silty clay, a fresh water alluvial deposit. Card house is an edge-to-face arrangement forming an open fabric similar to edge-to-face arrangement. (Goldschmidt, 1926) A domain (Aylmore and Quirk, 1960, 1962) or packet or book (Sloane and Kell, 1966) is an aggregate of parallel clay plates. An array of such fabrics is a termed a turbostratic fabric and is similar to the inter-weaving bunches. An edge-to-face association of packets or books is termed a book house and is similar to the arrangement of figure 2.2e. A cluster is a grouping of particles or aggregates into larger fabric units (Olsen, 1962; Yong and Sheeran, 1973).

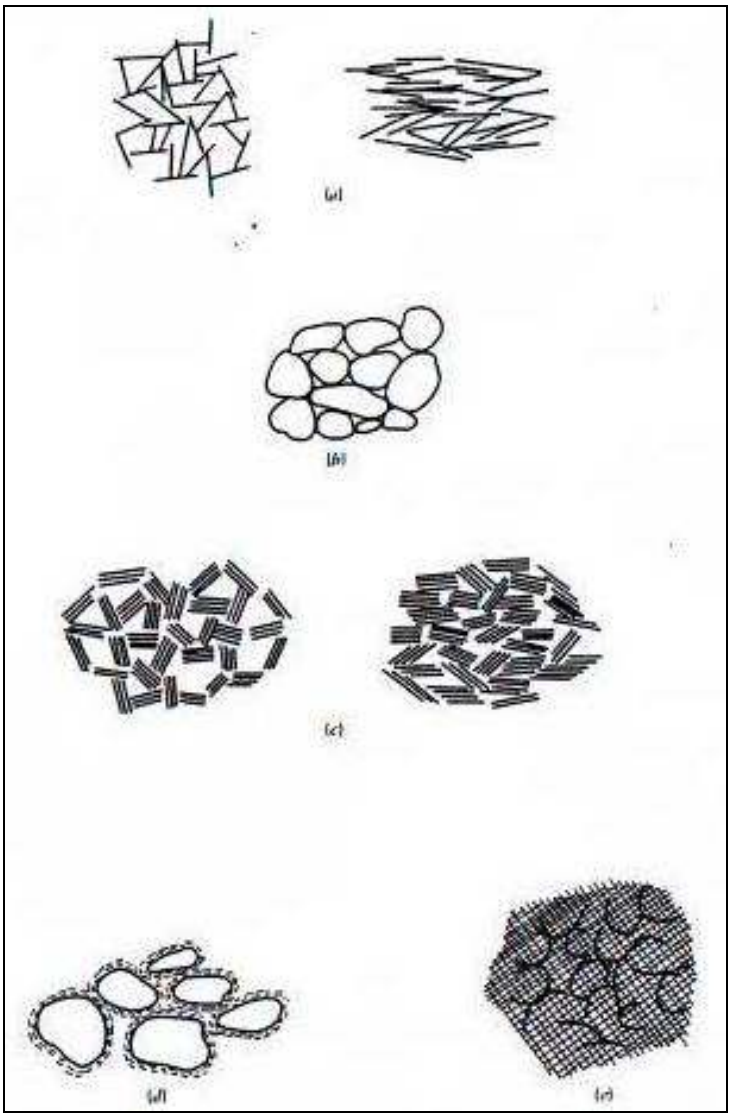

Figure 2.2. Schematic representations of elementary particle arrangements (a) Individual clay platelet interaction. (b) Individual silt or sand particle interaction. (c) Clay platelet group interaction. (d) Clothed silt or sand particle interaction. (e) Partly discernible particle interaction (Collins and Mc Gown, 1974).

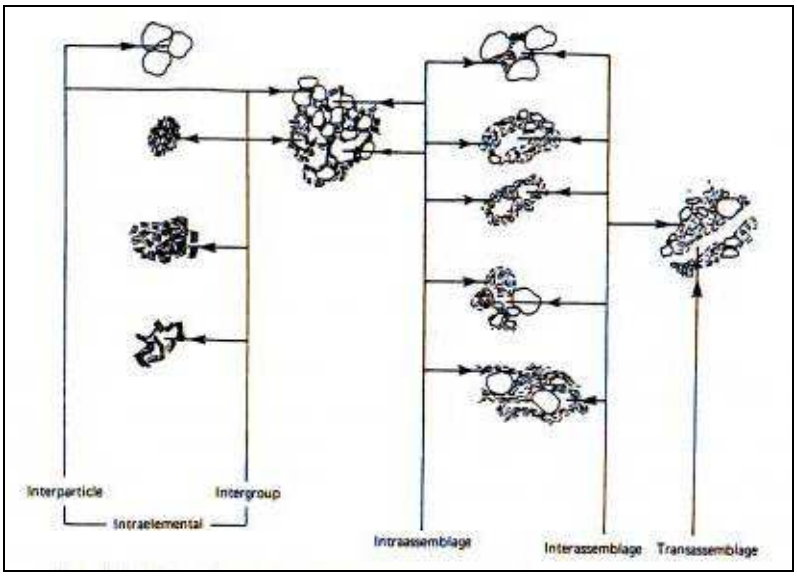

Figure 2.3. Schematic representations of pore space types (Collins and McGown, 1974).

2.2.3. Fabric Scale

1. Microfabric. The microfabric consists of the regular aggregations of particles and the very small pores between them. Typical fabric units are up to a few tens of micrometers across.
2. Minifabric. The minifabric contains the aggregations of the microfabric and the interassemblage pores between them.
3. Macrofabric. The macrofabric may contain cracks, fissures, root holes, laminations, etc. that correspond to the transassemblage pores.

The mechanical and flow properties of soil depend on details of these three levels fabric to varying degrees. For example, the hydraulic conductivity of a fine-grained soil will be almost totally dominated by the macro and the mini fabrics. Time-dependent deformations such as creep and secondary compression will be controlled most strongly by the mini and the micro fabrics.

2.2.4. Single-Grain Fabrics

The particle size of sand or gravel causes independent behavior. The stress-

deformation behavior of granular soils using particle mechanics theories are studied by various researchers; e.g., Rowe (1962, 1973), Horne (1965). The basic theories are shaped around elastic distortion of particles and the sliding and rolling of particles, usually of spherical or disc shape. In real granular soils, the irregular particle shapes and distribution of sizes invalidate the assumption of uniform spheres, and packing are usually far from regular.

2.2.5. Direct Observation of Cohesionless Soil Fabric

The study of fabric of a cohesionless soil is usually done by optical means. The particles are large enough so that they are easily seen in the petrographic microscope. Thin sections can be made from samples or in situ after impregnation of the sample by a suitable resin or plastic. In many cases, sand samples can be dried prior to impregnation, since sand fabrics are not generally affected by capillary stresses. A procedure for doing this to enable study of the fabrics produced in Monterey No. 0 sand by different methods of compaction is given by Mitchell et al. (1976).

2.2.6. Packings of Equal-Sized Spheres

Study of the possible regular packings of spheres of the same size provides insight into the maximum and minimum possible densities, porosities, and void ratios that are likely in single-grain fabrics. The range of possible porosities is from 25.95 percent to 47.64 percent, and the corresponding range of void ratios is from 0.34 to 0.91. Random packings of equal spheres can be considered to be composed of clusters of simple packings, each present in appropriate proportion to give the observed porosity. The relationship between coordination number N and porosity n in such systems is

$$N = 26.486 - 10726/n$$

Glass balls allowed falling freely from an anisotropic assembly, with the balls tending to arrange in chains (Kallstenius and Bergau, 1961).

2.2.7. Packings in Granular Soils

Particle sizes in any soil vary, and as a result, smaller particles can occupy pore spaces between larger particles. This results in a tendency toward higher densities and lower void ratios than for uniform spheres. On the other hand, irregular particle shapes result in a tendency toward lower densities and higher porosities and void ratios. Many studies have shown that a given cohesionless soil may have different fabrics at the same void ratio or relative density. Characterization of the fabric of a cohesionless soil can be done in terms of grain shape factors, grain orientations, and interparticle contact orientations (Lafeber, 1966; Oda, 1972; Mahmood and Mitchell, 1974; Mitchell, et al., 1976). The orientation of grains in a sand deposit can be described in terms of the inclination of the particle axes to a set of reference axes.

Fabric analyses are useful in research to show how mechanical properties are dependent on particle associations and arrangements. Fabric information can be used to deduce details of the depositional and post-depositional history of a deposit. The effects of different sampling methods can be assessed through study of fabric changes

.

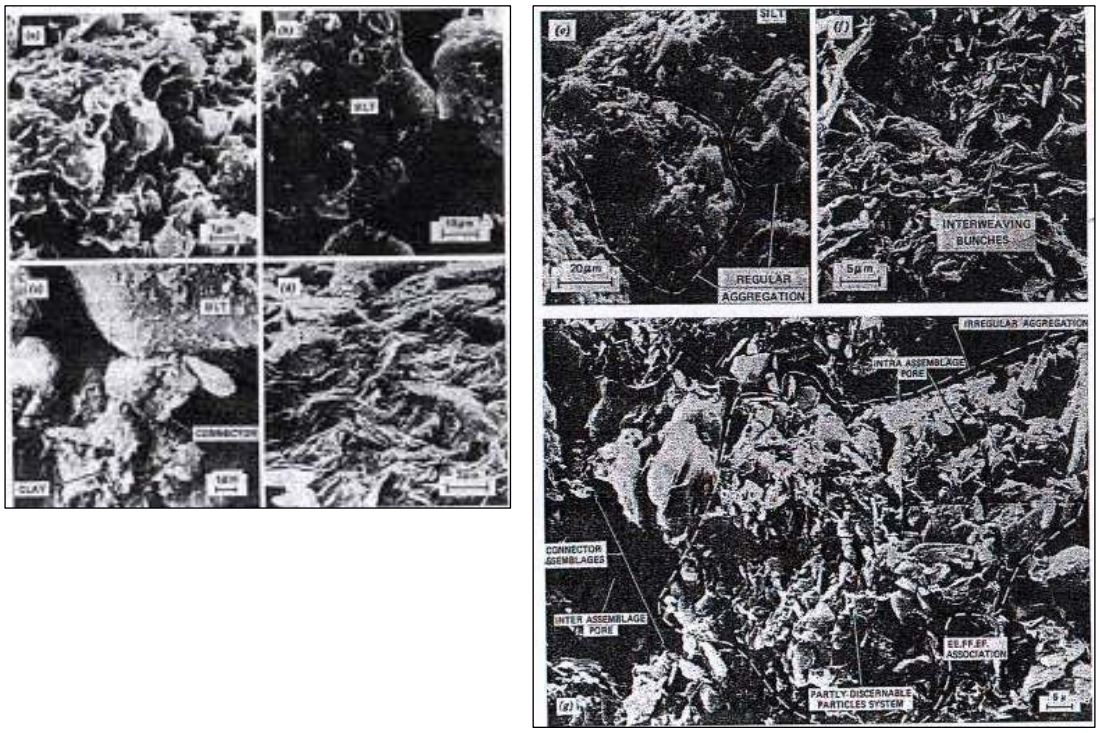

Figure 2.4. Scanning electron photomicrograph features of undisturbed soil fabric. (a) Partly discernible particle systems in Lydda silty clay, Isreal (fresh water alluvial deposit). (b) Grain-grain contacts in Ford silty loess, England (Aeolian deposit). (c) Connector assemblages in Breidmerkur silty till, Iceland (glacial ablation deposit). (d) Particle matrix assemblage in Immingham silty clay, England (estuarine deposit). (e) regular aggregation assemblage in Holon silty clay, Isreal (consisting of elementary particle arrangements interacting with each other and silt) freshwater alluvial deposit). (f) Interweaving bunch assemblage in Hurlford organic silty clay, Scotland (freshwater lacustrine deposit). (g) Irregular aggregation assemblage in Sunland silty clay, Norway (marine deposit). (Collins and McGown, 1974).

2.3. Shear Strength Parameters of Soil

If a structure is dependent on soil's shearing resistance, the importance of the shear strength of a soil is amplified. Increasing shear strength of kaolinite is good for two aspects. One it is basically curing the clay for making the site available for construction. Two, this may help us in shaping the clay in many different ways. Mainly the shear stress is needed for engineering situations such as determining the stability of slopes or cuts, finding the bearing capacity for foundations, and calculating the pressure exerted by a soil on a retaining wall. According to the ASTM D 3080 – Standard Test Method for Direct Shear Test of Soils under Unconsolidated Undrained Conditions, tests were performed on pure kaolinite, paper cut fiber added kaolinite, and also paper pulp added kaolinite.

$$\sigma = NormalStress = \frac{NormalForce}{Area}$$

$$\tau = ShearStress = \frac{\mathrm{Re}\,sistingForce}{Area}$$

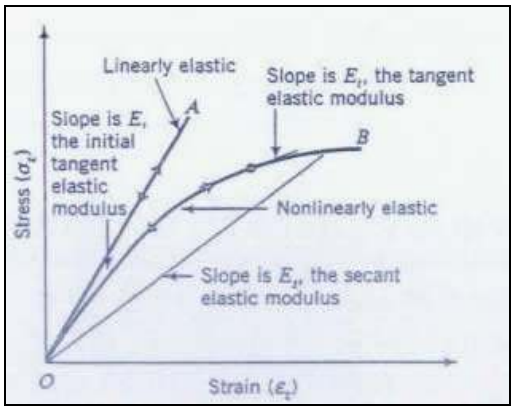

Figure 2.5. Linear and non-linear stress-strain curves of an elastic material

Linear and non-linear stress-strain curves of an elastic material are shown in figure 2.5. There are three important points on the normal stress – shear stress graph. Point A represent the normal stress and the shear stress on a plane in a soil mass which shear plane will not occur along that plane. Point B represents that shear plane occurs along the failure plane. C can not exist because failure already exists in a soil mass.

Mohr (1900) presented a theory for rupture in materials that contended that a material fails because of a critical combination of normal stress and shearing stress, and not from either maximum normal or shear stress alone. The functional relationship between normal stress and shear stress on a failure plane can be expressed as

$$\tau_f = f(\sigma)$$

Shear strength parameters are defined by Coulomb's shear strength equation

$$\tau_f = c + \sigma \tan \phi$$

where

τ = shear strength, kPa

c = soil cohesion or interparticle adhesion, kPa.

σ = intergranular pressure – may be either effective or total stress value, kPa

ø = angle of internal friction, degrees

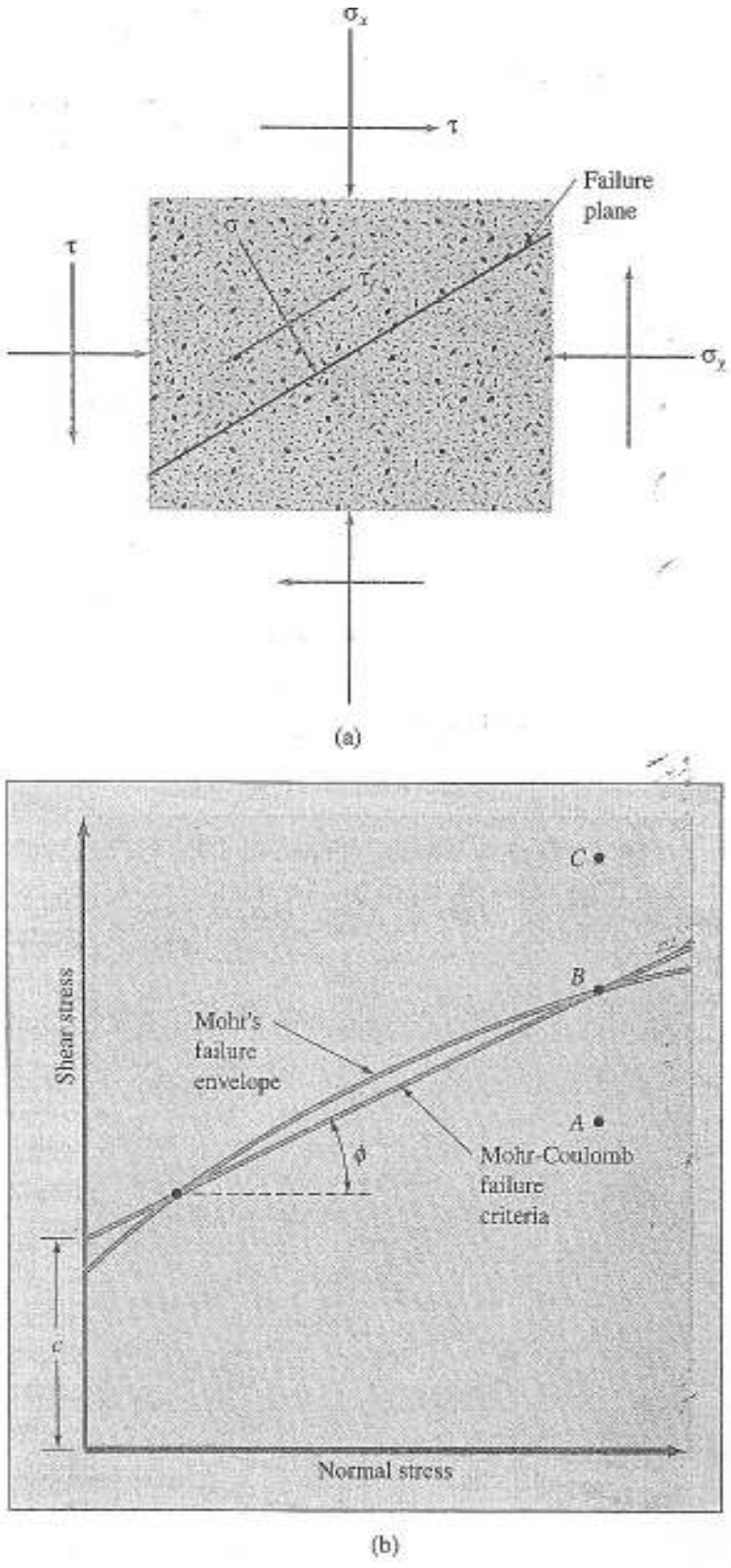

Figure 2.6. (a) The Mohr-Coulomb failure criteria (b) Mohr's failure envelope (Das, 2001)

The inclination of failure plane with the major principal line is determined with Figure 2.6(a). The failure plane EF makes an angle θ with the major principal plane. To determine the angle θ and the relationship between σ_1 and σ_3, refer to Figure 2.6(b).

Gray and Ohashi (1983) developed a theoretical model based on limiting equilibrium of forces to examine the effects of fiber reinforcement and to obtain test parameters for fiber-reinforced sand composites. The model developed is shown in figure 2.8. In this model, shearing results the fiber to distort and mobilize the tensile resistance in fiber. This force consists of a component normal and tangential to the shear plane. The normal component causes an increase in confining stress and the tangential component directly effects shear resistance.

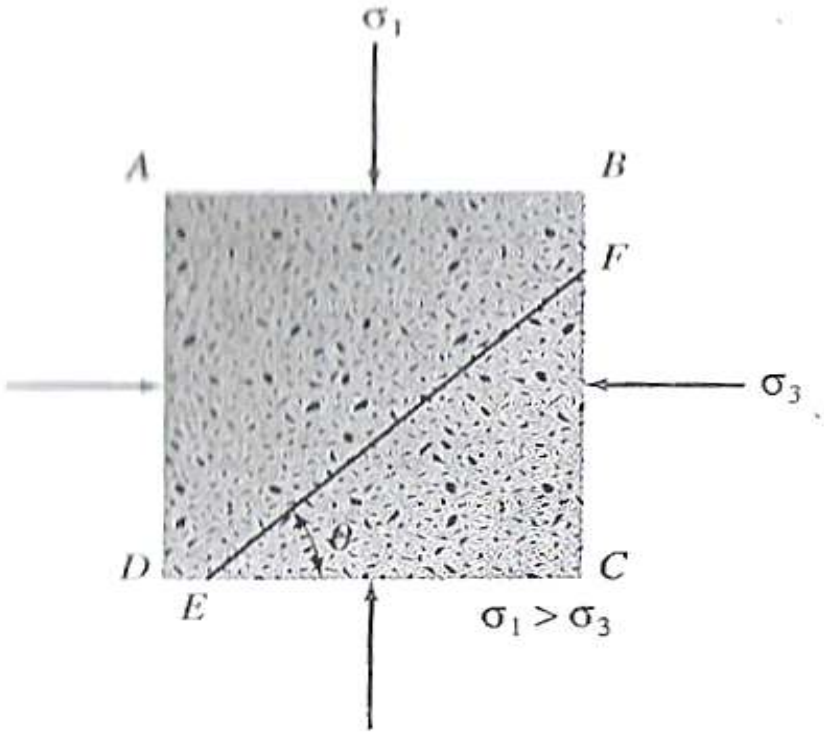

Figure 2.7. Inclination of failure plane in soil with major principle plane (Das, 2001)

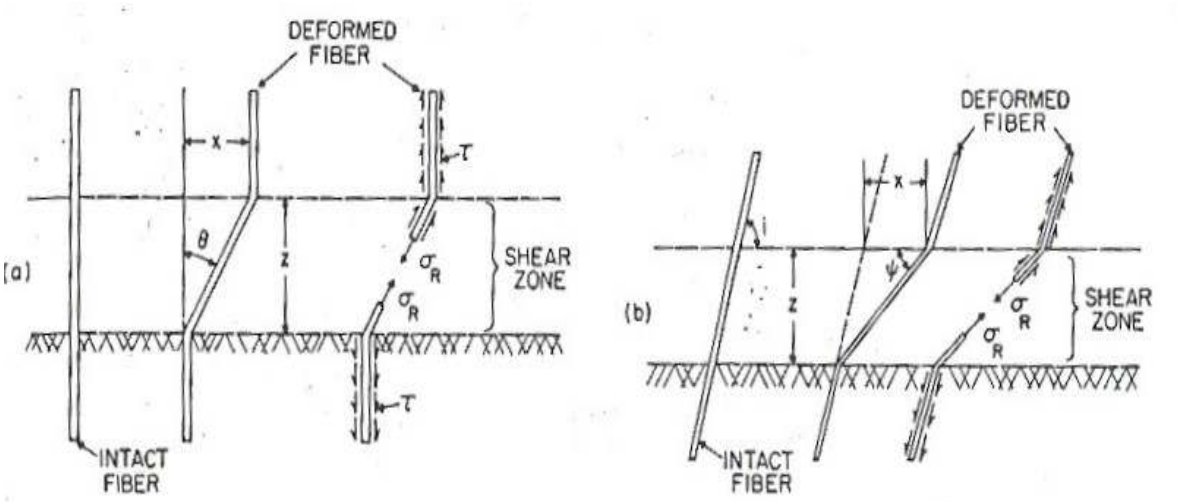

Figure 2.8. Model for oriented fiber reinforcement in sand; (a) perpendicular fibers; (b) inclined fibers (Gray and Ohashi, 1983)

From these principles, different kinds of direct shear tests can be applied. For example in a drained test the rate of loading can be kept low enough on a saturated soil specimen, so that excess pore water pressure in the soil will be absorbed by the drainage. Pore water from the specimen is drained with the help of porous stones. Although all of the direct shear tests share the same characteristic that the soil is not allowed to fail along the weakest plane, but rather is forced along the plane of split of the shear box, the direct shear test is still the most economical, and practical one.

Andersland and Khattak (1979) tested kaolinite clay reinforced with paper pulp fibers in triaxial testing under confining stress of 294 kPa to 441 kPa. On the basis of test results, they concluded that the addition of fibers increased both stiffness and undrained strength of clay. The effective angle of internal friction (Ø) of reinforced soil was reported to range 20˚ for unreinforced clay to 31˚ for all fiber added samples under consolidated drained condition. Also, consolidated undrained tests exhibited the values of Ø ranging from 20˚ for unreinforced clay to 80.4˚ for samples of fibers only (Andersland, and Khattak, 1979).

Özkul (1998) conducted an experimental study to investigate the effects of overburden stress on the hydraulic conductivity kaolinite and kaolinite-rubber liner and to investigate the effects of rubber particles on the permeability to these liners (under normal conditions and when exposed to gasoline). Hydraulic conductivity in consolidation permeameter and consolidation experiments was performed. Water and gasoline were used as permeants. Kaolin-rubber samples in water didn't have significantly larger k values than those of the kaolinite in water.

Öztürk (2007) conducted a laboratory-testing program to investigate the influence of fiber inclusion on clay soils. Fiber inclusion ratios of 0.25%, 0.50% and 1.00% by weight were selected and results of those tests were compared for reinforced soil and clay soil alone. A series of direct shear, CBR, unconfined compression, splitting tensile and linear shrinkage tests were conducted. The objective of this research is to investigate the effect of fiber reinforcement to the shear strength properties of kaolinite clay.

Ranjan et al. (1996) conducted a series of triaxial compression tests on cohesionless soils reinforced with discrete, randomly distributed fibers, both synthetic and natural, to study the influence of fiber characteristics in terms of weight fraction, aspect ratio, and surface friction. They have studied soil characteristics and its density, and confining stress on shear strength of reinforced soils and developed a mathematical model to bring out the effect of these factors on the shear strength of reinforced soil. Their test result indicate that the failure envelopes of soil-fiber composites have curvilinear failure envelope, with a transition occurring at a certain confining stress, termed as critical confining stress is affected by the fiber aspect ratio. Fiber inclusion significantly increases the shear strength of soil.

Hoare (1979) analyzed the results of a series of laboratory compression and CBR tests on sandy gravel reinforced with randomly distributed synthetic fibers less than two percent by weight. It was observed that the presence of fibers increased the apparent angle of internal friction and ductility of the soil particularly at low confining stress. Similar observations have been reported by Verma and Char. They performed triaxial tests on mild

steel fiber-reinforced medium/fine sand. They observed an increase in angle of internal friction from 36˚ to 45˚ with increase in fiber content from zero to seven percent by volume (Verma and Char, 1978).

2.4. Hydraulic Conductivity

Another important parameter for geotechnical design is hydraulic conductivity. Hydraulic conductivity influences the rate of the settlement of a saturated soil under load. The rate of flow to wells from an aquifer is dependent on hydraulic conductivity. Also the design of earth dams, the performance of landfill liners, the stability of slopes and retaining structures, and filters to prevent piping and erosion are influenced by hydraulic conductivity of the soil around the site.

A network of interconnected pores in the soil structure allows water pass through. The degree to which soils are permeable depends upon a number of factors, such as soil type, grain size distribution and soil history. This degree of hydraulic conductivity is characterized by the coefficient of hydraulic conductivity.

Darcy (1856) proposed that average flow velocity through soils is proportional to the gradient of the total head.

$$v_j = k_j \frac{dH}{dx_j}$$

Where v is the average flow velocity, k is a coefficient of proportionally called the coefficient of permeability or hydraulic conductivity, and *dH* is the change in the total head versus a distance *dx*.

Darcy's law is essentially derived from the flow of fluids. It is based on the assumption that the flow is laminar:

$$q = -kiA$$

Where q is the flow rate, i is the hydraulic gradient, A is the total cross-sectional area of flow, and k is the proportionality constant.

2.5. Literature Research

In table 2.1., the collection of the papers, thesis studies, and previous work done by many researchers are shown with the arrangement of author(s), objective of the study, and result of the studies.

Table 2.1. Summary of previous studies

Author(s)	Objective of the study	Results
Gray and Ohashi (1983)	-To establish a mathematical model for predicting the increase in shear strength -To determine the increase in shear strength of soils experimentally with addition of fibers.	-The addition of fibers increase shear strength of soils -Fiber orientation does not affect the shear strength of soil
Maher and Ho (1994)	-Mechanical properties of kaolinite-fiber soil were investigated by a series of unconfined compression, splitting tension, three-point bending and hydraulic conductivity tests.	-Inclusion of fibers increased peak compressive strength and ductility -Splitting tensile strength of kaolinite clay increased with addition of fibers -Inclusion of fibers increased both toughness and hydraulic conductivity.

Ranjan, Vasan and Charan (1994)	-Triaxial tests were performed on fiber-reinforced soil to observe influence of fiber properties (weight, fiber content and aspect ratio)	-Critical confining stress decrease with increase in aspect ratio -Shear strength increase with increase in fiber content and aspect ratio -Residual strength increases with inclusion of fibers
Michalowski and Zhao (1996)	-To present a mathematical modeling of failure criterion for fiber-reinforced soils. -Triaxial tests were conducted for that purpose. -Results of mathematical model and experiments were compared.	-The presence of fibers inhibited the dilation effect. -Polyamide fibers produced a significant increase in peak shear strength. -Increase in fiber content, while aspect ratio is kept constant, increases strain rate and decreases stiffness. -Mathematical model gives approximate solution to the effect of fibers in soil strength
Santoni, Tingle and Webster (2001)	-Unconfined compression tests were performed on fiber-reinforced sand specimens to identify the effect of numerous variables on performance of fiber-reinforced soils for road construction.	-Inclusion of fibers increased unconfined compressive strength of soils -Optimum fiber length is found 51 mm -Maximum performance is achieved at fiber dosage between 0.6% and 1.0% by weight. -Specimen performance is enhanced in both wet and dry optimum conditions

Consoli, Montardo, Prietto and Pasa (2002)	-Unconfined compression, splitting tensile and triaxial tests were conducted on sandy soil which is reinforced with polyethylene fibers obtained from recycled waste bottles -Effects of fiber content, fiber length, cement content and initial mean effective stress were investigated.	-Unconfined compressive and splitting tensile strength of specimens significantly increased with addition of fibers. -Both peak and ultimate strength increased with addition of fibers for cemented and uncemented soil. -Initial stiffness does not change significantly
Michalowski and Cermak (2003)	-Triaxial tests were performed on specimens in order to set a model for predicting failure stress for reinforced-soils.	-Substantial increase in shear strength can be achieved by addition of 2% fibers by volume -Fibers are more effective with larger aspect ratios -The reinforcement is more effective when the fiber length is large compared to the size of the grains
Miller (2004)	-To understand the impact of fiber addition on the development of cracks, compaction characteristics and hydraulic conductivity. -To find the optimum amount of fiber ratio for waste containment soil liners	-Addition of fibers reduce crack occurrence whereas the hydraulic conductivity increases -The optimum fiber content is between 0.4% and 0.5% -Compaction behavior does not change with addition of fibers

Özkul (2005)	-To understand the mechanical behavior of low plasticity kaolinite clay with 10% tire buffing by weight. -A series of triaxial, direct shear, hydraulic conductivity and odometer tests were performed	-Inclusion of tire buffing decreases dry unit weight. -Soil composite is more compressible than clay alone. -Hydraulic conductivity does not change significantly with addition of tire buffing. -Shear strength of the composite does not improve significantly with addition of tires.
Edinçliler, Baykal and Saygılı (2006)	-To understand the effect of tire shred, tire chip and tire buffing addition to shear strength parameters of sand. -Large size direct shear tests were performed to understand the behavior of road embankments reinforced with granular tire material.	-Addition of tires affects shear strength and deformation of sand. Tires are more effective at lower normal stresses. -Tire reinforcement gives satisfactory results up to 2m. Embankment depth. -Usage of waste tires for road embankment reduces environmental and storage problems caused by waste tires.
Chew, Kamruzzan, Lee (2004)	- To examine the relationship between microstructure and engineering of cement treated marine clay	- Immediate increase in water content, increase in effective increase permeability.

Consoli, Prietto and Ulbrich (1998)	- Evaluation the effect of randomly distributed fiber reinforcement and cement inclusion on the response of a sandy soil to load.	- Cement addition increases stiffness and peak strength, fiber reinforcement both the peak and residual triaxial strength decreases because of the brittle behavior.
Briaud, Zhang, Moon (2003)	- Estimation of the vertical movement of ground surface for soil that swells and shrinks.	- A method is described to calculate the shrink and swell of shallow foundations.
Hsuan (2002)	To describe the potential physical and chemical degradation of polypropylene fibers in the needlepunched and stitch bonded GCL	- GCL fibers durability is important with respect to sloping surfaces and canyon landfill liners.

3. METHODOLOGY

3.1. Materials

Kaolinite clay, straw paper pulp, and straw paper cut fibers were mainly used as materials for this study. Well-graded kaolinite clay soil from Balıkesir region was tested with the code number K401M. The optimum water content that was previously discussed was achieved by the usage of distilled water. For reference, kaolinite clay will be stated as "K" and kaolinite-paper pulp mixture will be referred as "KPP" and kaolinite-paper cut fiber mixture will be referred as "KPC" in further stages of this study. The physical and engineering properties of the clay and straw paper mentioned above are given below.

3.1.1. Clay

As the name implies, the clay used in this study contained high amounts of kaolinite. Silt is also highly abundant in this kind of clay. Kaolinite has a chemical formula of $Al_2Si_2O_5(OH)_4$. The geotechnical properties of clay can be found in Table 3.1. The mineralogical composition is shown in Table 3.2. It is classified as Cl in the Unified Classification System.

Table 3.1. Atterberg limits of kaolinite K401 M

Specific Gravity	2,63
Liquid Limit (%)	25
Plastic Limit (%)	19
Plasticity Index	6
Activity	0.22

Table 3.2. Mineralogical composition of kaolinite clay

K 401 M Kaolinite		
Chemical Analysis	**Percentage**	
SiO_2	%	62,19
Al_2O_3	%	26,18
Fe_2O_3	%	0,37
TiO_2	%	0,38
CaO	%	0,17
MgO	%	0,13
Na_2O	%	0,20
K_2O	%	0,14
SO_3	%	0,10
L.O.I. (Loss of ignition)	%	9,94

Table 3.3. Sieve analyses of kaolinite clay

K 401 M Granular Analysis		
No	**Sieve**	**Percentage**
1	> 60 M	0,50%
2	0 - 60 M	99,50%
3	0 - 50 M	97,55%
4	0 - 40 M	96,80%
5	0 - 30 M	93,00%
6	0 - 20 M	86,50%
7	0 - 10 M	73,30%
8	0 - 5 M	58,90%
9	0 - 2.7 M	47,35%

3.1.2. Paper

3.1.2.1. Major Paper Properties & Definitions

Table 3.4. Properties of paper

PROPERTIES OF PAPER							
Properties	**Unit**	**Testing Method**	**50 g/m2**	**60 g/m2**	**80 g/m2**	**90 g/m2**	**120 g/m2**
Basis Weight	g/m2	T410 om 93	50±2.5	60±3	80±4	90±4.5	120±6.0
Moisture	%	T412 om 94	4-6	4-6	4-6	4-6	4-6
COBB Value	g/m2	T441 om 90	21±2	21±2	25±3	29±3	25±3
Whiteness	%	ISO 2470	62±2	62±2	62±2	62±2	62±2
Opacity	%	ISO 2471	Min. 80	Min. 85	Min. 90	Min. 95	Min. 95
Tearing Resistance (Width)	N	T494 om 88	Min. 18	Min. 18	Min. 20	Min. 25	Min. 30
Tearing Resistance (Length)	N		Min. 36	Min. 36	Min. 40	Min. 45	Min. 60
Smoothness (W)	ml/min.	T538 om 96	Max. 450	Max. 450	Max. 500	Max. 500	Max. 600
Smoothness (L)	ml/min.		Max. 400	Max. 400	Max. 450	Max. 450	Max. 500

It is easy to perceive that weight or substance per unit area is an important property in paper, and paper based products. The basis weight of the paper can be described as the weight of paper per unit area. This can be expressed as the weight in grams per square meter (GSM or g/m^2) of a specific size. The weight of a lot or batch of paper is commonly signified by the term REAM WEIGHT. A change in basis weight is significant in the sense that this affects all the other properties of paper. The weight in grams varies with the changes in the moisture content of paper. The basis weight of the paper used throughout the study was 50±2.5 g/m^2.

Brightness is defined as the percentage reflectance of blue light only at a wavelength of 457 nm. Whiteness, on the other hand, determines how much paper can reflect light of all wave lengths included in the visible spectrum. Therefore, brightness, and

whiteness are two distinct terms that should not be used as substitutes for each other. However, the maximum value of whiteness that can be achieved by tinting of the paper is determined by the brightness values of the pulps, and pigments going into that particular paper product. Whiteness affects the way an object appears, whereas the color is an aesthetic value. Color can appear different when viewed under a different light source. Although, the definition of brightness is arbitrary, careful standardization enables blue reflectance values to be used in the paper, and pulp industry for the control of mill processes, and in certain types of research and development programs. The color of paper, like of other materials, depends in a complicated way on the characteristics of the observer and a number of physical factors such as the spectral energy distribution of the illuminant, the geometry of illuminating and viewing, the nature and extent of the surround and the optical characteristics of the paper itself. The whiteness of the paper used throughout the study was 62±2 %.

Bulk is defined as the ratio of volume or thickness of paper relative to its weight. Therefore, it is simply the reciprocal of density (density per unit volume). It is calculated from caliper and basis weight. As density, the sheet bulk is closely related to all other major properties of paper, and affects smoothness, gloss, opacity, strength, and darkness.

Dimensional change, along with a change in moisture content, as a result of absorption and de-absorption of moisture by paper. Such changes in dimension may seriously affect register in printing processes and interfere with the use of such items as tabulating cards. Uneven dimensional changes cause undesirable cockling and curling. Dimensional changes in paper originate in the swelling and contraction of the individual fibers. It has been observed that cellulose fibers swell in diameter from 15 to 20% in passing from the dry condition to the fiber saturation point. The degree of swelling is very difficult to determine as there are many paper-making fibers that allow different degrees of swelling, and also the irregular cross-section of fibers do not allow precise definition of diameter. Change that occurs in the dimensions of paper with variation in the moisture content is an important consideration in the use of paper. All papers expand with increased moisture content and contract with decreased moisture content, but the rate and extent of changes vary with different papers.

Folding endurance is the paper's capability of withstanding multiple folds before it breaks. It is defined as the number of double folds that a strip of 15 mm wide and 100 mm length can withstand under a specified load before it breaks. It is important for printing grades where the paper is subjected to multiple folds like in books, maps, or pamphlets. Fold test is also important for carton, box boards, ammonia print paper, and cover paper etc. Folding endurance is a requirement in Bond, Ledger, Currency, Map, Blue Print and Record Papers.

Formation determines the distribution of fibers, and fillers within the sheet. The fact that most of the other properties of paper depend on formation amplifies the importance of this property. Paper that is poorly formed will have weak, thin spots and thick spots. These will affect properties like caliper, opacity, strength etc. Paper formation also affects the coating capabilities and printing characteristics of the paper.

Gloss is the diffusely reflected light component that is measured against a known standard. Gloss is important for printing such things as magazine advertisements. The level of gloss desired is very dependent on the end use of the paper. Gloss and smoothness are different properties and are not dependent on each other.

Paper has a definite grain direction due to greater orientation of fibers in the direction of travel of the paper machine. This grain direction is known as machine direction. The cross direction is the direction of paper at right angles to the machine direction. Some of the properties vary with the MD and CD and hence the values are reported in both the directions. While sheeting the paper, machine and cross direction are to be kept in mind and the sheet cutting to be done to suit the end use requirements. Examples: 1. all printing papers are to be cut in long grain (The biggest dimension in the grain direction). 2. Book papers fold better and the book stays open better if the sheets are out so that the machine direction runs up and down the pages. 3. Wrap around labels for metal cans and bottles are to be cut with the machine direction vertical to obtain greater flexibility about the can. Long grain and Short grain: The sheet is in long grain if the larger dimension is parallel to grain (MD) direction. The sheet is said to be in short grain if the larger dimension is parallel to cross direction (CD).

Most physical properties of paper are affected by variations in moisture content. Poor moisture control can adversely affect many paper properties. Water has the effect of plasticizing the cellulose fiber and of relaxing and weakening the inter fiber bonding. The electrical resistance and the dielectric constant of paper both vary with moisture content. The absorption and reflectance of certain bands of infrared and microwave radiation by paper are affected by its moisture content. The amount of water present in a sheet of paper is usually expressed as percentage. The amount of water plays an important role in calendaring, printing and converting process. Moisture control is also significant to the economic aspect of paper making. The moisture of the paper used throughout the study was 4-6 %.

Opacity refers to the ability of a paper sheet to hold light from passing through. Perfect opacity is achieved when no visible light can pass trough the sheet. It is the ratio of diffused reflectance and the reflectance of single sheet backed by a black body. Opacity is important in Printing Papers, Book Papers, etc. The opacity of the paper used throughout the study was min.80 %.

Because paper is composed of a randomly felted layer of fibers, it follows that the structure has a varying degree of porosity. The extent that fluids, both liquid and gaseous, can penetrate the structure of paper as a paper property is highly significant to the use of paper. Paper is a highly porous material and contains as much as 70% air. Porosity is a highly critical factor in printing papers, laminating paper, filter paper, cigarette paper, bag paper, anti tarnish paper and label paper. Porosity is the measurement of the total connecting air voids, both vertical and horizontal, that exists in a sheet. Porosity of sheet is an indication of absorptive ability or the ability of the sheets to accept ink or water. Porosity can also be a factor in a vacuum feeding operation on a printing press.

The need to limit the spreading of ink resulted in "sizing" the paper with gelatinous vegetable materials which had the effect of sealing or filling the surface pores. Later, the term "sizing" was applied to the treatment of paper stock prior to the formation of the sheet, with water-repellent materials such as resin or wax. Resistance towards the penetration of aqueous solution / water is measured by Sizing or Cobb values. The Cobb value of the paper used throughout the study was 21±2 g/m^2.

Smoothness is concerned with the surface contour of paper. It is the flatness of the surface under testing conditions which considers roughness, liveliness, and compressibility. In most of the uses of paper, the character of the surface is of great importance. It is common to say that paper has a "smooth" or a "rough" texture. The terms "finish" and "pattern" are frequently used in describing the contour or appearance of paper surfaces. Smoothness in important for writing, where it affects the ease of travel of the pen over the paper surface. Finish is important in bag paper as it is related to the tendency of the bag to slide when stacked. Successful printing operation depends on the smoothness of the paper. Smoothness is also related to how well paper can appear as rough paper looks unattractive. The smoothness (width) value of the paper used throughout the study was max.450 ml/min, and smoothness (length) value of the paper was max.400 ml/min.

Stiffness is the measure of force required to bend a paper through a specified angle. Stiffness is an important property for box boards, corrugating medium and to certain extent for printing papers also. Paper that can easily be bent can cause feeding and delivery problems in larger sheet presses. Stiff paper will cause problems such as in copier machines where it will have difficulty traveling through feeder rollers. Bond papers also require certain stiffness to be flat in typewriters etc.

Stretch is the amount of distortion which paper undergoes under tensile stress. Stretch elongation is usually expressed, as percent stretch to rupture. Stretch can be related to the paper's ability to conform and maintain conformance to a particular contour, e.g. Copier paper, multicolor offset printing papers, liquids packing cartons base papers etc. It is an important property in sack Kraft papers which are used for cement bags etc. Stretch is higher in cross direction than machine direction.

Tearing resistance indicates the behavior of paper in various end use situations; such as evaluating web run ability, controlling the quality of newsprint and characterizing the toughness of packaging papers where the ability to absorb shocks is essential. Tearing strength depends on fiber length and inter-fiber bonding. Longer fibers will result in better tearing strength. Longer fibers will diffuse the stress over a greater area, and more fibers, and bonds, whereas shorter fibers will result in stress to be concentrated over a smaller area. The tearing resistance (width) value of the paper used throughout the study was

min.18 N, and tearing resistance (length) value of the paper was min.36 N.

Conditioning of paper is also of importance in many printing and converting operations. Besides its effect on the physical properties of paper, moisture content determines the extent of static build up in paper subjected to pressure, and friction. The tendency for paper to develop static becomes greater with increasing dryness. Cellulose fibers are hygroscopic i.e. they are capable of absorbing water from the surrounding atmosphere. The amount of absorbed water depends on the humidity and the temperature of the air in contact with the paper. Thus, test results will be affected with even small changes in temperature, and humidity. Therefore, it is important that standard conditions are maintained throughout the experiments in terms of humidity, and temperature to achieve reliable test results.

Thickness or Caliper of paper is measured with a micrometer as the perpendicular distance between two circular planes, parallel surfaces under a pressure of 1 kg/cm^2. Caliper is a critical measurement of uniformity. Variations in caliper can affect several basic properties including strength, optical and roll quality. Thickness is important in filling cards, printing papers, condenser paper, saturating papers etc.

Wax pick no. indicates the surface strength of the paper. This test is important for all uncoated printing papers.

Wire side and felt side also referred as wire side, and top side, the side which is in contact with the paper machine wire during paper manufacture is called the wire side, where as the other side is called top side. Certain properties differ between wire and felt side and it is common to measure these properties on both the sides. When printing is to be made on only one side only, it is preferable to print on the felt side. Postage stamps are printed on wire side and then glued on felt side, where the smoothness is helpful for attaining an even application.

3.1.2.2. Papermaking process. As in almost every industry, technological improvements, and advances have been observed in the production of paper based products, especially in terms of automation, and increase in the rate and capacity of production thanks to mechanization. Despite this, the main production processes and methods have virtually stayed the same for well over a century. Papermaking process takes place in five steps. These steps are chipping, pulping, bleaching, inclusion of additives, removing water.

For economical operation of pulping plant as well as for better penetration of cooking liquor, wood logs/bamboo are to be chipped into small pieces (some wood species can not be chipped directly and needs debarking). The process is called chipping and the equipment used for chipping are called chippers. During chipping, chips are generated in various sizes. For better operation of the process, only chips of size 5-35 mm are taken. Chips of size less than 5 mm (dust and pin chips) are taken to boiler house for burning as fuel for generating steam. Chips of size more than 35 mm are taken into chippers again to be chipped to an acceptable size.

By some cooking process, lignin, which is the glue that holds the fibers of the wood together in their form, and other purities are removed from the wood & other raw materials. The cooking process requires wood, bamboo or other raw material chips. The cooking process requires wood, bamboo or other raw material chips. The chips are loaded into a digester and cooking liquor is added. Then, by pressure cooking, the wood, bamboo or other raw material fibers are separated from unwanted ingredients. Either batch digester or continuous digesters are used in cooking.

The cooking process requires wood, bamboo or other raw material chips. The chips are loaded into a digester and cooking liquor is added. Then, by pressure cooking, the wood, bamboo or other raw material fibers are separated from unwanted ingredients. Either batch digester or continuous digesters are used in cooking.

The chips and liquor are mixed as the chips are pumped to the top of the digester. The top section of the digester is pressurized to 160 psi and more. As the chip mass passes downward, the cooking liquor penetrates the chip. After about 45 minutes or more as per

raw material the chips have to be passed through the impregnation zone where hot liquor (171 ˚C) is circulated through the chips for heating. The actual pulping occurs at 179 ˚C in about 90 minutes, a period known as the cooking period. After passing through the cooking zone, the chips (which have not yet become pulp) are washed with weak liquor through washing stages that follow.

Within the chemical process there are two types:

- Sulphate Process "(Alkaline process)"
- Sulphite Process "(Acid process)"

Some hard woods may be dissolved with difficulty by the sulphite process. On the other hand, by the sulphate process most of the chemicals are recovered and reused.

In its natural form, the cellulose fiber is white in color. Despite this, some unwanted elements in the pulp like residual lignin give unbleached pulp its cream color. Bleaching is utilized for removing this cream color, and achieving whiteness. During this process avoiding any possible damages to the fiber is of high importance. This process is also supposed to improve other properties of paper pulp. Therefore there are multiple objectives to be achieved by bleaching process:

- To increase brightness of the pulp by removal or modification of some of the unwanted elements in the unbleached pulp. These deleterious elements are lignin traces, resins, metal ions, non-celluloid carbon hydrates etc.
- The unbleached pulp will turn yellow, lose its brightness, and strength as time passes. Removing these elements by bleaching will also eliminate these effects of aging, and provide stability.
- To lower viscosity of the pulp for optimum flow, during subsequent operations.
- Bleaching also should help reduce the fiber bundles and bark fragments.

Bleaching should be done with minimum mechanical action of fibers, while dissolving lignin and other unwanted residuals. Bleaching pulp is normally done in a step-wise sequence using different chemicals and process conditions at each stage, with washing in between stages.

Additives are added to paper pulp, to both act as fillers, and to increase brightness of paper pulp. Addition of fillers like talcum & calcium carbonate is very common. These additives must be finely ground. Additives like dyes & starch are also added. Other fillers are Titanium Dioxide, Barium Sulphate & Zinc Sulphide.

Removing water is the next important stage. For this the pulp is passed through a rapidly moving wire mesh called fourdriner. The objective is to remove 93% to 95% of the water in the finished paper.

As the paper flows along the wire mesh and water is drained along the way, a dandy roller near the end helps to smooth out the paper. The dandy roller improves the formation of the paper web by application of pressure. When the paper reaches the end of the wire mesh it is transferred to a felt blanket which conveys it through many steam heated driers to remove the excess moisture. In the process the paper gets some glaze like coating also. Then it is made to pass through a series of calendar stacks. The calendars are series of polished iron rollers stacked one on top of the other, through which the finished paper will pass to smoothen down. The next step is rewinding on a metal or fiber core. The last stages after this are sheeting, packing & testing.

3.2. Experiments

3.2.1. Sample Preparation

The first step in sample preparation was the preparation of the main materials to be used in the study, namely kaolinite clay, and straw paper (along with kaolinite clay specimens reinforced with straw paper).

The paper was used in two forms: (1) Cut form and (2) Pulp form. First, water was heated to 100 ˚C. Then paper was left in the boiling water for one to two hours. Paper saturated with water was then put in a container and mixed with a mechanical mixer until uniform pulp form achieved. In paper cut form, Eraysan manual shredder was used. The standard A4 form paper was cut into two parts. Paper was shredded by the help of the shredder. Paper cut fibers were 6 mm in width, 297 mm in length. The tearing resistance

of paper was very important at this point.

Paper in cut from, and pulp form was then added to clay to begin preparation of the samples to be used in the tests. The first important point was uniformity within the samples. Achieving optimum moisture level and also minimizing pores in the samples were also crucial factors. The samples being at optimum moisture levels ensured that maximum unit weight was also achieved.

The clay was mixed in a mechanical mixer for approximately 5 minutes to make sure that all the clay particles within the samples were uniformly distributed. Mixing was continued manually with the help of a spatula, this time to ensure proper and uniform distribution of paper cut fiber and paper pulp, and kaolinite. The mechanical mixer was again used for the mixing of the paper cut fibers, and paper pulp with clay.

The second phase of the sample preparation was to obtain the optimum water content within the samples, which was done by pouring the samples in a container, and spraying water over the samples. The water enriched samples were finally again put, and mixed in the mechanical mixer. The same preparation procedure was applied to all of the samples to be used in all of the tests. (I.e. direct shear, unconfined compression, splitting tensile and shrinkage test specimens).

The optimum water content of the samples was tested with standard proctor tests for pure koalinite, and kaolinite mixed with straw paper 1% by weight. Through this test, the main aim was to identify the maximum dry unit weight of clay.

Samples were compacted at their optimum water content for direct shear tests. Both standard and modified compaction energies were used for compaction of samples according to ASTM D1557-78.

Harvard compaction mold was used to obtain unconfined compression test, and splitting tensile test samples. The samples were prepared at optimum water content and Harvard compaction type cylindrical mold with diameter of 3.30 cm and height of 7.10 cm was used. Both rammer and a specially designed hammer were used for standard compaction.

3.2.2. Equipment and Testing Methods

Compaction tests were conducted using a standard 101.6 mm compaction mold and a collar assembly extending 50.8 mm above the top of the mold to retail soil during preparation of compacted specimens of the desired height and volume. Standard rammers with a weight of 2.5 kg and falling height of 305 mm were used during compaction process. The compacted specimen within the mold was removed with a lifting jack and the sample was sliced vertically through the center. Two representative specimens were taken from the compacted soil and the water content of each specimen is determined. In compaction tests, standard test procedures as outlined in ASTM D698-78 were followed.

Direct shear test specimens were obtained from compaction molds, which were compacted with standard and modified energies. Samples with dimensions 6 x 6 x 2 cm were used in order to conduct direct shear tests. Samples, which were trimmed from compacted soil, were packed in airtight plastic bags and stored overnight in a curing room. Three specimens for each percentage of paper cut fiber and paper pulp inclusions were tested. The specimens were carefully pushed into the shear box with a rammer with an end cap slightly smaller than the inside dimensions of the shear box. The bottom porous stone and filter paper had already been placed in the bottom of the box. The top filter paper was in place during placement of the specimen box. The shear box was adjusted by using alignment pins and elevating screws. The two halves of shearing box were separated 2-3 mm before shearing in order to eliminate shearing between two parts. After placement of the specimen in the direct shear box, the box was mounted into the direct shear machine and a seating load was applied. Normal stresses of 100 kPa, 200 kPa and 300 kPa were applied respectively. Shearing rate of 0.50 mm/min was applied to specimens and it took approximately 10 minutes for each specimen to reach total deformation state. The specimens were sheared to a total displacement of approximately 10 mm. Manual readings were taken from dial gauges for recording vertical-horizontal deformations and applied load. Upon completion of the shear stage, each specimen was removed from the shear box and the shear plane was visually examined.

Unconfined compression tests were conducted on clay; clay-paper cut fibers, clay paper pulp composites according to ASTM D2166 standards. Harvard miniature

compaction mold with an inner diameter of 33 mm and height of 71 mm was used to obtain test specimens. The specimens were treated in moisture controlled curing room for two days. Three specimens for each ratio of paper content and kaolinite clay were tested. After the curing of unconfined compression test samples, the specimens were trimmed from top and bottom ends to obtain flat planes which helped the specimen perfectly interact with loading plate. Three height and three diameter measurements were taken. The averages of those measurements were used as specimen dimensions. In addition, weight of the specimen was measured. After those procedures, specimens were placed in the loading device and the upper platen was adjusted to make contact only with the specimen. The deformation indicator and LVDT were set to zero. Axial strain rate of 0.5 mm/min was chosen in order not to let failure time exceed 15 minutes. Load dial readings were recorded at each 0.2 mm displacement intervals and readings continued until load values decrease with increasing displacement, or until 15% strain was reached.

Similar sample preparation and curing procedure was used in splitting tensile strength tests. ASTM D3967 testing standards were followed during splitting experiments. Three specimens were prepared for each percentage of fiber inclusion and pure kaolinite clay. After the curing period, samples were prepared according to standards with thickness-to-diameter (t/D) ratio between 0.2 and 0.75. The ends of specimens were cut parallel to each other and at right angles to the longitudinal axis. The dimensions and the weight of the specimens were recorded prior to splitting test. The specimens were positioned so that the diametric plane of the specimen lined up with the center of loading plane. 0.5 mm/min of loading rate was selected to ensure that failure occurred within 1 to 10 minutes and deflection-load readings were recorded.

Compaction mold permeameter was used and samples were compacted using standard proctor energy. ASTM D5084 testing standards were followed during hydraulic conductivity tests. Before testing, specimens were completely saturated with distilled water in order to avoid the presence of air which may restrict the flow of water.

Linear shrinkage tests were conducted in a 140 mm length mold with inner radius of 12.5 mm. Soil sample weighing approximately 150g was used with moisture content close to liquid limit. In order to prevent the soil adhering the mold, a thin film of grease was used on the surface. The soil paste was placed in the mold, and sample was gently jarred to ensure no air pockets present. The soil was leveled with a palette knife and soil adhering to the rim of the mold was removed. After this procedure, the mold was placed in a drying oven with a temperature of 105ºC. The mold was left in the oven for 1 day until the soil had finished drying. The mean length of dried sample was measured and percentage of linear shrinkage was determined.

4. TEST RESULTS AND DISCUSSION

In this chapter, results of compaction, direct shear, unconfined compression, splitting tensile strength, hydraulic conductivity and linear shrinkage tests are shown and briefly discussed. Standard compaction effort is abbreviated as “St” and modified compaction effort is abbreviated as “Md”. Clay compacted at standard and modified energy is referred as “K-St” and “K-Md” respectively. Paper cut fibers and kaolinite compacted with standard and modified energy are stated as “KPC-St” and “KPC-Md” respectively. Paper pulp and kaolinite compacted with standard and modified energy are stated as KPP-St and KPP-Md respectively.

4.1. Compaction Tests and Determination of Optimum Water Content

Standard Proctor and Modified Proctor tests were conducted in order to find moisture-unit weight relationships for pure kaolinite, kaolinite + 1% paper cut fiber mixture by weight. Standard Proctor test was started with target water content of 15% up to a limit of 23% with increments of 2%. Modified compaction test was started with a target water content of 14% to a limit of 22% with 2% increments. The achievement of the optimum water content within the samples ensures maximum dry unit weight which in turn gives minimum pore ratio. Due to both paper cut fibers, and paper pulp having the same paper content by weight in their respective mixtures, the optimum water content for the two different types of additives was the same. The figures 4.1-4.4 include the Standard, Modified and Harvard compaction test results, and the corresponding graphs.

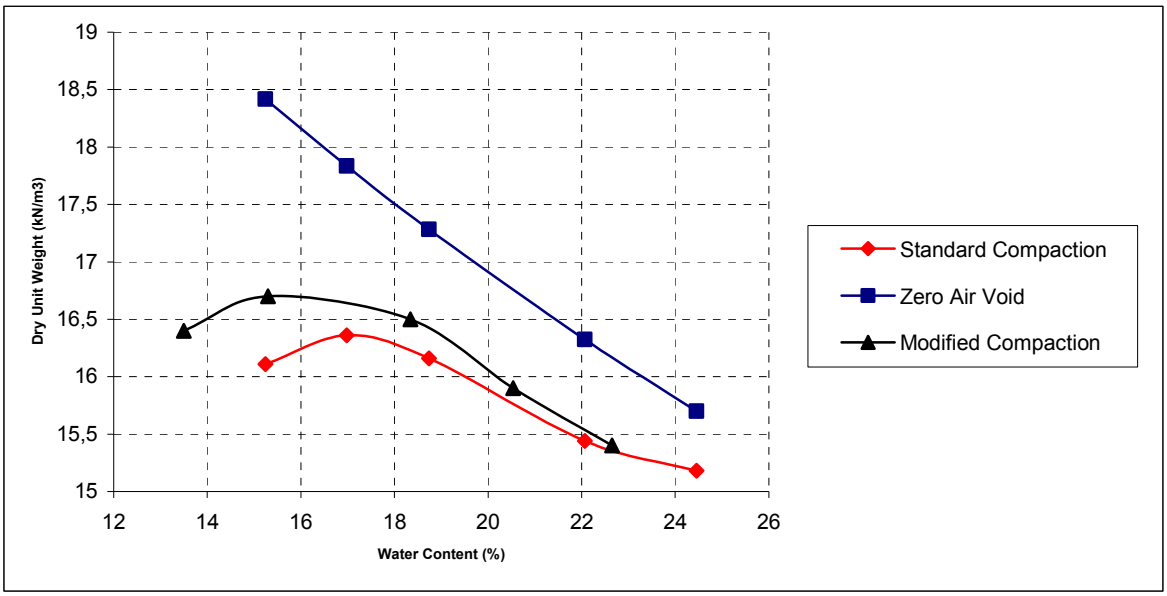

Figure 4.1. Moisture - unit weight relationship curve for K samples

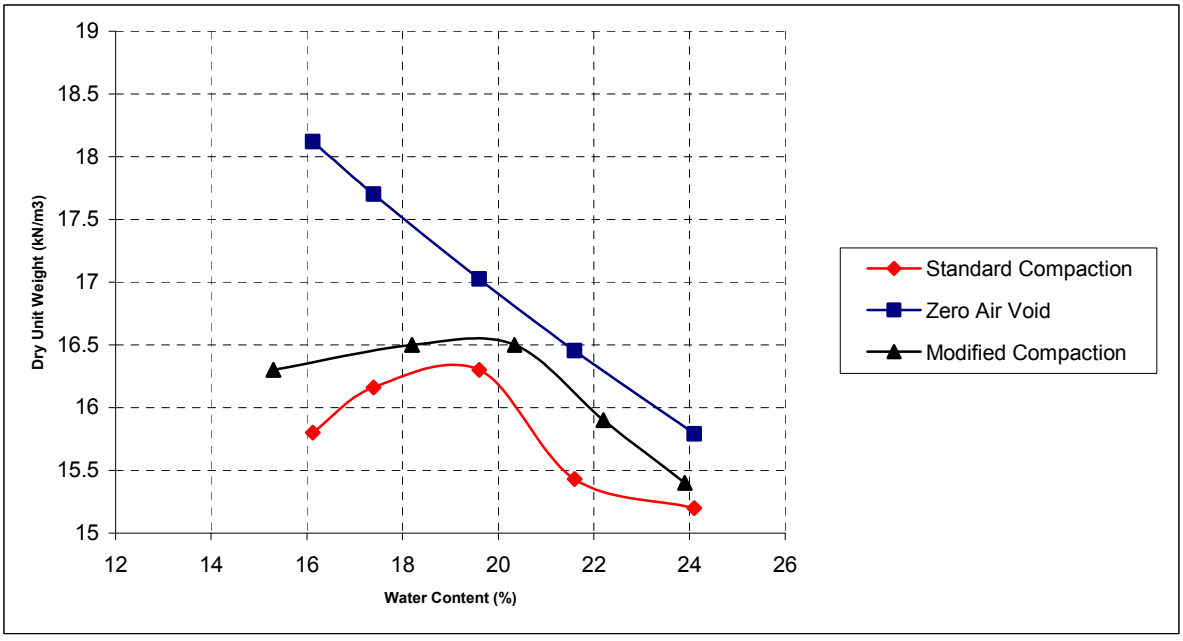

Figure 4.2. Moisture - unit weight relationship curve for KPC-1.00 samples

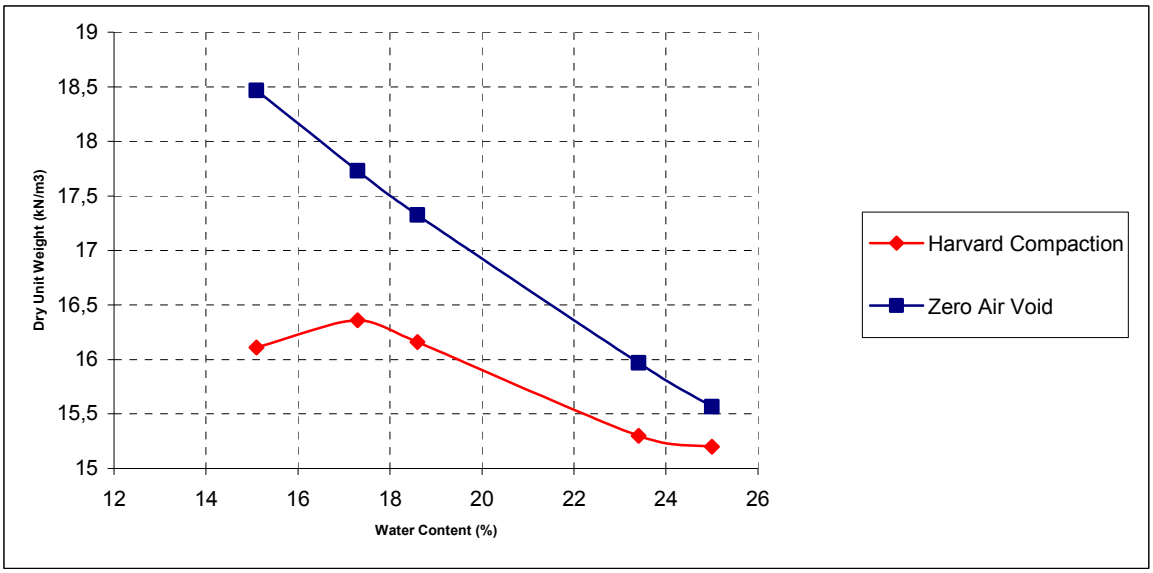

Figure 4.3. Moisture - unit weight relationship curve for K samples compacted with Harvard miniature compaction equipment (spring tamper)

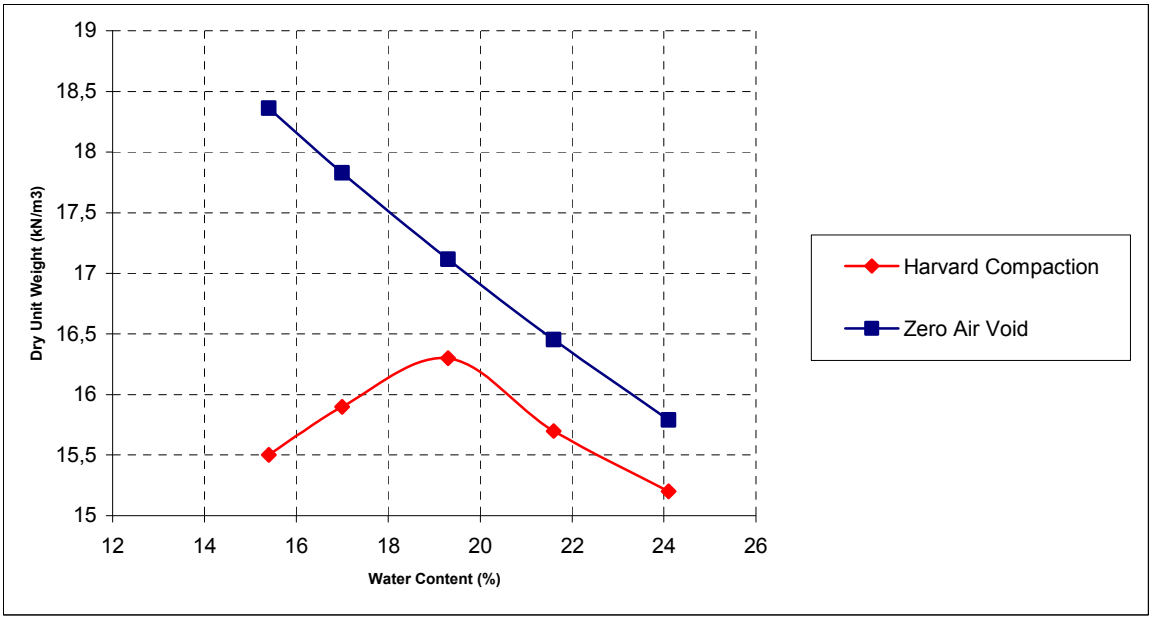

Figure 4.4. Moisture - unit weight relationship curve for KPC-1.00 samples compacted with Harvard miniature compaction equipment (spring tamper)

For Standard Proctor tests conducted using pure kaolinite the optimum water content for kaolinite is 16.98%. The maximum dry unit weight of pure kaolinite at the optimum water content is 16.35kN/m^3. In Modified Proctor tests, pure kaolinite has an optimum water content of 15.30% with a maximum dry unit weight of 16.70kN/m^3.

Although the optimum water content in the Modified Proctor tests decreases by 2% relative to Standard Proctor tests, the compaction effort had only a small effect in the maximum dry unit weight of the samples.

Moreover, to understand the effect of adding paper cut fibers to pure kaolinite, compaction tests were performed on kaolinite-paper cut fibers mixed %1 by weight and standard, modified, Harvard compaction hammer energies were applied. According to KPC 1% by weight standard Proctor test, optimum water content is 19.6% with a maximum dry unit weight of 16.30kN/m^3. Modified Proctor test results of KPC 1% samples has an optimum water content of 20.34 % and maximum dry unit weight of 16.50 kN/m^3. In addition, K samples and KPC 1.0% samples compacted with spring tamper in a Harvard miniature mold have optimum water content of 17.30%, 19.30% and dry unit weight of 16.36 kN/m^3, 16.30 kN/m^3 respectively.

From the test results, and the corresponding graphs, adding paper cut fibers 1% by weight increases the optimum water content by 3% in standard Proctor Tests, and by 5% in modified Proctor Tests. KPC 1% samples have correlation between standard and modified proctor tests, but unlike K samples optimum water content increases. Adding paper pulp and paper cut fiber by weight affects optimum water content and also dry unit weight. Adding paper to kaolinite increased the water content because during the mixing process, added water was sucked by paper uniformly. The addition of water in a gradual manner guarantees uniform absorption. The optimum water content was applied to all tests for observing the most realistic behavior of kaolinite reinforced with paper cut fibers, and paper pulp. Mixing problems occurred when water was added instantly.

4.2. Direct Shear Test Results

All direct shear tests were performed in a 6 cm by 6 cm direct shear box on K, KPP, KPC soil samples. Samples were prepared at optimum water content and compacted with standard and modified energies. Paper pulp content 1% by weight was added to kaolinite and will be referred as KPP-1.00%. Also paper cut fibers contents of 0.25%, 0.50%, 1.00 % by weight was added to kaolinite. Paper cut fibers inclusion of 0.25%, 0.50

%, and 1.00% by weight will be referred as KPC-0.25%, KPC-0.50%, and KPC-1.00%. Again for the specimen compacted with standard energy is labeled with St, the specimen compacted with modified energy is labeled with Md.

The results of direct shear tests for K, KPC and KPP soil samples are shown in Table 4.1. Shear stress versus horizontal displacement, vertical displacement versus horizontal displacement and vertical stress versus normal stress graphs of each tests are plotted, and the information and discussions about each graph are given below. The results of each test are given in figures 4.5 – 4.50.

From the summarized results of direct shear tests given in Table 4.1, addition of paper pulp and paper cut fibers increased the shear strength parameters of soil. The cohesion shows significant variation between K samples and KPC samples with 0.25% - 1.00% paper fiber added by weight. Addition of paper pulp and paper cut fibers up to an amount of 1.00% by weight decrease cohesion in soil. The internal friction angle (Ø) increases with correspondence to paper cut fiber inclusion ratio. The friction angle value increased from 21.50º to 53º with addition of fibers to soil, which were compacted with standard energy. Samples compacted with modified energy almost showed the same behavior on friction angle which changed from 32.50º to 55.40º. Adding paper pulp and paper cut fibers to kaolinite increased shear strength. Pure samples didn't show dilation whereas paper cut fiber, and paper pulp added samples dilate in direct shear tests in general.

Type of Specimen	Normal Stress	Dry Unit Weight	Peak Values		Shear Strength Parameters		Increase According To Pure Kaolinite	
	(kPa)	kN/m3	Stress (kPa)	Deformation (mm)	c (kPa)	Ø (˚)	c (kPa)	Ø (˚)
K-St	100	16,30	78,42	-0,25	29,5	21,47	0,00	0,00
	200		133,45	-0,60				
	300		191,35	-0,89				
KPC-0.25%-St	100	16,20	90,23	0,76	5,23	39,1	-82,27	82,11
	200		159,64	0,16				
	300		252,43	0,40				
KPC-0.50%-St	100	15,90	105,00	0,52	3,12	50,7	-89,42	136,14
	200		234,95	0,73				
	300		322,80	1,02				
KPC-1.00%-St	100	16,00	126,90	0,64	4,39	53	-85,12	146,86
	200		290,23	0,79				
	300		392,23	1,07				
KPP-1.00%-St	100	16,40	75,94	-0,16	2,08	35,8	-92,95	66,74
	200		142,80	-0,47				
	300		220,16	-0,54				
K-Md	100	16,40	102,21	0,34	36,03	32,5	22,14	51,37
	200		158,09	-0,31				
	300		229,42	-0,45				
KPC-0.25 % Md	100	16,60	100,06	0,44	4,39	53	-85,12	146,86
	200		290,23	-0,04				
	300		392,32	-0,40				
KPC-0.50 % Md	100	16,50	127,50	0,34	2,08	51,5	-92,95	139,87
	200		245,04	0,49				
	300		375,46	0,72				
KPC-1.0 % Md	100	16,30	135,23	-0,45	4,78	55,4	-83,80	158,03
	200		323,45	-1,06				
	300		425,01	-3,02				
KPP-1.0 % Md	100	16,00	102,21	-0,31	10,4	40,8	-64,75	90,03
	200		171,28	-0,55				
	300		274,66	-0,85				

Table 4.1. Results of direct shear tests

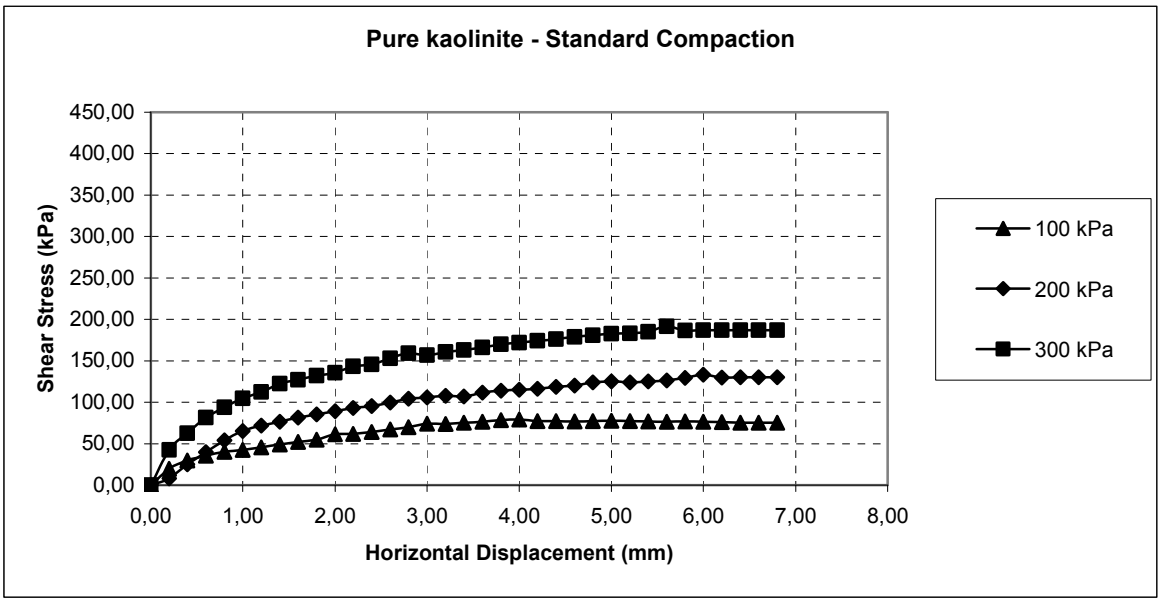

Figure 4.5. The shear stress-horizontal displacement curves of K-St group samples under 100 kPa, 200 kPa and 300 kPa normal stresses

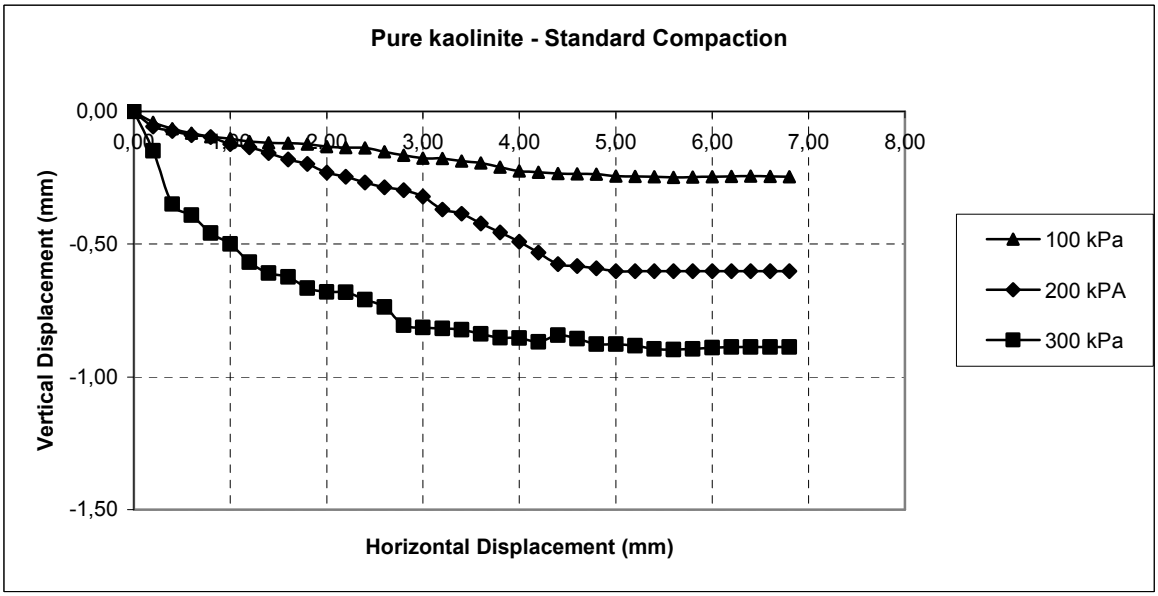

Figure 4.6. The vertical displacement - horizontal displacement curves of K-St group samples under 100 kPa, 200 kPa and 300 kPa normal stresses

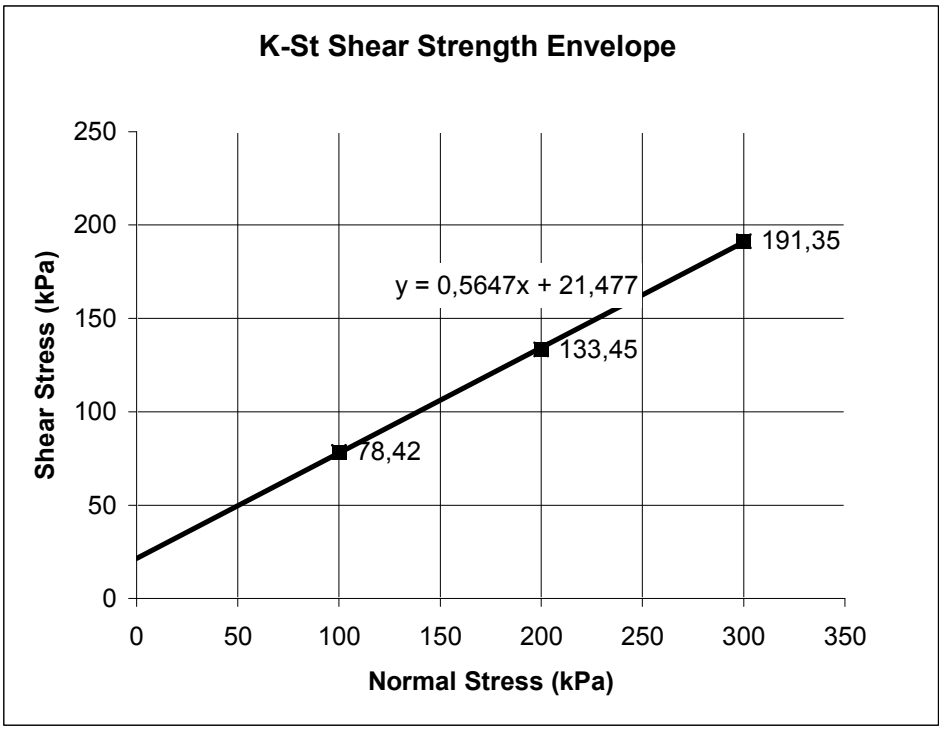

Figure 4.7. Shear stress envelope of K-St group samples under 100 kPa, 200 kPa and 300 kPa normal stresses

Test results for pure kaolinite samples which were compacted at standard energy are shown in Figures 4.5 – 4.7. K-St samples compacted at standard energy have peak stresses of 78.42, 133.45, 191.35 kPa respectively for 100, 200 and 300 kPa normal stresses. The internal friction and the cohesion are 29.5˚ and 21.47 kPa respectively. K-St samples compacted at standard energy have peak vertical displacements of -0.247 mm, -0.602 mm, -0.897 mm with respect to 100,200 and 300 kPa normal stresses. Contraction was occurred under 100 kPa, 200 kPa, 300 kPa. Compared to K-Md samples compacted at modified energy, K-St samples had lower peak shear stresses.

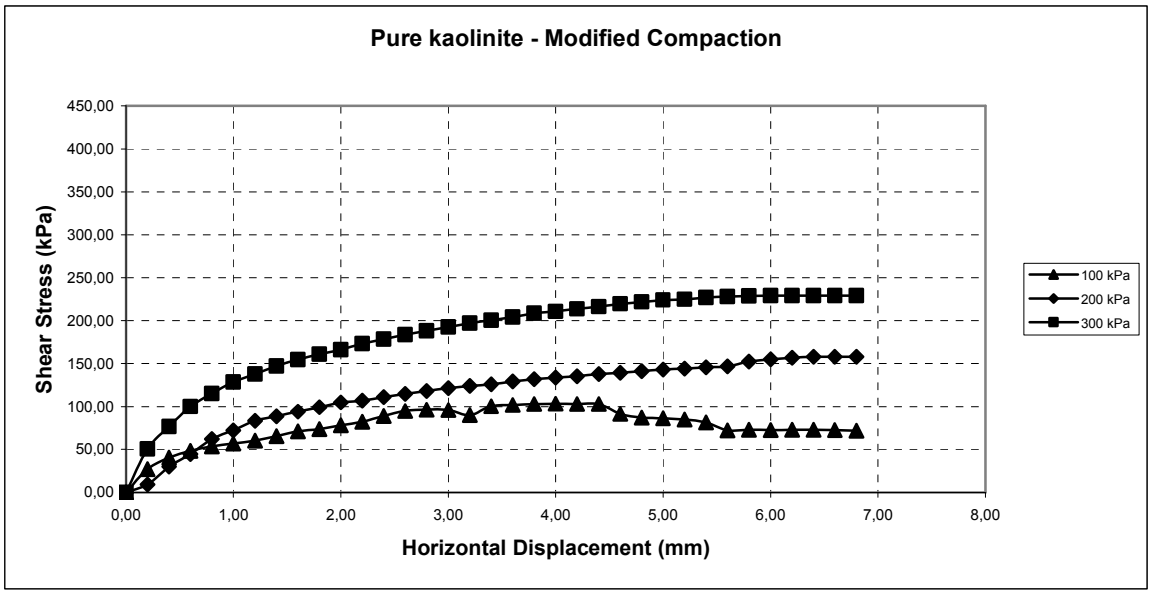

Figure 4.8. The shear stress-horizontal displacement curves of K-Md group under 100 kPa, 200 kPa and 300 kPa normal stresses

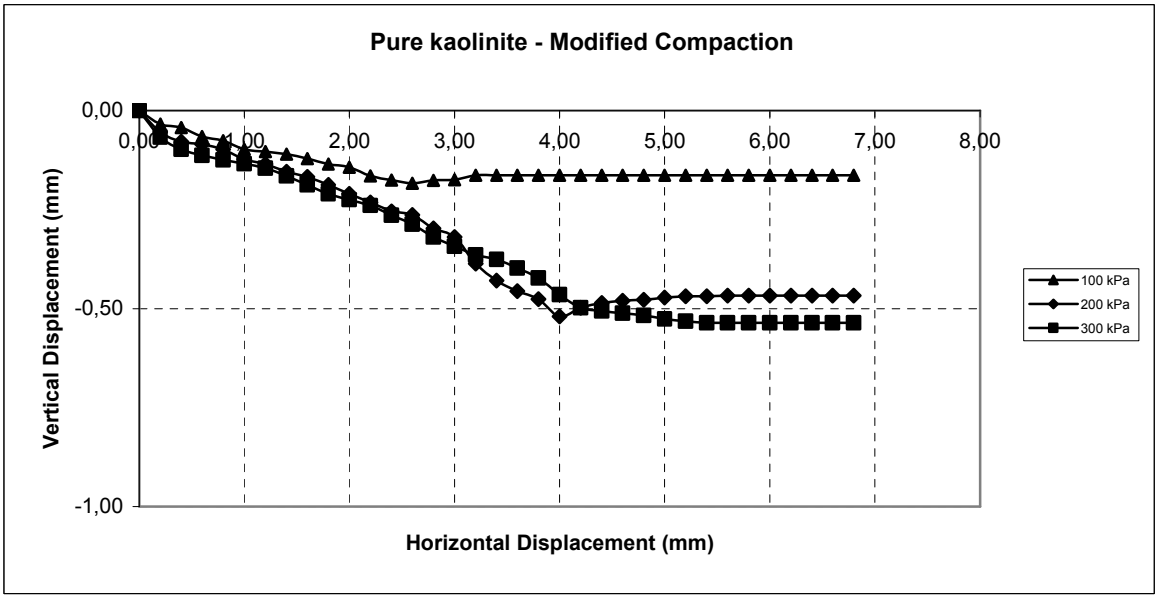

Figure 4.9. The vertical displacement - horizontal displacement curves of K-Md group samples under 100 kPa, 200 kPa and 300 kPa normal stresses

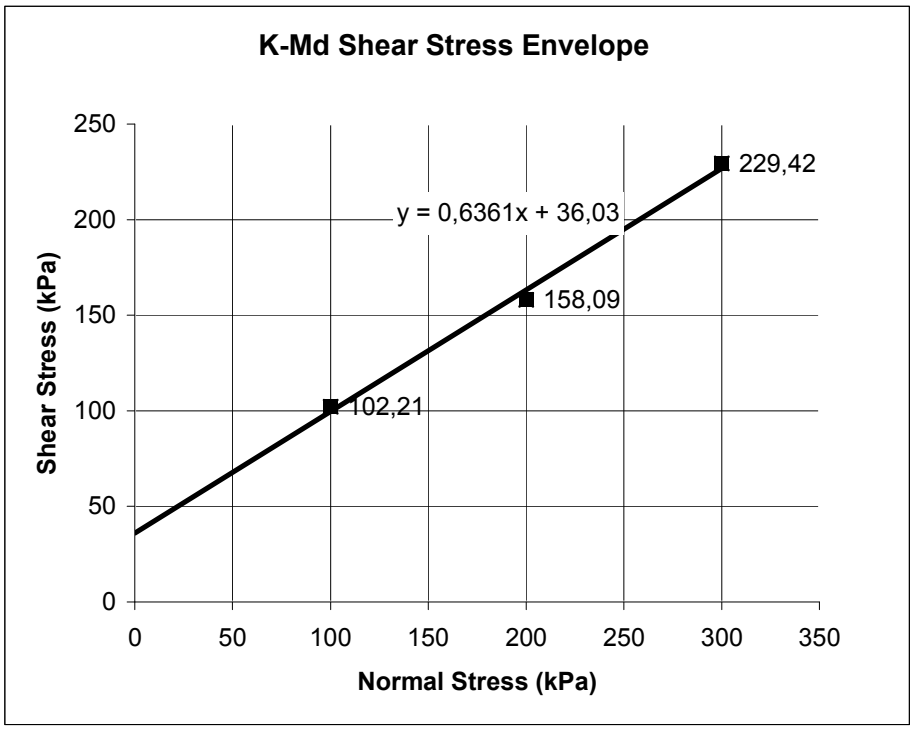

Figure 4.10. Shear stress envelope of K-Md group samples under 100 kPa, 200 kPa and 300 kPa normal stresses

Test results for pure kaolinite samples which were compacted at modified energy are shown in Figures 4.8 – 4.10. K-Md samples compacted at modified energy have peak stresses of 102.21, 158.09, 229.42 kPa respectively for 100, 200 and 300 kPa normal stresses. The internal friction angle and the cohesion are 32.5˚ and 36.03 kPa respectively. Cohesion and internal friction angle values increase both with respect to K-St samples. K-Md samples compacted at modified energy have peak vertical displacements of -0.16 mm, -0.45 mm, -0.54 mm with respect to 100,200 and 300 kPa normal stresses. Compaction effort affected shear strength parameters. Contraction occurred under normal stresses both for K-St, and K-Md samples, but vertical displacement for K-Md samples was lower than K-St samples.

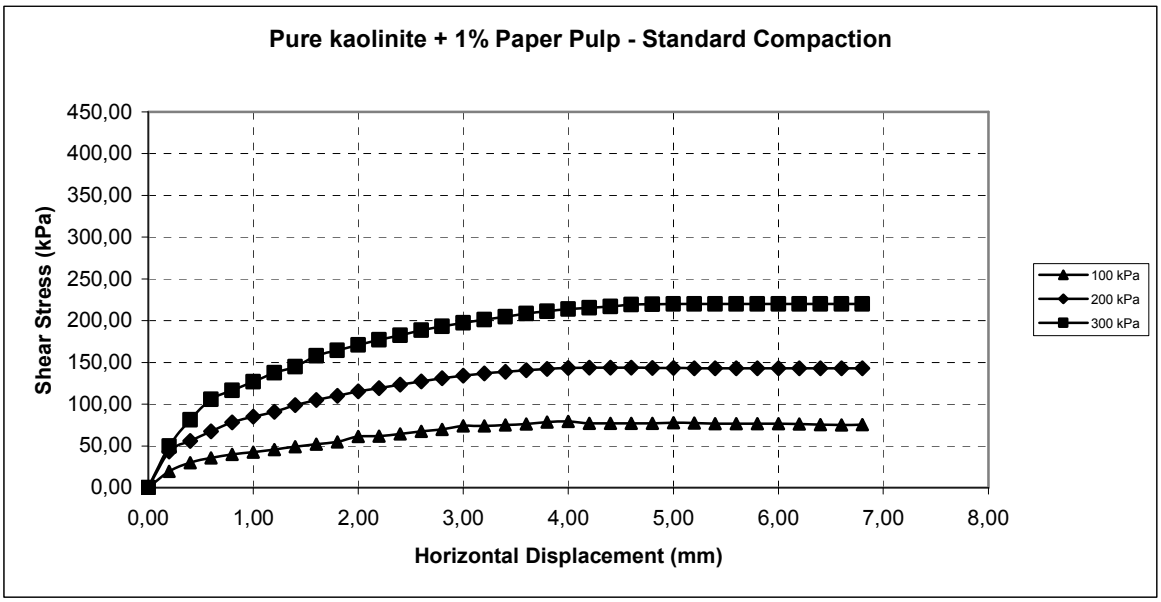

Figure 4.11. The shear stress-horizontal displacement curves of KPP 1%-St group samples under 100 kPa, 200 kPa and 300 kPa normal stresses

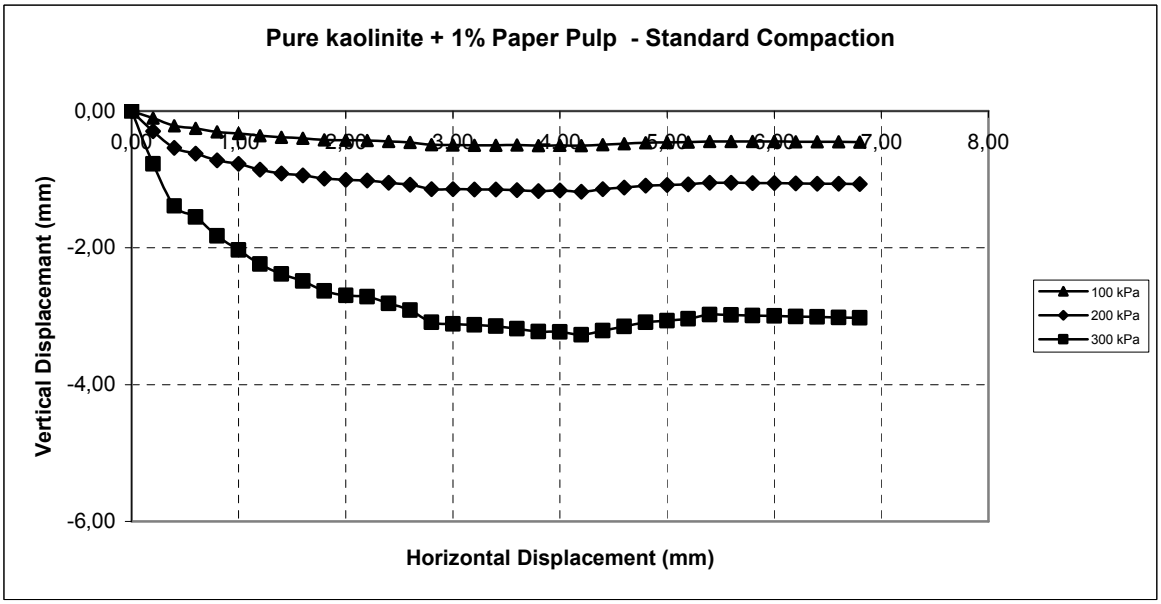

Figure 4.12. The vertical displacement – horizontal displacement curves of KPP 1%-St group samples under 100 kPa, 200 kPa and 300 kPa normal stresses

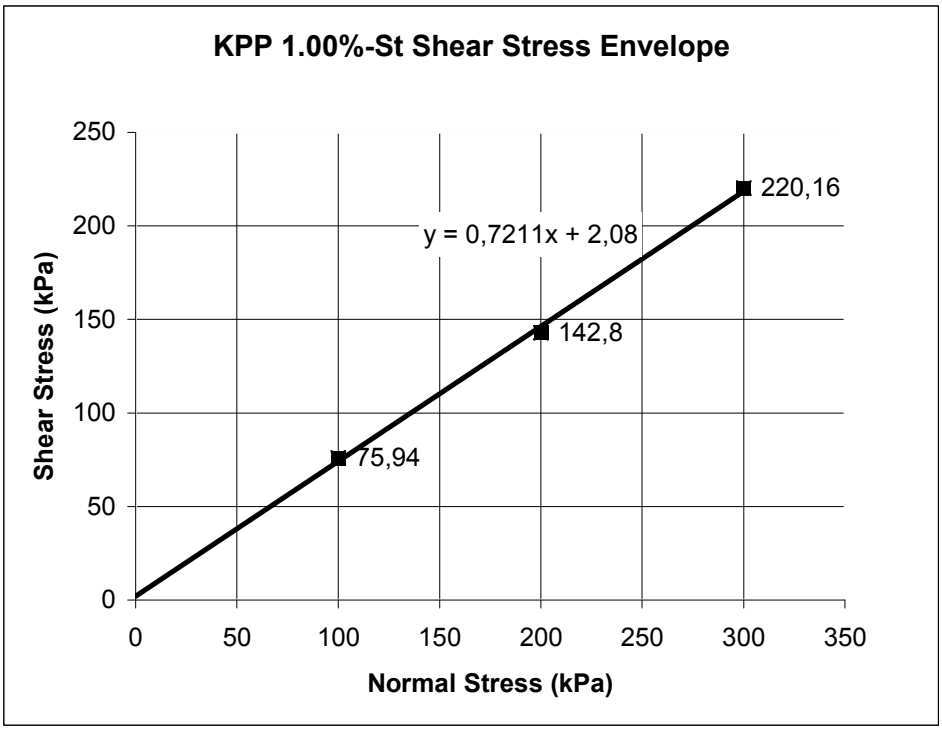

Figure 4.13. Shear stress envelope of KPP 1%-St group samples under 100 kPa, 200 kPa and 300 kPa normal stresses

Test results for KPP 1%-St samples which were compacted at standard energy are shown in Figures 4.11 – 4.13. KPP 1%-St samples have peak stresses of 75.94, 142.8, 220.16 kPa respectively for 100, 200 and 300 kPa normal stresses. Using paper pulp in the modification of kaolinite increases the shear strength and the optimum water content of kaolinite simultaneously, and causes uniform distribution within kaolinite. KPP 1%-St samples have peak vertical displacements of -0.451 mm, -1.06 mm, - 3.023 mm with respect to 100,200 and 300 kPa normal stresses. All samples showed contraction behavior under normal stresses. The internal friction angle and the cohesion are 35.8˚ and 2.08 kPa respectively.

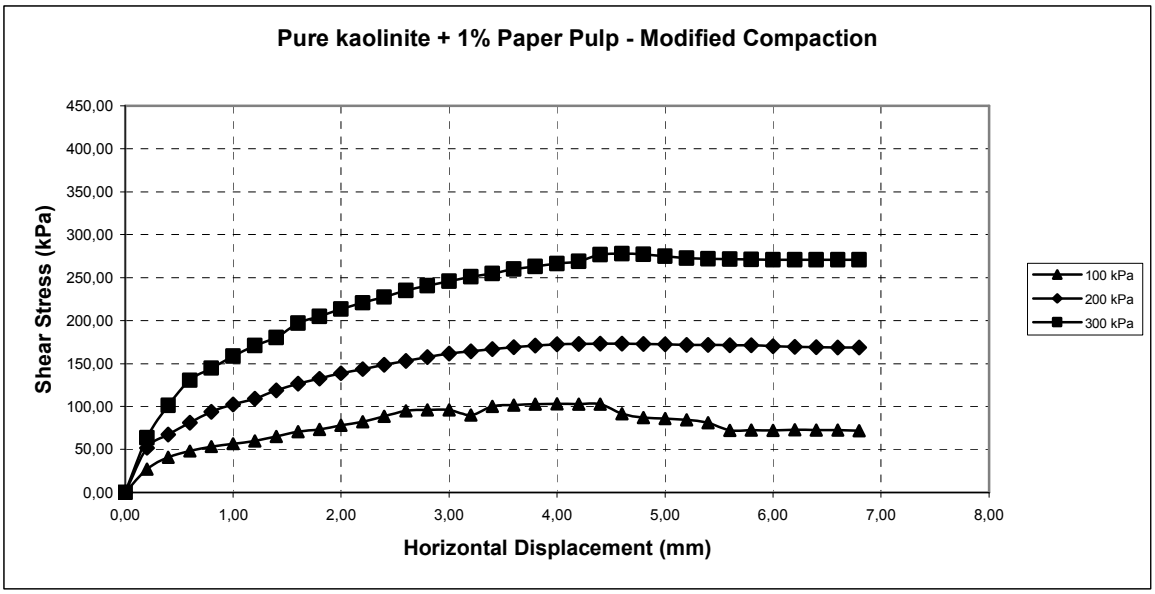

Figure 4.14. The shear stress-horizontal displacement curves of KPP 1%-Md group samples under 100 kPa, 200 kPa and 300 kPa normal stresses

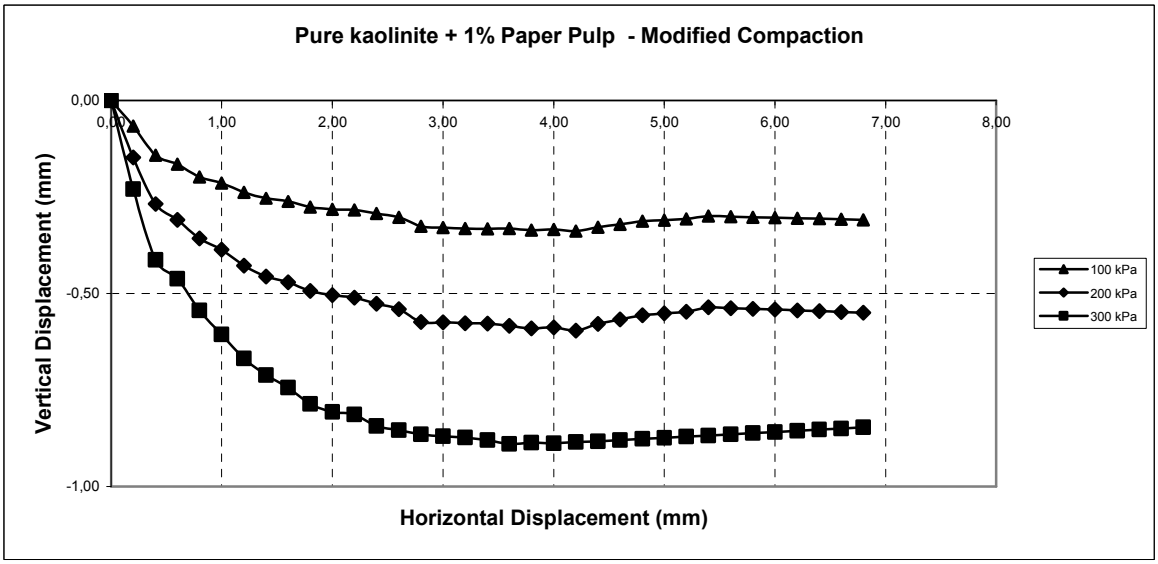

Figure 4.15. The vertical displacement - horizontal displacement curves of KPP 1%-Md group samples under 100 kPa, 200 kPa and 300 kPa normal stresses

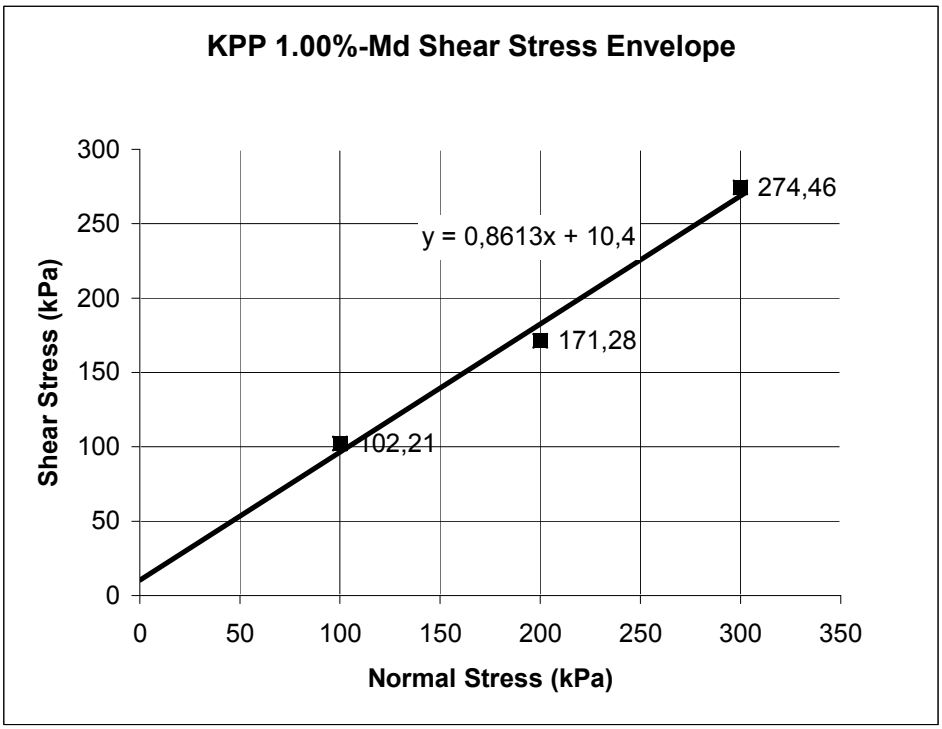

Figure 4.16. Shear stress envelope results of KPP 1%-Md group samples under 100 kPa, 200 kPa and 300 kPa normal stresses

KPP 1%-Md samples compacted at modified energy have peak stresses of 102.21, 171.28, 274.46 kPa respectively for 100, 200 and 300 kPa normal stresses. KPP 1%-Md samples compacted at modified energy have peak vertical displacements of -0.31 mm, -0.55 mm, -0.85 mm with respect to 100,200 and 300 kPa normal stresses. The internal friction and the cohesion are 40.8˚ and 10.4 kPa respectively. Cohesion increases from 2.08 to 10.4 with respect to KPP 1%-St samples. Compaction effort affected the cohesion value of paper pulp samples.

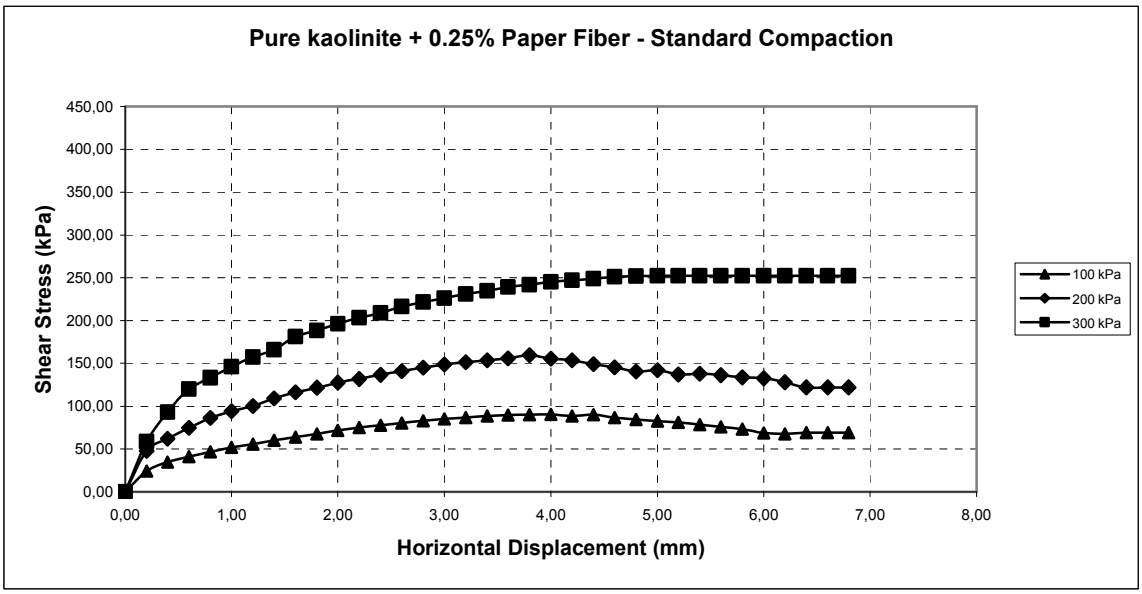

Figure 4.17. The shear stress-horizontal displacement curves of KPC 0.25 %-St group samples under 100 kPa, 200 kPa and 300 kPa normal stresses

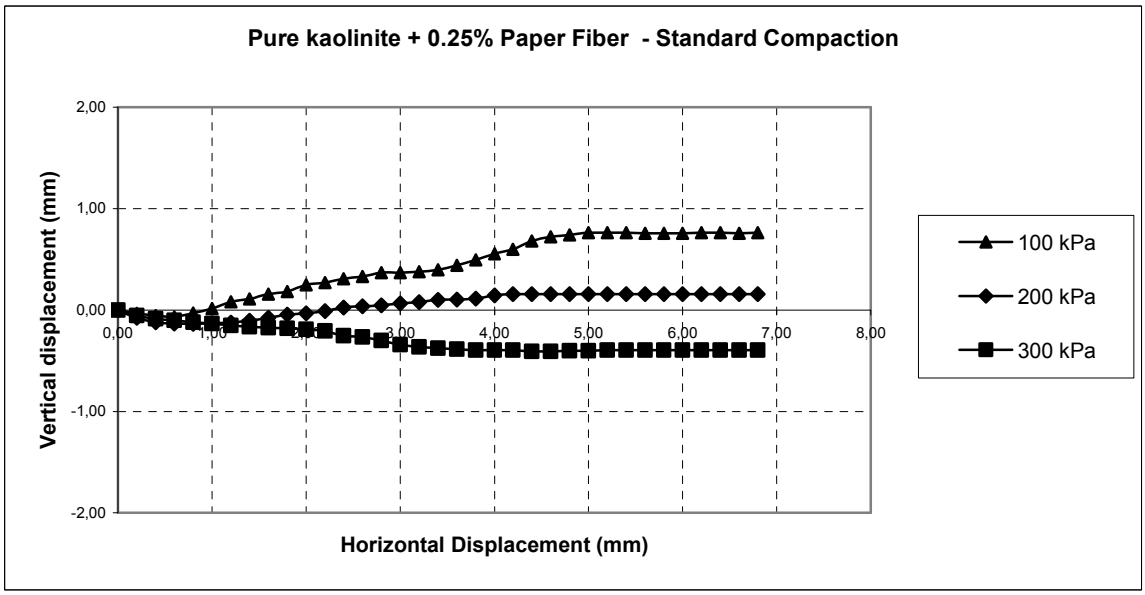

Figure 4.18. The vertical displacement - horizontal displacement curves of KPC 0.25 %-St group samples under 100 kPa, 200 kPa and 300 kPa normal stresses

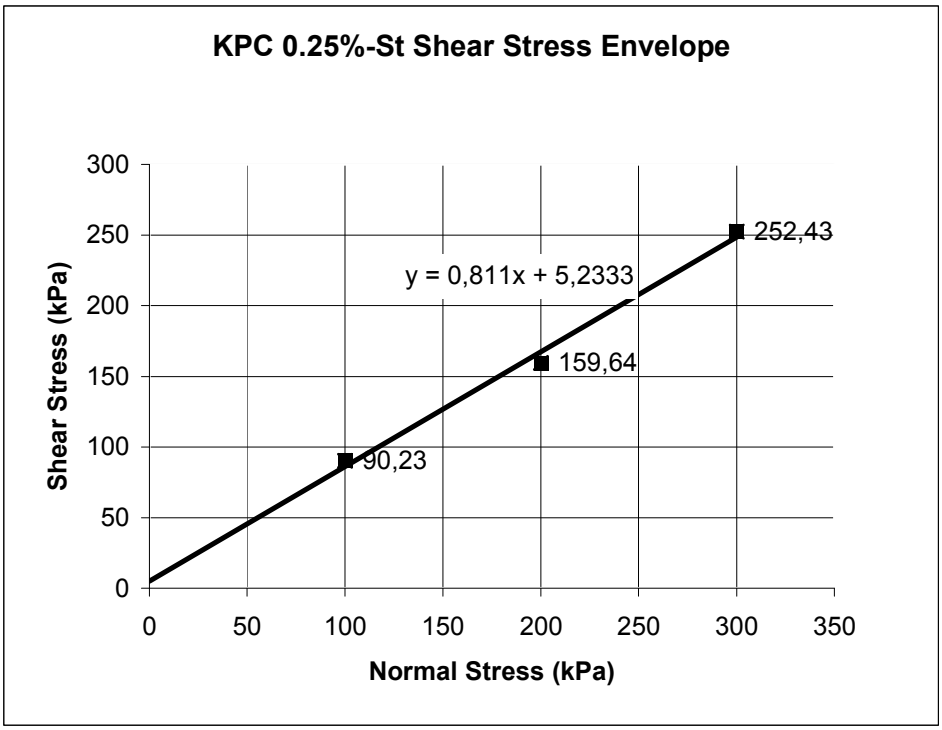

Figure 4.19. Shear stress envelope results of KPC 0.25 %-St group samples under 100 kPa, 200 kPa and 300 kPa normal stresses

Test results for KPC 0.25 %-St samples which were compacted at standard energy are shown in Figures 4.17-4.19. KPC 0.25 %-St samples have peak stresses of 90.23, 159.64, 252.43 kPa and have peak vertical displacements of 0.76 mm, 0.16 mm, -0.40 mm under 100 kPa, 200 kPa, 300 kPa normal stresses respectively. KPC 0.25 %-St samples in contrast to K-St and KPP-St samples showed dilation under 100 kPa, and 200 kPa. Under 300 kPa normal stresses, 0.25 % paper cut fiber inclusion ratio by weight increased the shear strength. The internal friction and the cohesion are 39.1˚ and 5.23 kPa respectively. Cohesion increased due to KPP samples, but in comparison to K-St samples cohesion decreased. Internal friction angle increased to 39.1˚ which is larger than both K-St and KPP-St value. Adding paper cut fibers decreased the cohesion like paper pulp did. At the beginning of the tests under 100 kPa, and 200 kPa, contraction occurred then dilation was observed.

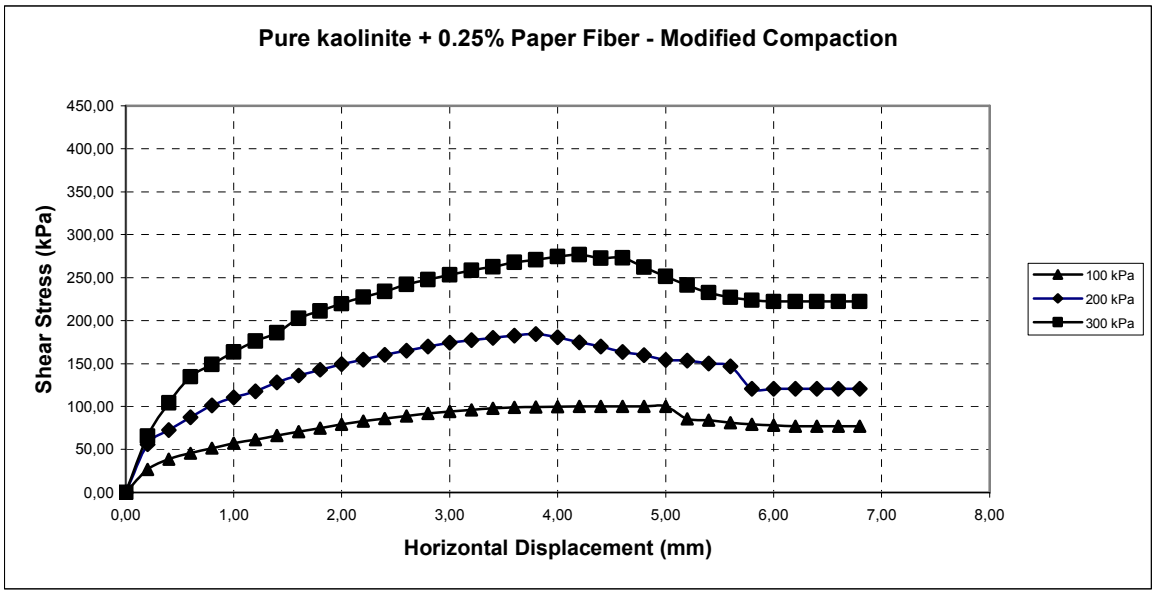

Figure 4.20. The shear stress-horizontal displacement curves of KPC 0.25 %-Md group samples under 100 kPa, 200 kPa and 300 kPa normal stresses

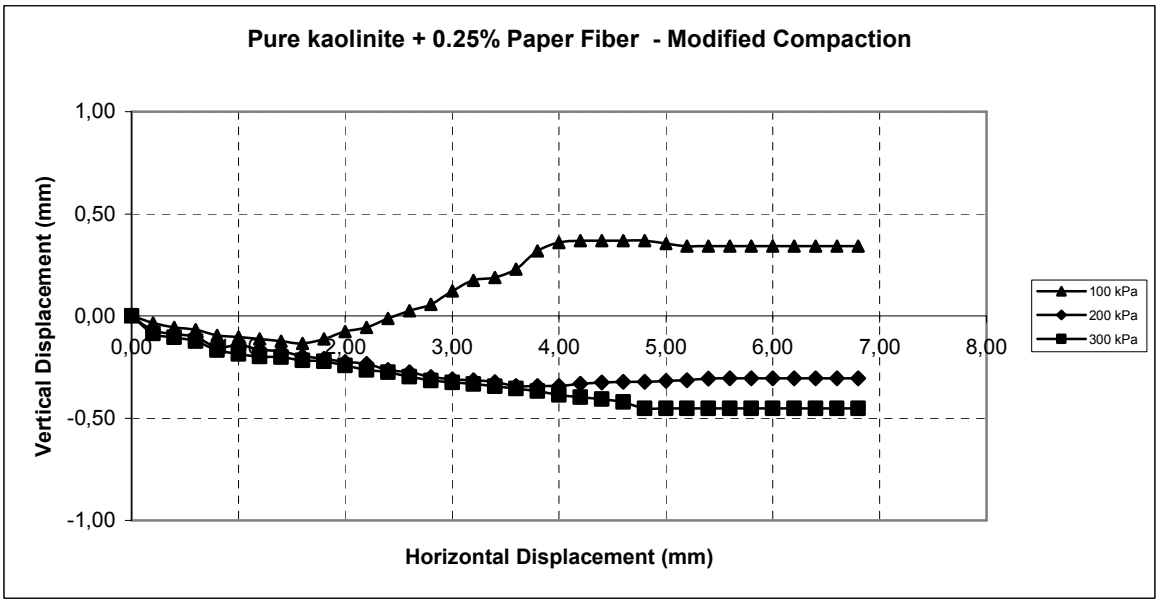

Figure 4.21. The vertical displacement - horizontal displacement curves of KPC 0.25 % - Md group samples under 100 kPa, 200 kPa and 300 kPa normal stresses

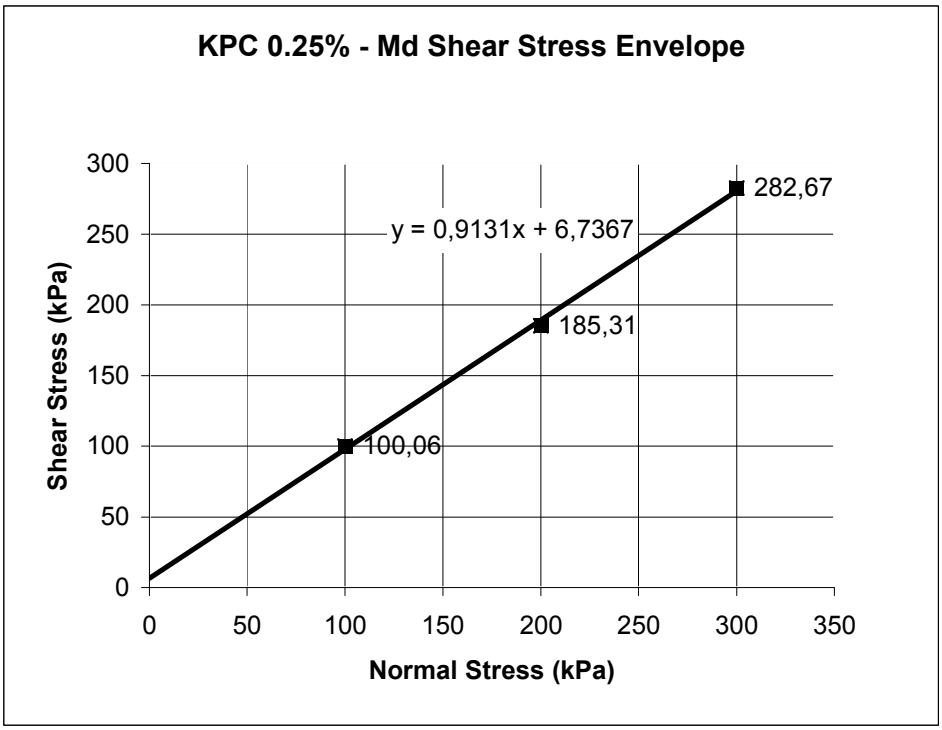

Figure 4.22. Shear stress envelope results of KPC - 0.25 %-Md group samples under 100 kPa, 200 kPa and 300 kPa normal stresses

Test results for KPC 0.25 % - Md samples which were compacted at modified energy are shown in Figures 4.20 - 4.22. KPC 0.25 % - Md samples have peak stresses of 100.60, 185.31, 282.67 and have peak vertical displacements of 0.34 mm, -0.31 mm, -0.453 mm under 100 kPa, 200 kPa, 300 kPa respectively. Only under 100 kPa normal forces, dilation was observed. KPC 0.25% - Md samples under 200 kPa and 300 kPa as the normal stress and compaction effort increased; contraction was observed. The internal friction and the cohesion are 42.4˚ and 6.74 kPa respectively.

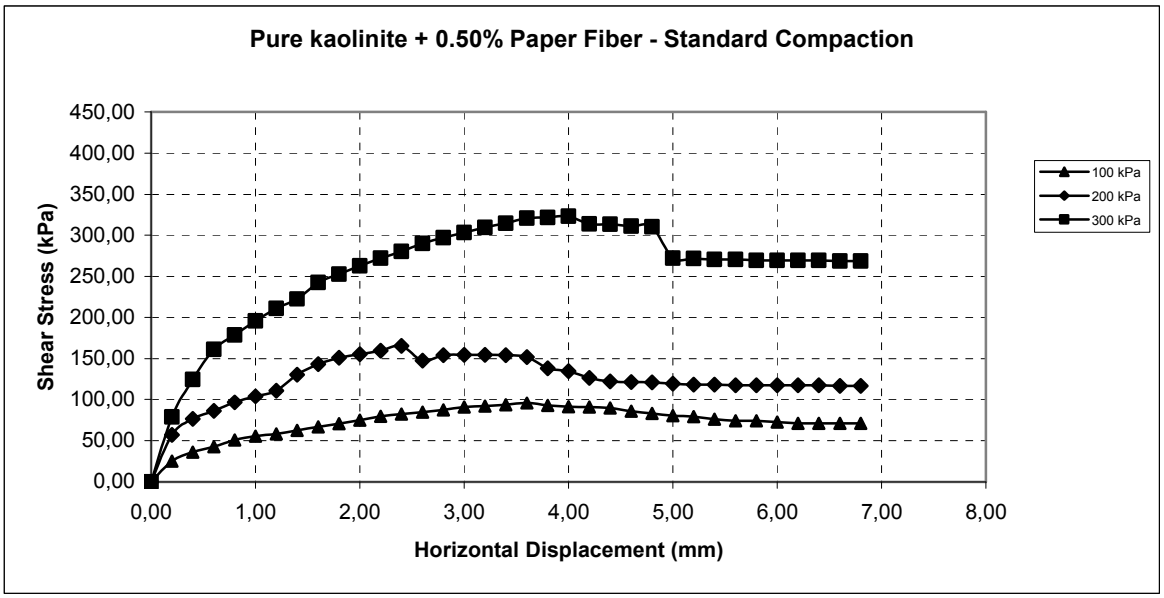

Figure 4.23. The shear stress - horizontal displacement curves of KPC 0.50 %-St group samples under 100 kPa, 200 kPa and 300 kPa normal stresses

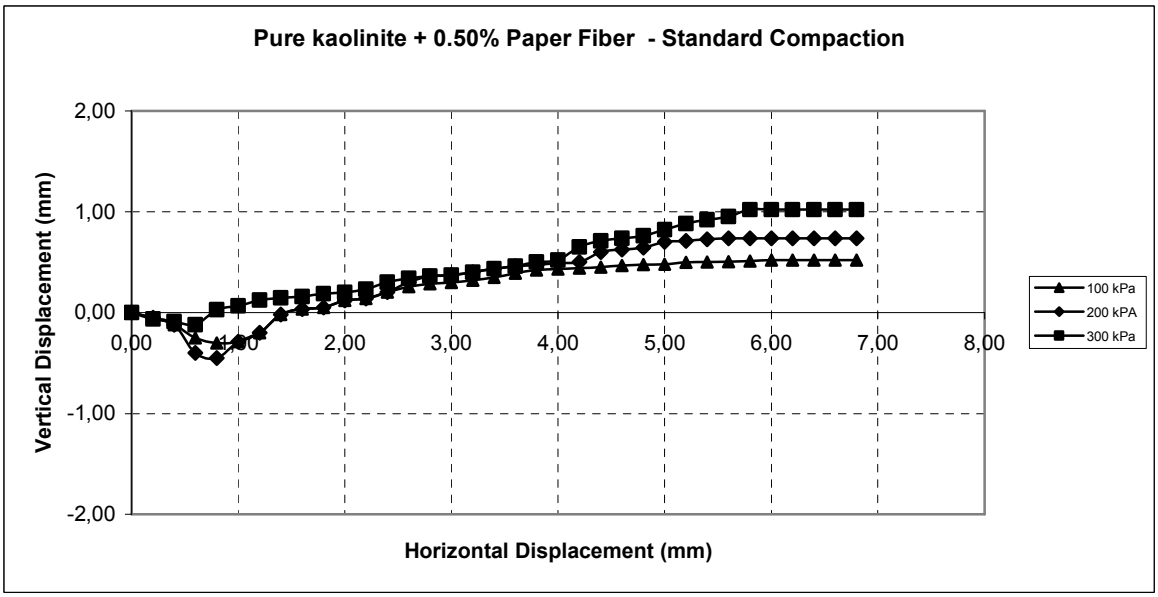

Figure 4.24. The vertical displacement - horizontal displacement curves of KPC 0.50 %-St group samples under 100 kPa, 200 kPa and 300 kPa normal stresses

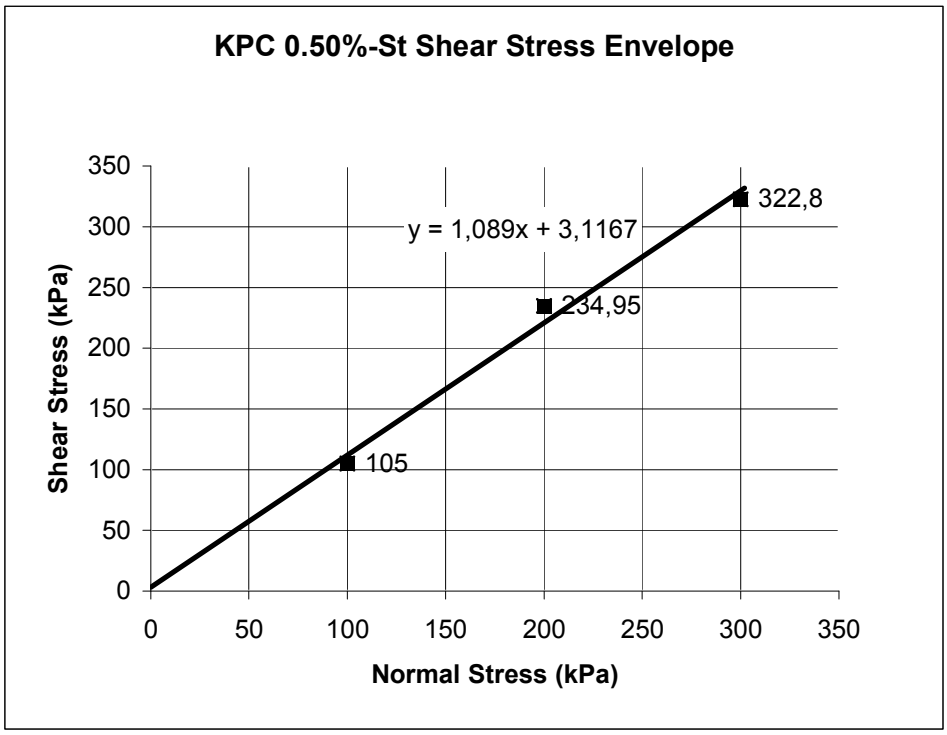

Figure 4.25. Shear stress envelope results of KPC 0.50 %-St samples under 100 kPa, 200 kPa and 300 kPa normal stresses

Test results for KPC 0.50 %-St samples which were compacted at standard energy are shown in Figures 4.23-4.25. KPC 0.50%-St samples have peak stresses of 105, 234.95, 322.80 kPa and have peak vertical displacements of 0.520 mm, 0.734 mm, 1.020 mm under 100 kPa, 200 kPa, 300 kPa normal stresses respectively. The internal friction and the cohesion are 50.70˚ and 3.12 kPa respectively. Distribution of paper cut fibers affected shear stress behavior, immediate loss of strength was observed. Under 100 kPa, 200 kPa, 300 kPa normal stresses; at first contraction observed, with rise in the shear strength dilation behavior continued till steady state.

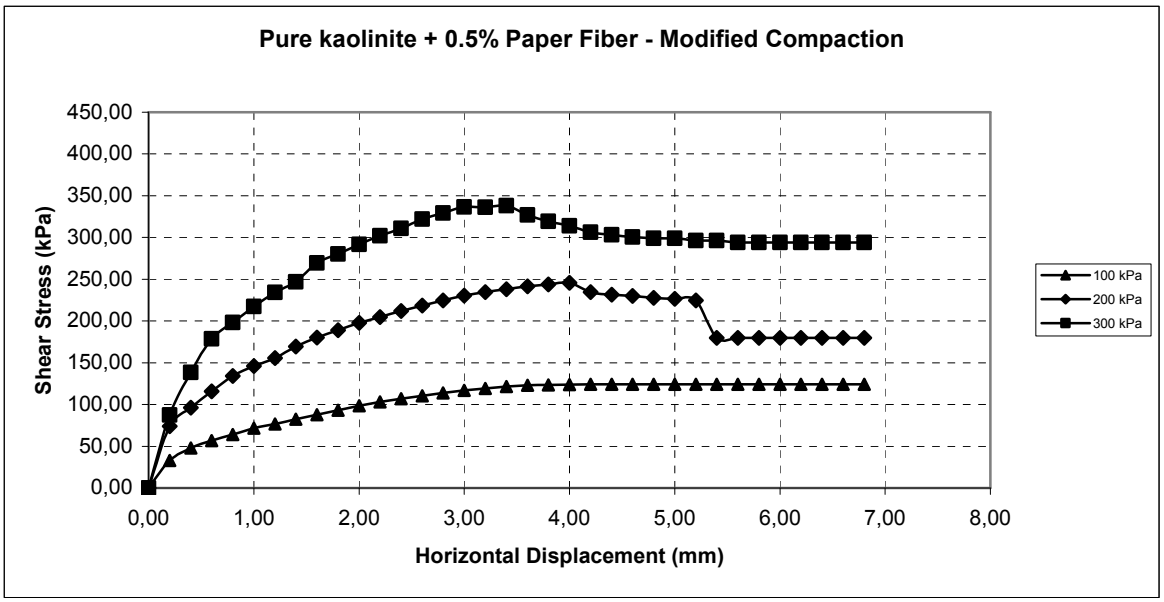

Figure 4.26. The shear stress-horizontal displacement curves of KPC - 0.50 %-Md group samples under 100 kPa, 200 kPa and 300 kPa normal stresses

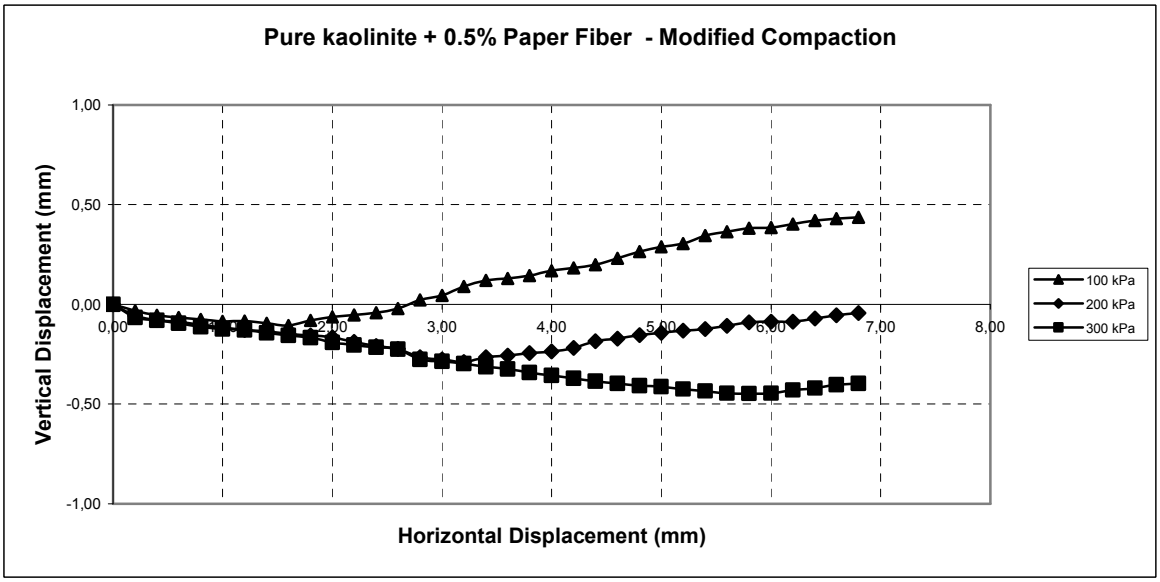

Figure 4.27. The vertical displacement – horizontal displacement curves of KPC - 0.50 %-Md samples under 100 kPa, 200 kPa and 300 kPa normal stresses

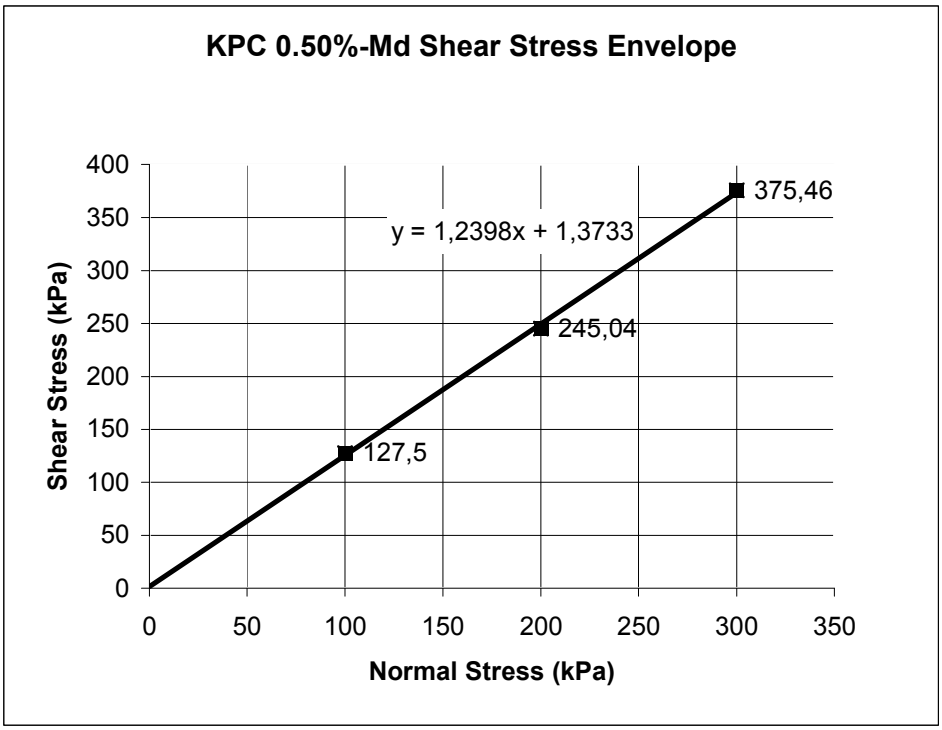

Figure 4.28. Shear stress envelope results of KPC - 0.50 %-Md group samples under 100 kPa, 200 kPa and 300 kPa normal stresses

Test results for KPC - 0.50 %-Md which were compacted at modified energy are shown in Figures 4.26-4.28. KPC - 0.50 %-Md samples compacted at modified energy have peak stresses of 127.50, 245.04, 375.46 kPa and have peak vertical displacements of 0.44 mm, -0.040 mm, -0.40 mm under 100 kPa, 200 kPa, 300 kPa normal stresses respectively. The internal friction and the cohesion are 51.50˚ and 2.08 kPa respectively. Both KPC 0.50%-St and KPC 0.50%-Md samples showed dilation behavior under normal stresses. Paper cut fiber addition 0.50% by weight under standard compaction effort caused contraction was observed, and then dilation was observed till 2.00 mm horizontal displacement. KPC 0.50%-St samples had contraction and dilation behavior although shear strength increased. Fiber distribution of samples affected the shear stress behavior. Under 300 kPa normal stresses, immediate loss of strength was observed.

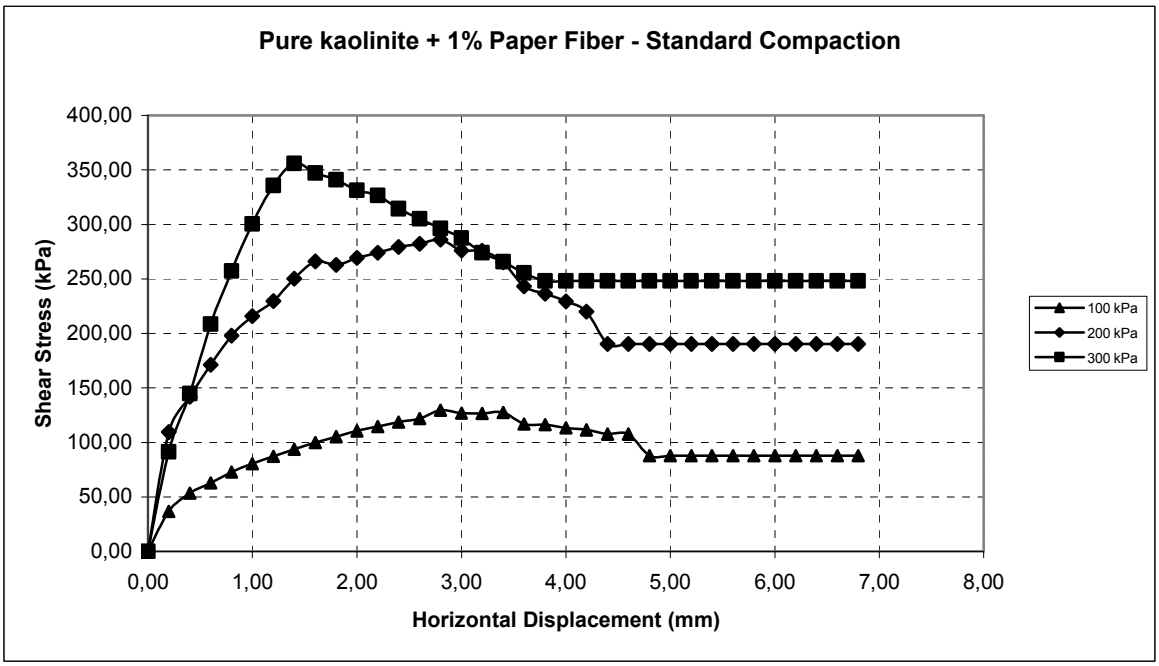

Figure 4.29. The shear stress-horizontal displacement curves of KPC - 1.00 %-St group samples under 100 kPa, 200 kPa and 300 kPa normal stresses

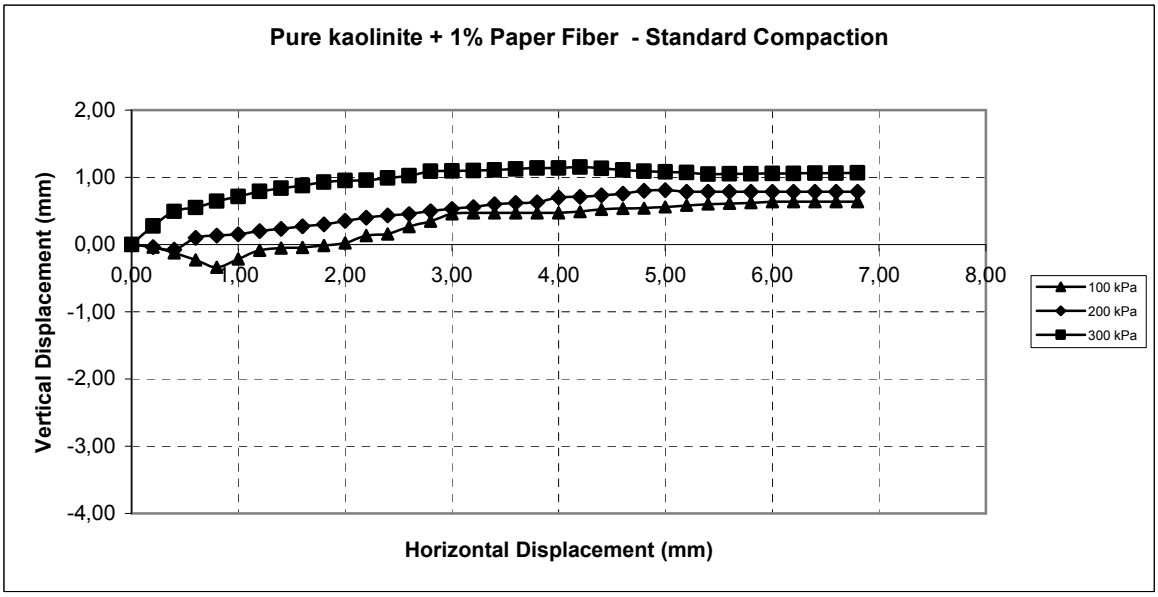

Figure 4.30. The vertical displacement - horizontal displacement curves of KPC - 1.00 %-St group samples under 100 kPa, 200 kPa and 300 kPa normal stresses

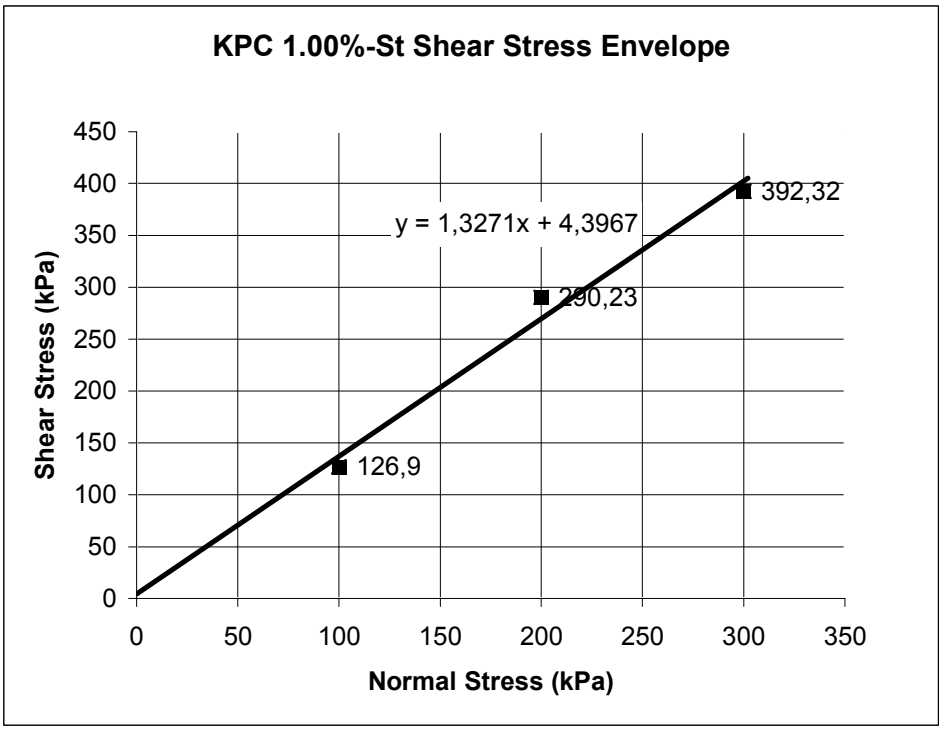

Figure 4.31. Shear stress envelope of KPC 1.00 %-St group samples under 100 kPa, 200 kPa and 300 kPa normal stresses

Test results for KPC - 1.00 %-St samples which were compacted at standard energy are shown in Figures 4.29-4.31. KPC - 1.00 %-St have peak stresses of 126.90, 290.23, 392.32 kPa and have peak vertical displacements of 0.640 mm, 0.790 mm, 1.067 mm under 100 kPa, 200 kPa, 300 kPa normal stresses respectively. The internal friction and the cohesion are 53˚ and 4.40 kPa respectively.

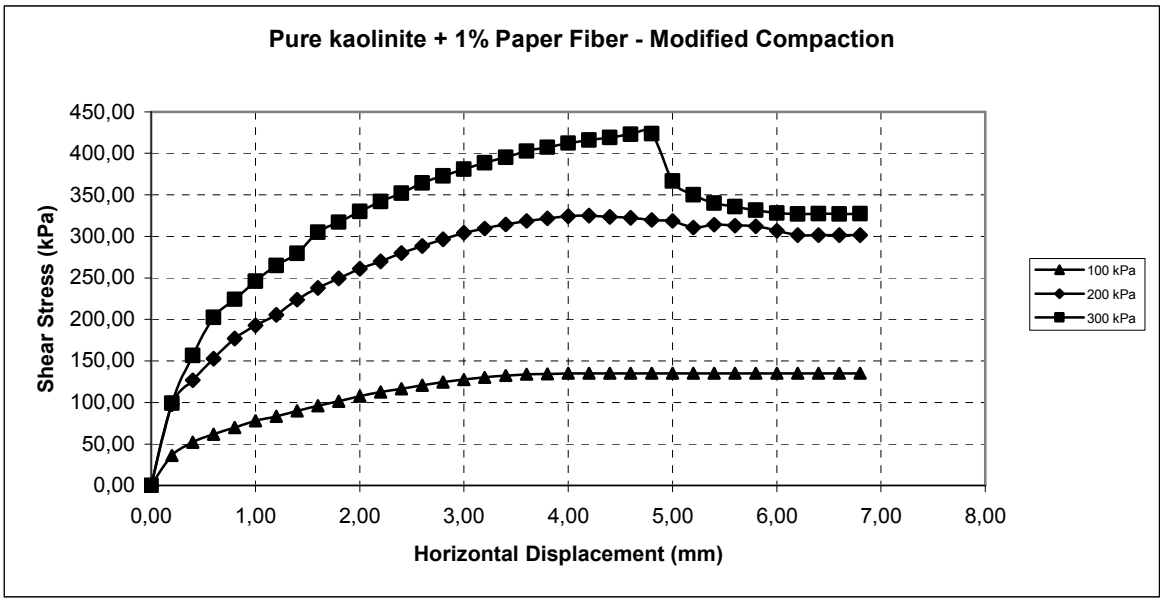

Figure 4.32. The shear stress-horizontal displacement curves of KPC 1.00 %-Md group samples under 100 kPa, 200 kPa and 300 kPa normal stresses

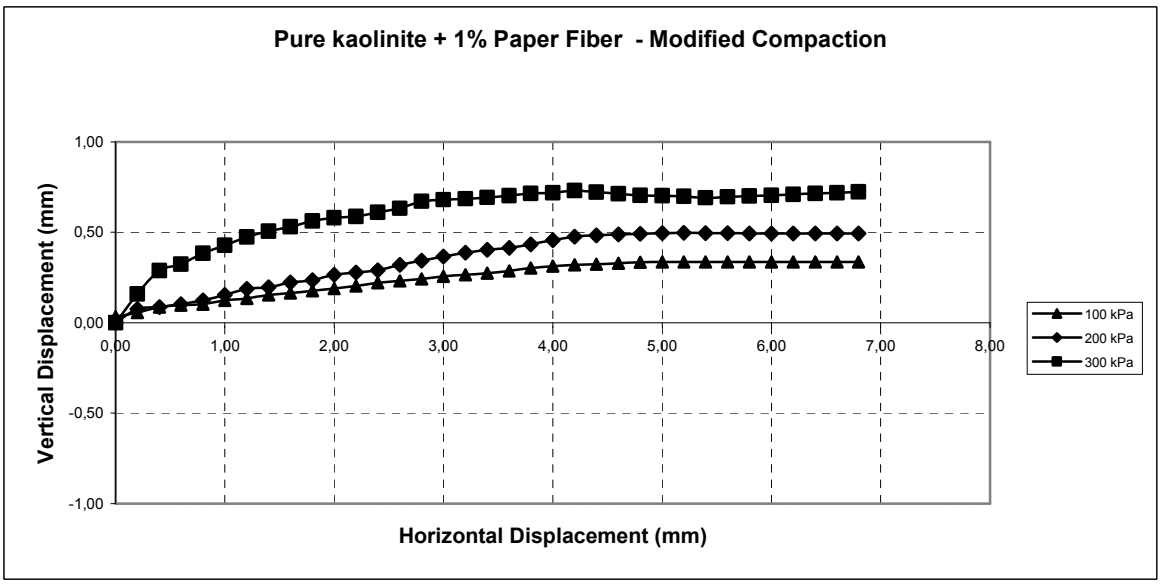

Figure 4.33. The vertical displacement - horizontal displacement curves of KPC - 1.00 %-Md group samples under 100 kPa, 200 kPa and 300 kPa normal stresses

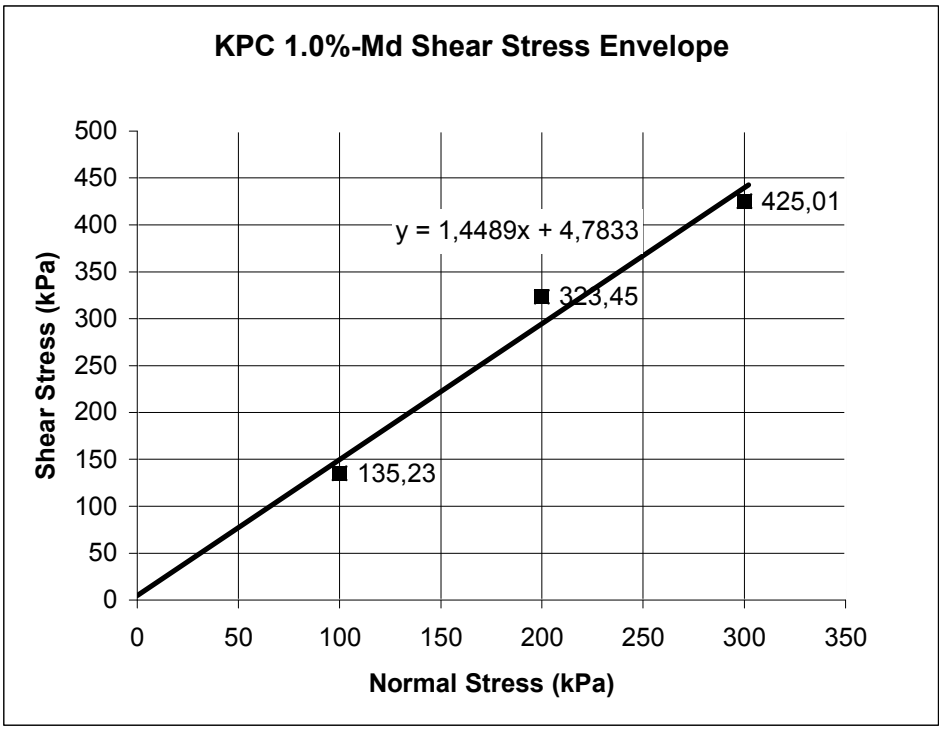

Figure 4.34. Shear stress envelope of KPC 1.00 %-Md group samples under 100 kPa, 200 kPa and 300 kPa normal stresses

The results for KPC - 1.00 %-Md which were compacted at modified energy are shown in Figures 4.32-4.34. KPC - 1.00 %-Md samples have peak stresses of 135.23, 323.45, 425.01 kPa and have peak vertical displacements of 0.335 mm, 0.493 mm, 0.724 mm under 100 kPa, 200 kPa, 300 kPa normal stresses respectively. The internal friction and the cohesion are 55.4˚ and 4.783 kPa respectively.

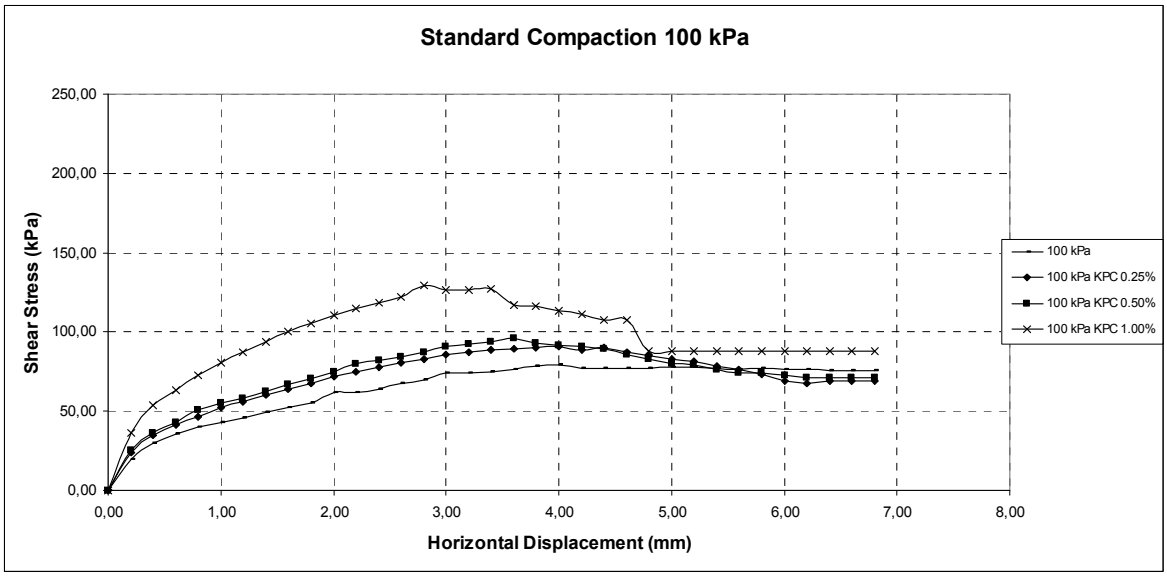

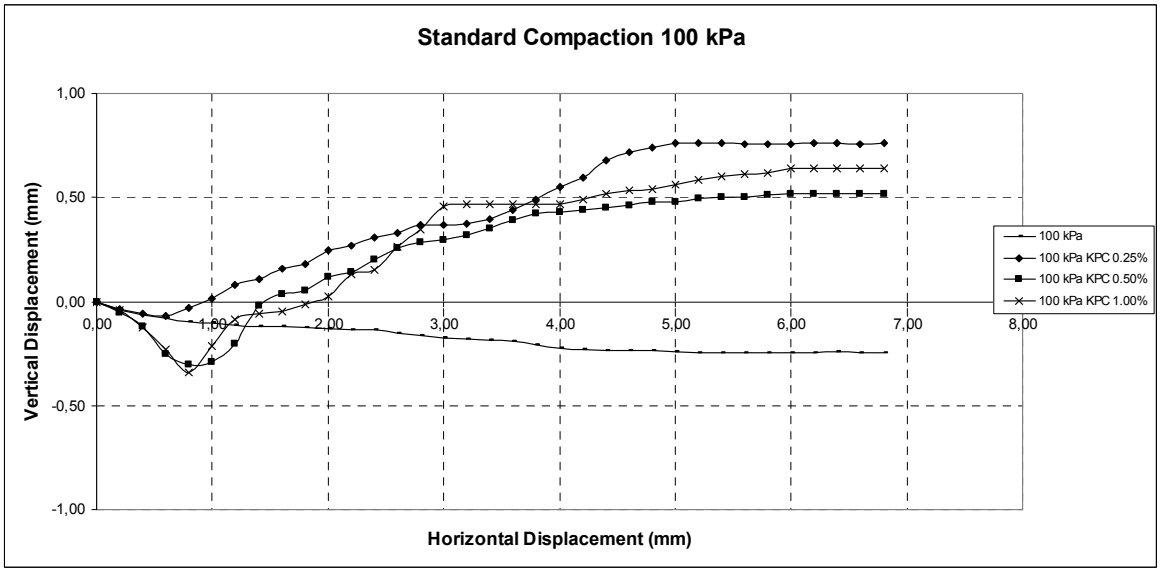

Figure 4.35. The direct shear test results of K, KPC 0.25%-St, KPC 0.50%-St, KPC 1.00 %-St group samples under 100 kPa normal stresses

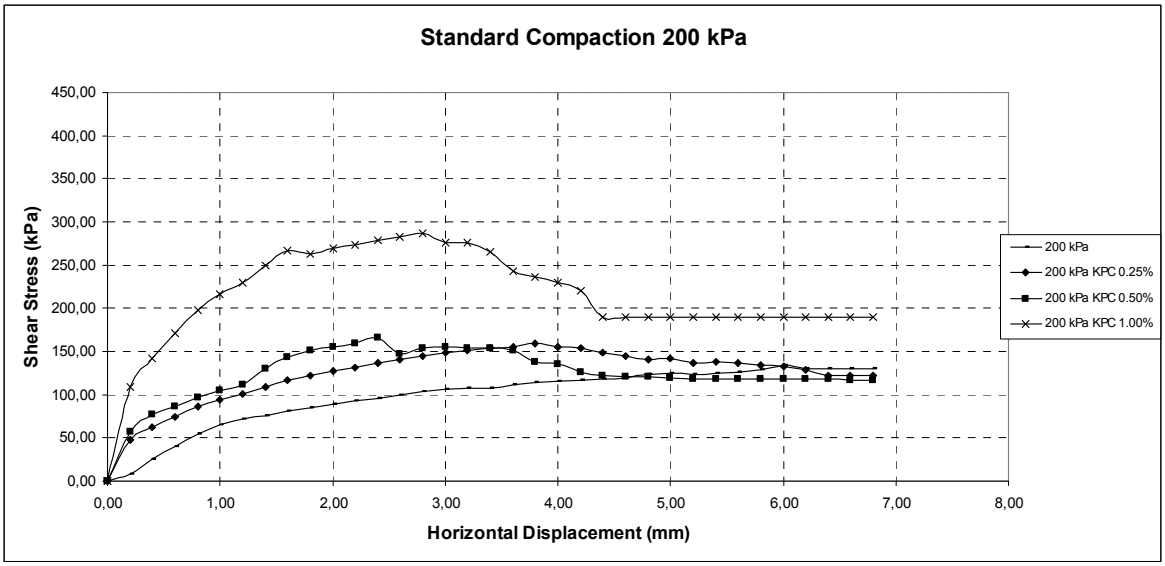

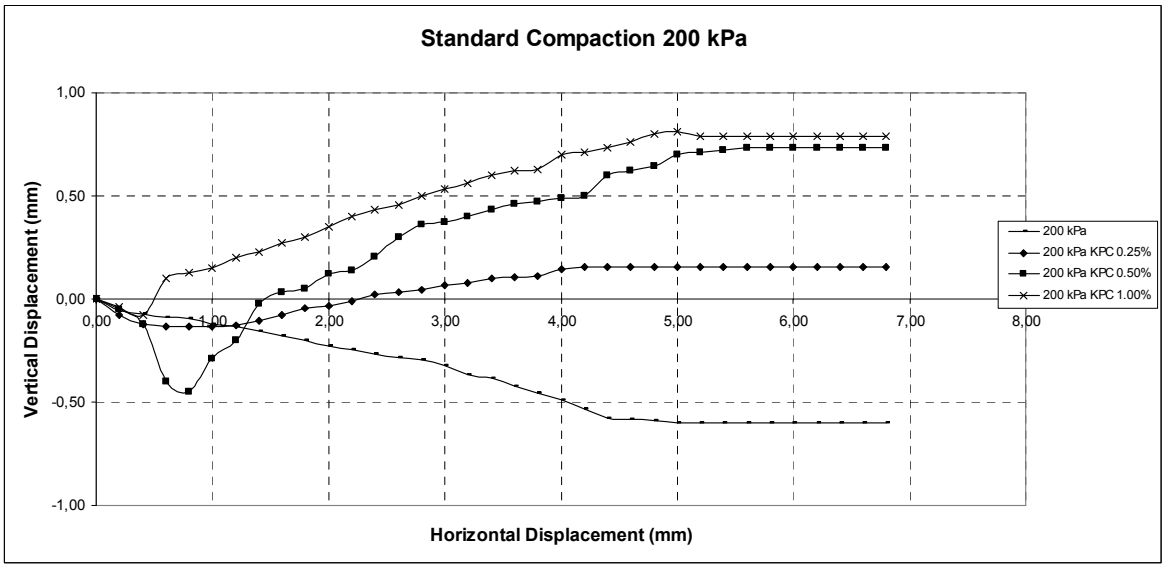

Figure 4.36. The direct shear test results of K, KPC 0.25%-St, KPC 0.50%-St, KPC 1.00 %-St group samples under 200 kPa normal stresses

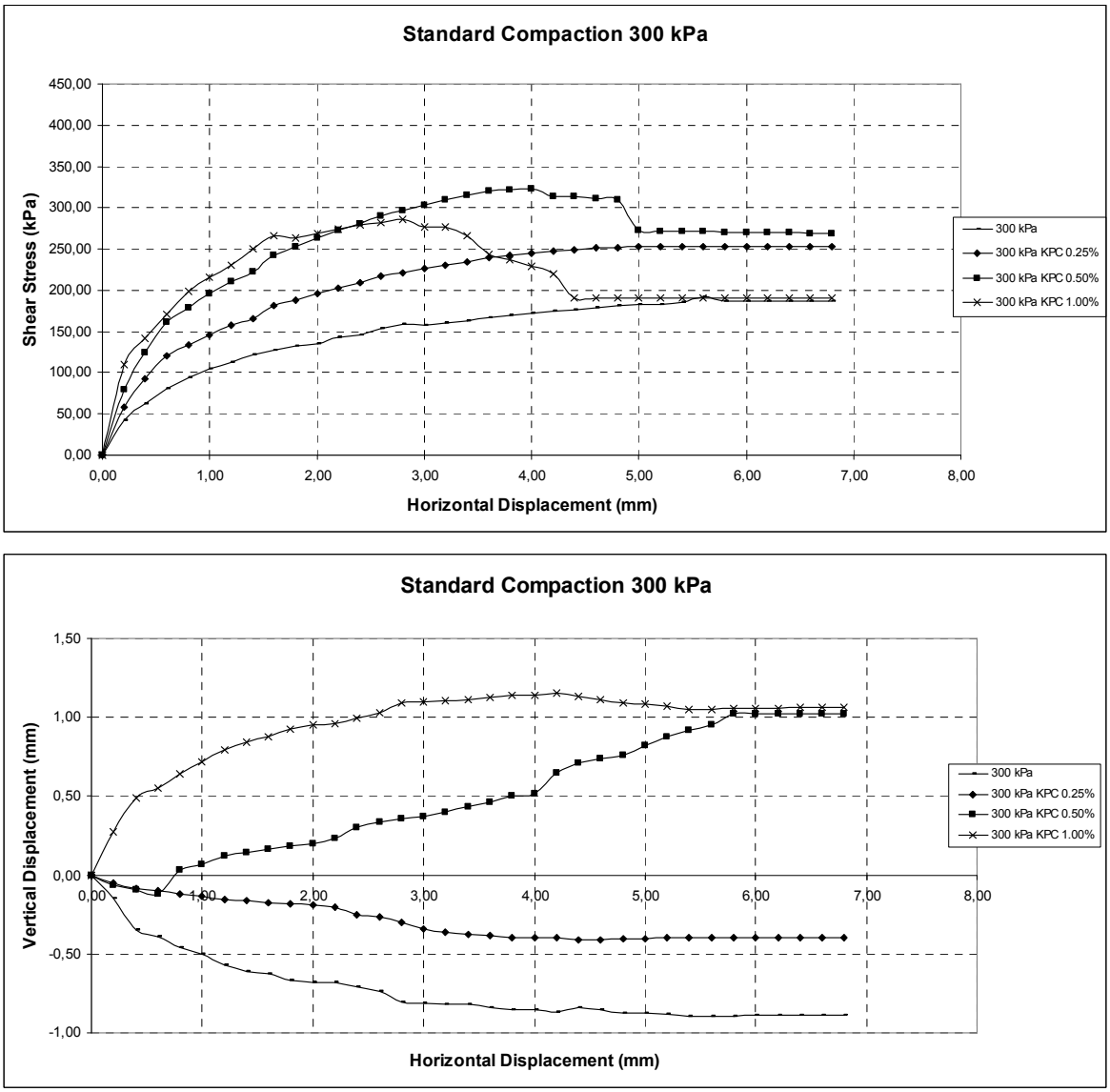

Figure 4.37. The direct shear test results of K, KPC 0.25%-St, KPC 0.50%-St, KPC 1.00 %-St group samples under 300 kPa normal stresses

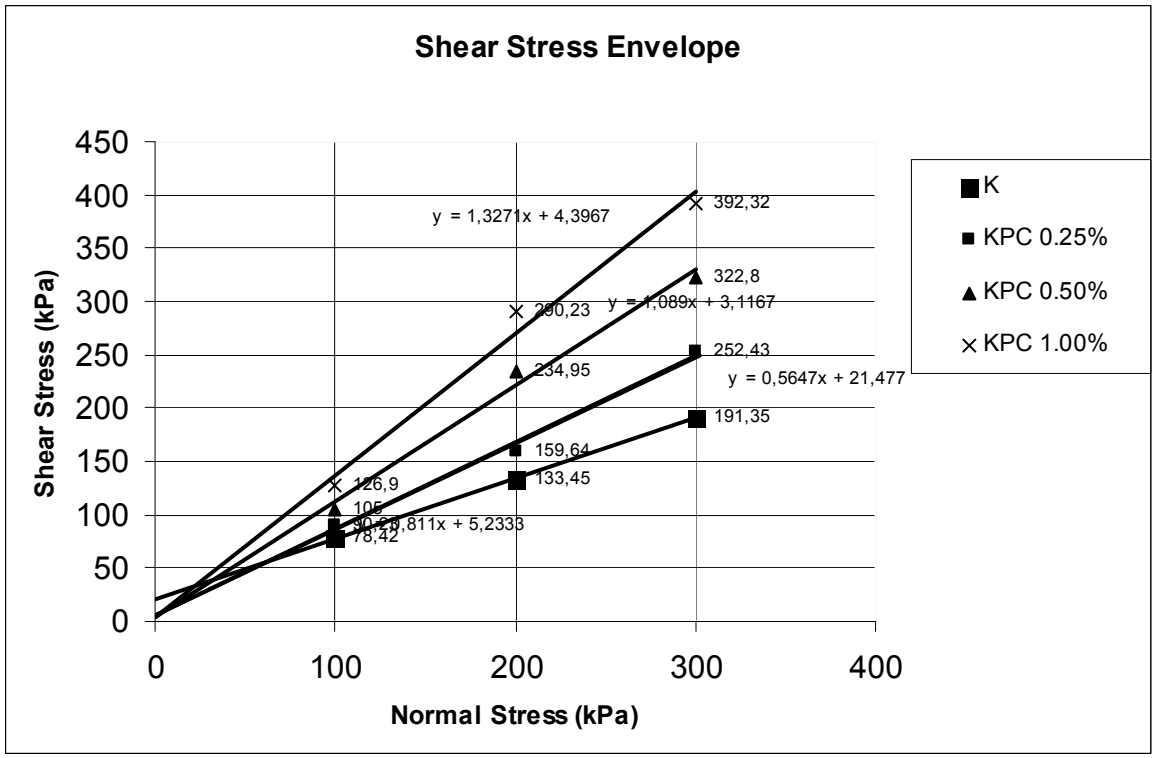

Figure 4.38. The shear stress envelope of K-St, KPC 0.25%-St, KPC 0.50%-St, KPC 1.00 %-St group samples

Between figures 4.35-4.38 direct shear test results, and graphs of K-St, KPC 0.25%-St, KPC 0.50%-St, KPC 1.00 %-St group samples under 100 kPa, 200 kPa, 300 kPa normal stresses are shown. Addition of paper cut fibers increased the shear strength of pure kaolinite. During direct shear experiments under different stresses, uniformity of paper cut fiber and kaolinite mixture affected the shear strength parameters. The inclusion ratio of paper cut fibers by weight changed the deformation behavior of the samples. The internal friction angle increased, and at the same time cohesion decreased with the addition of paper cut fibers. As paper inclusion ratio increased from 0.25% by weight to 1.00 % by weight, dilation behavior observed. Paper cut fibers decreased workability of kaolinite due to hardening the mixture. Although mixing procedures under great attention was applied during sample preparation, non-homogenous distribution of paper cut fibers affected contraction and dilation behavior of samples. Under 300 kPa sudden dilation behavior was observed in the KPC 1.00%-St samples. In general at the end of tests steady state was observed. KPC 1.00%-St samples had sudden loss of shear strength.

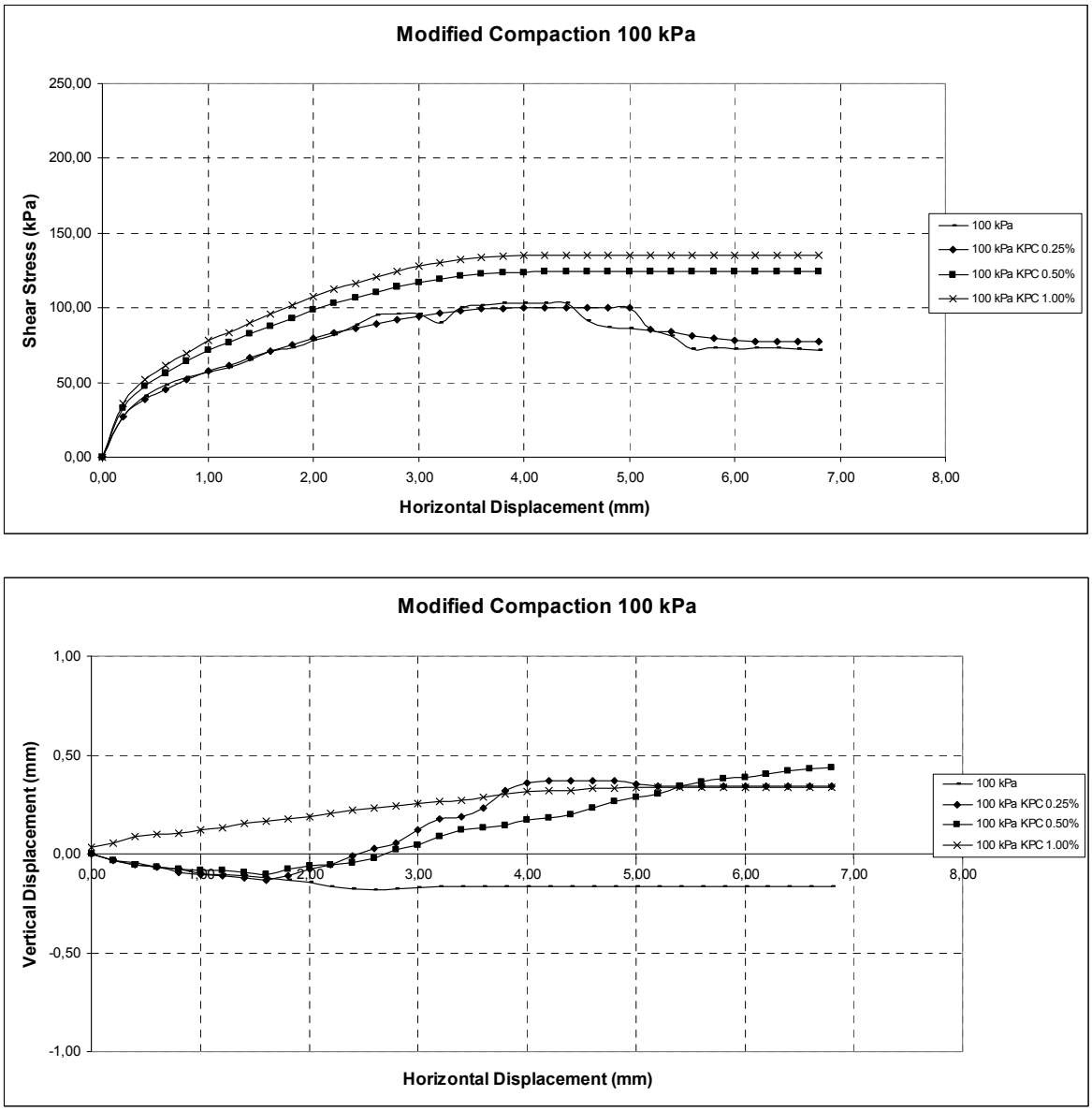

Figure 4.39. The direct shear test results of K-Md, KPC 0.25%-Md, KPC 0.50%-Md, KPC 1.00 %-Md group samples under 100 kPa normal stresses

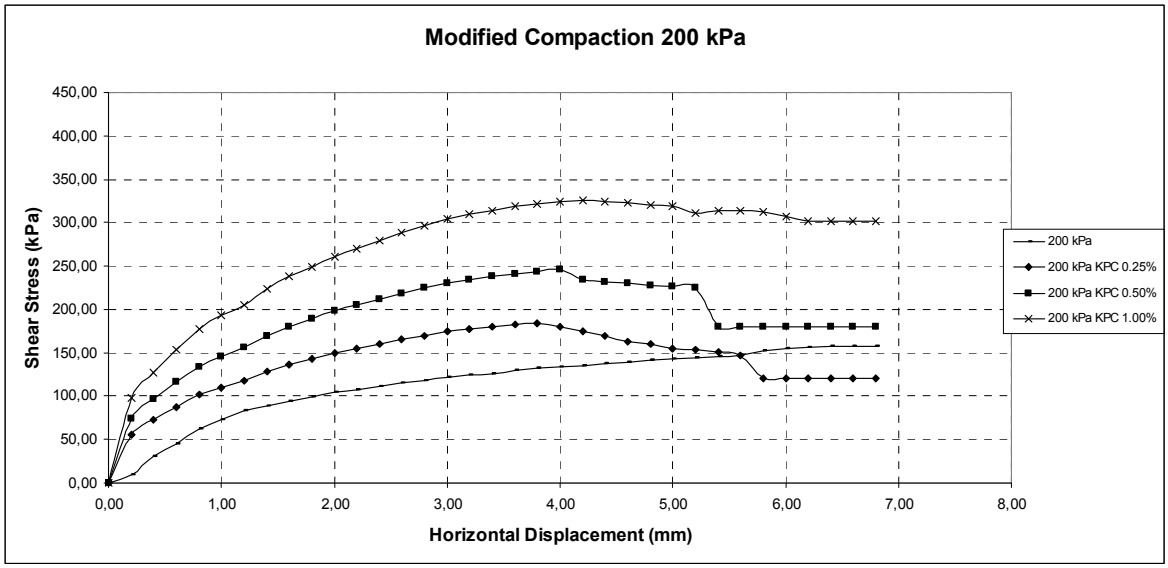

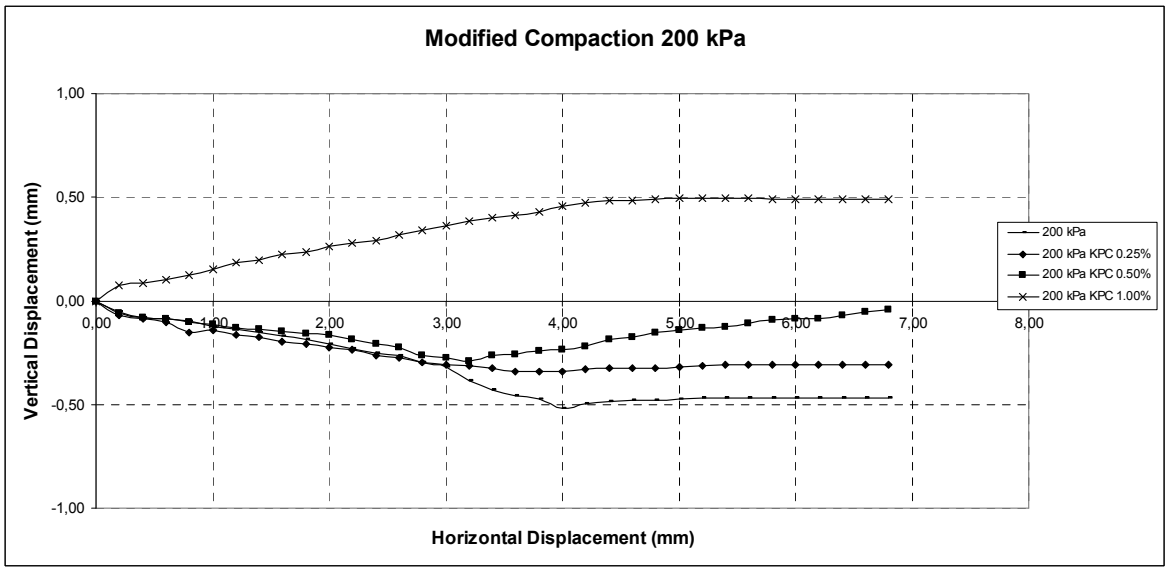

Figure 4.40. The direct shear test results of K-Md, KPC 0.25%-Md, KPC 0.50%-Md, KPC 1.00 %-Md group samples under 200 kPa normal stresses

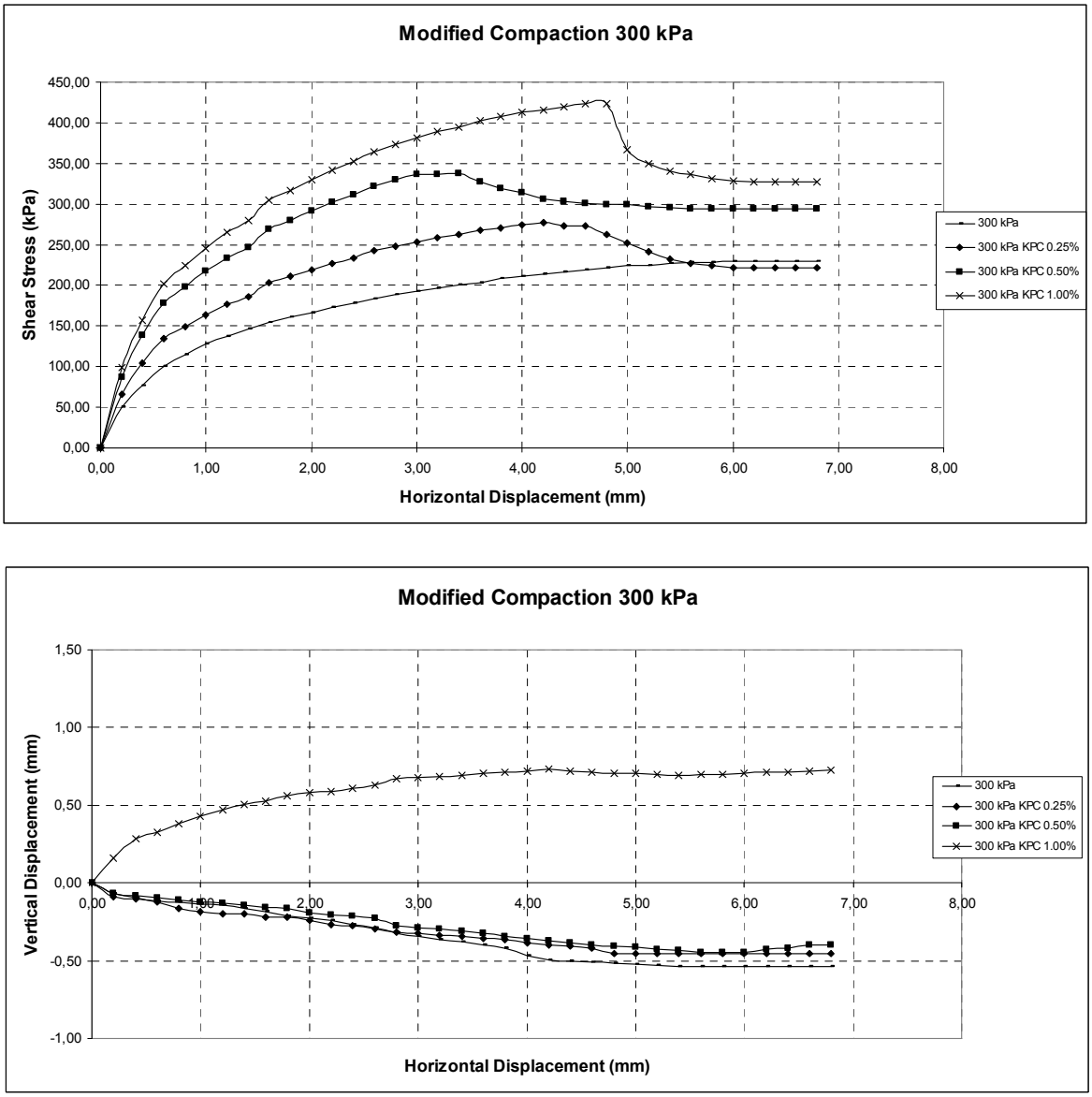

Figure 4.41. The direct shear test results of K-Md, KPC 0.25%-Md, KPC 0.50%-Md, KPC 1.00 %-Md group samples under 300 kPa normal stresses

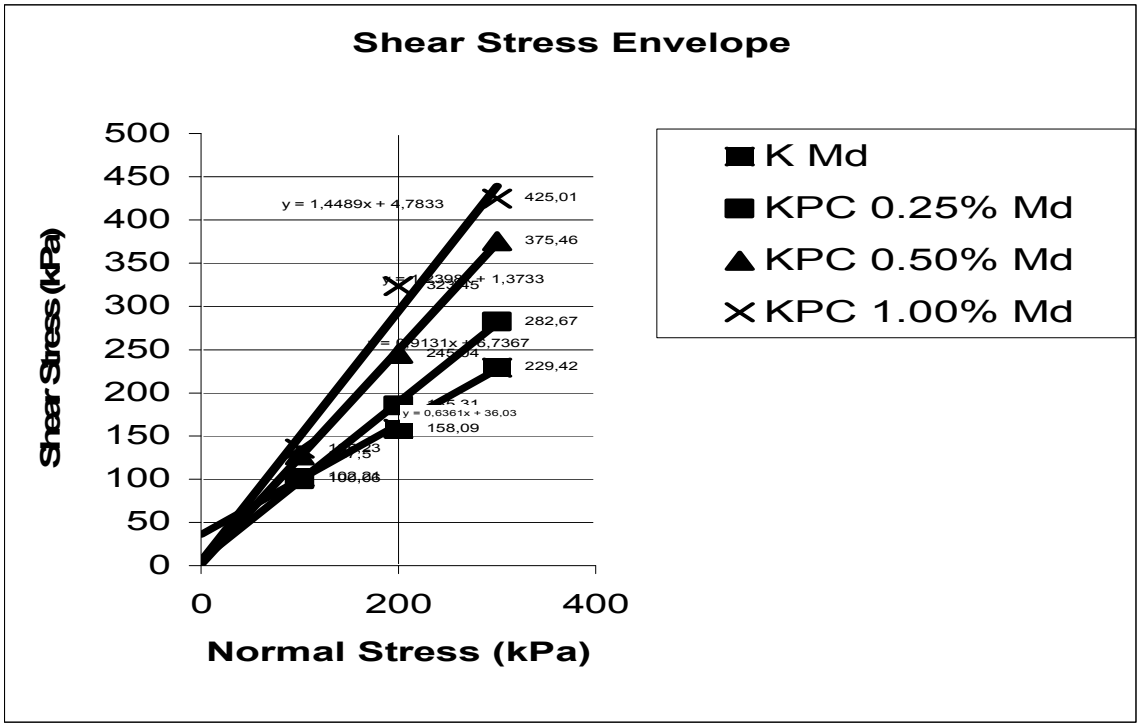

Figure 4.42. The shear stress envelope of K-Md, KPC 0.25%-Md, KPC 0.50%-Md, KPC 1.00 %-Md group samples under normal stress

Between Figures 4.39–4.42 direct shear test results, and graphs of K-Md, KPC 0.25%-Md, KPC 0.50%-Md, KPC 1.00 %-Md group samples under 100 kPa, 200 kPa, 300 kPa normal stresses are shown. In contrast to standard compaction effort, modified compaction effort affected deflection behavior of kaolinite reinforced with paper cut fiber. Under 200 kPa, and 300 kPa normal stresses, KPC-Md samples showed contraction behavior. Only KPC 1.00%-Md samples showed dilation. Under 300 kPa sudden loss of strength was observed. Addition of paper cut fiber increased shear stress.

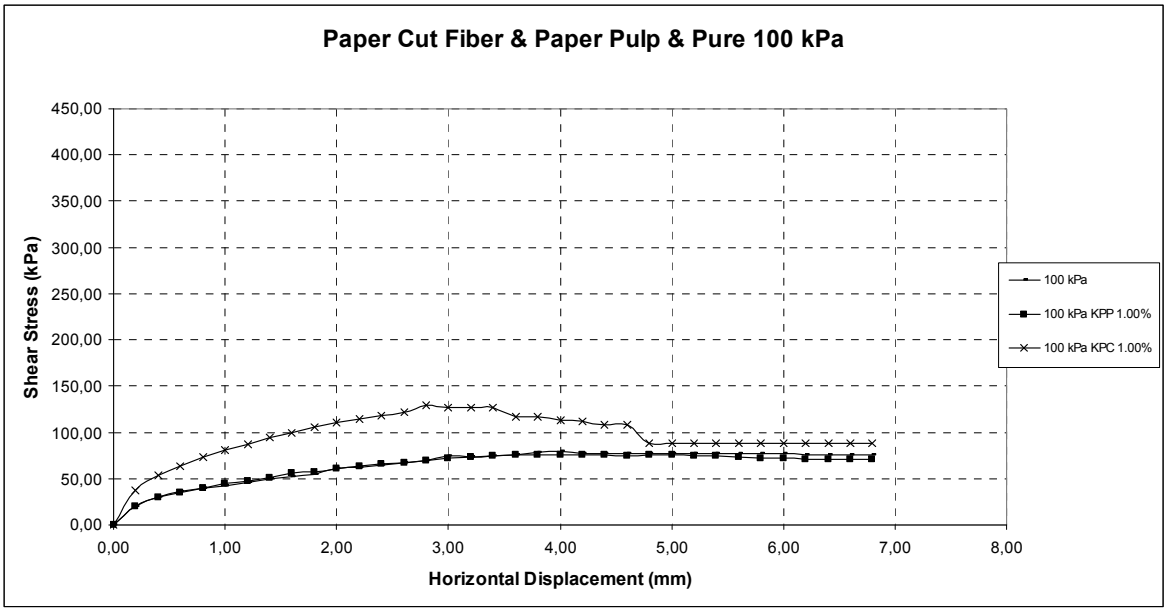

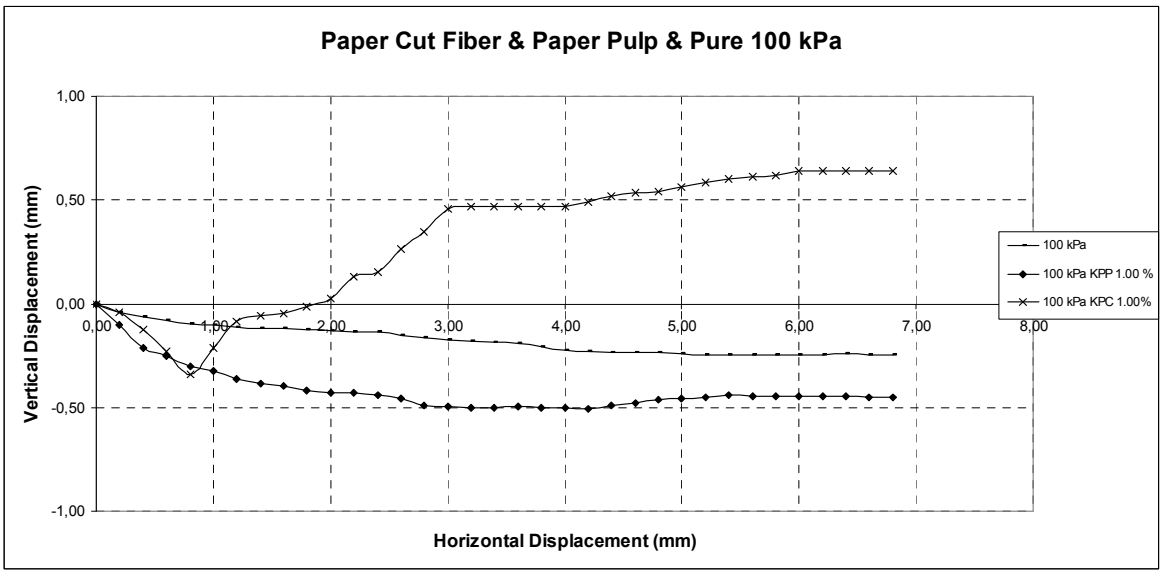

Figure 4.43. The direct shear test results of K-St, KPC 1.00%-St, KPP1.00%-St group samples under 100 kPa normal stresses

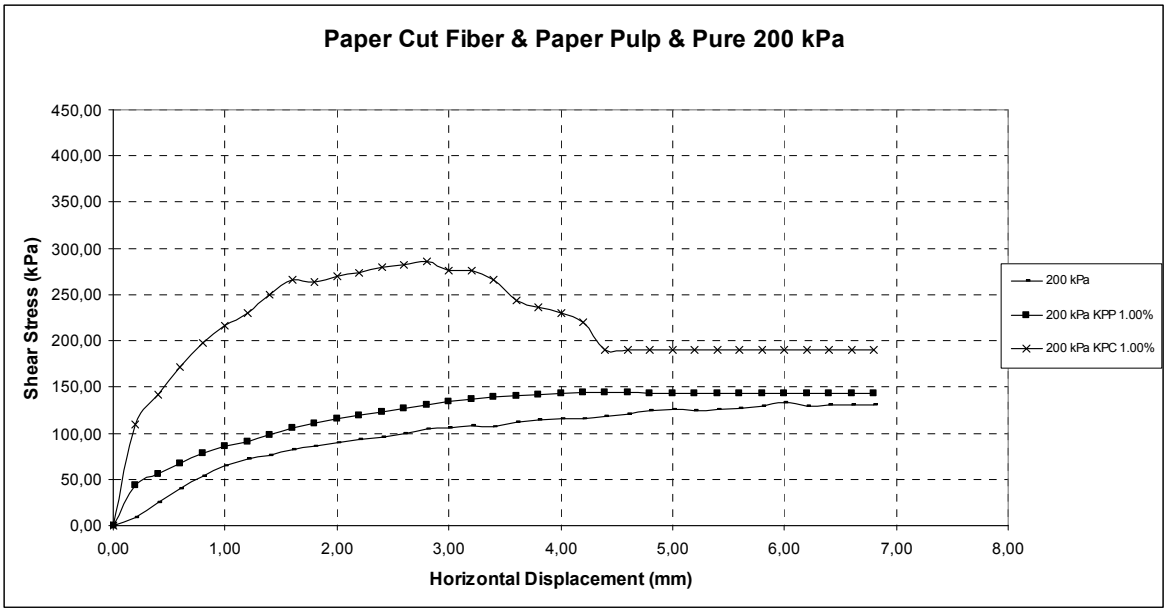

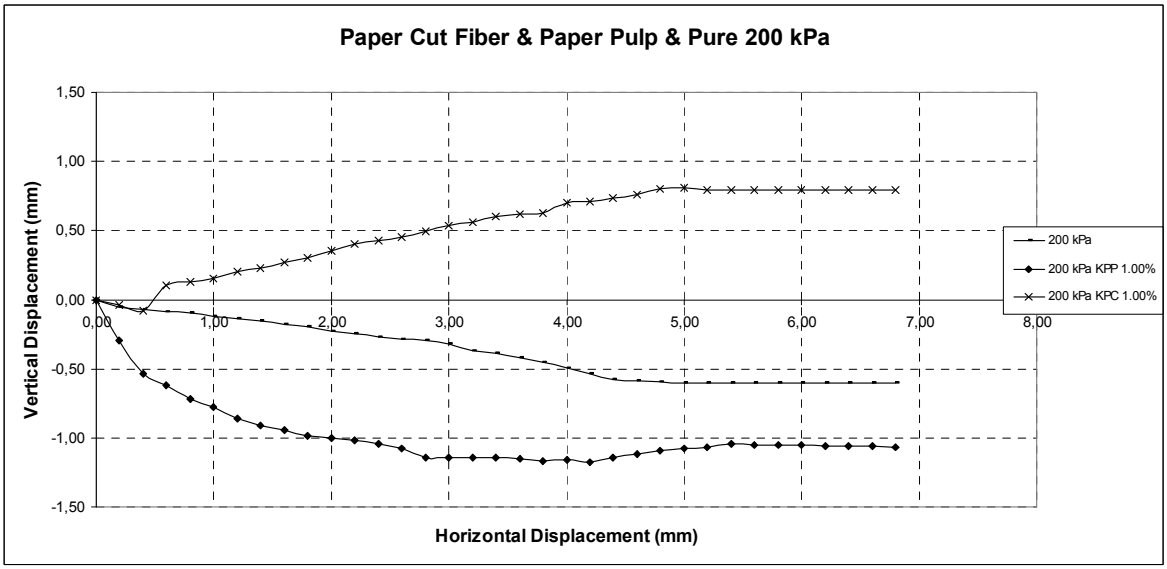

Figure 4.44. The direct shear test results of K-St, KPC 1.00%-St, KPP1.00%-St group samples under 200 kPa normal stresses

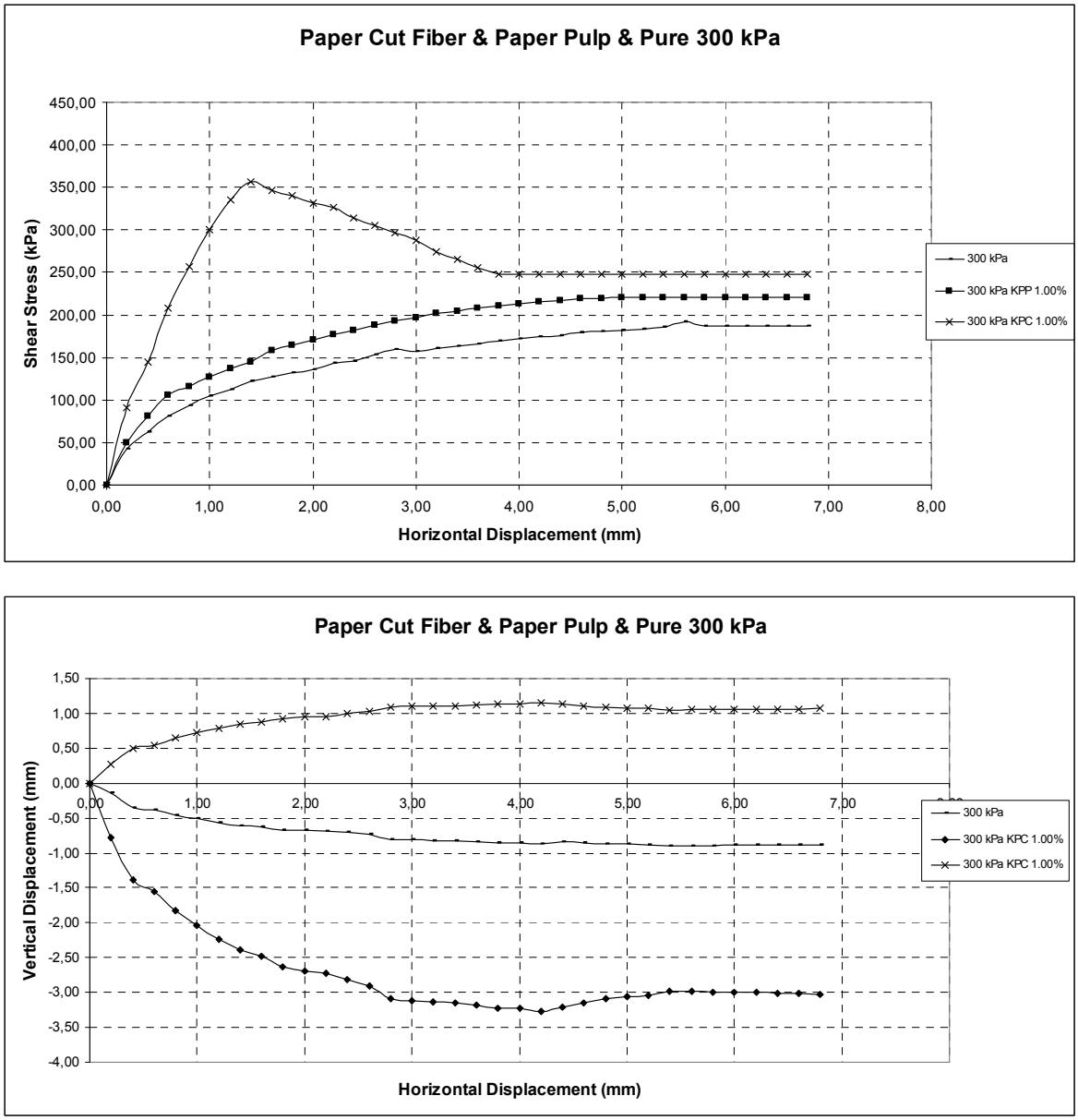

Figure 4.45. The direct shear test results of K-St, KPC 1.00%-St, KPP1.00%-St group samples under 300 kPa normal stresses

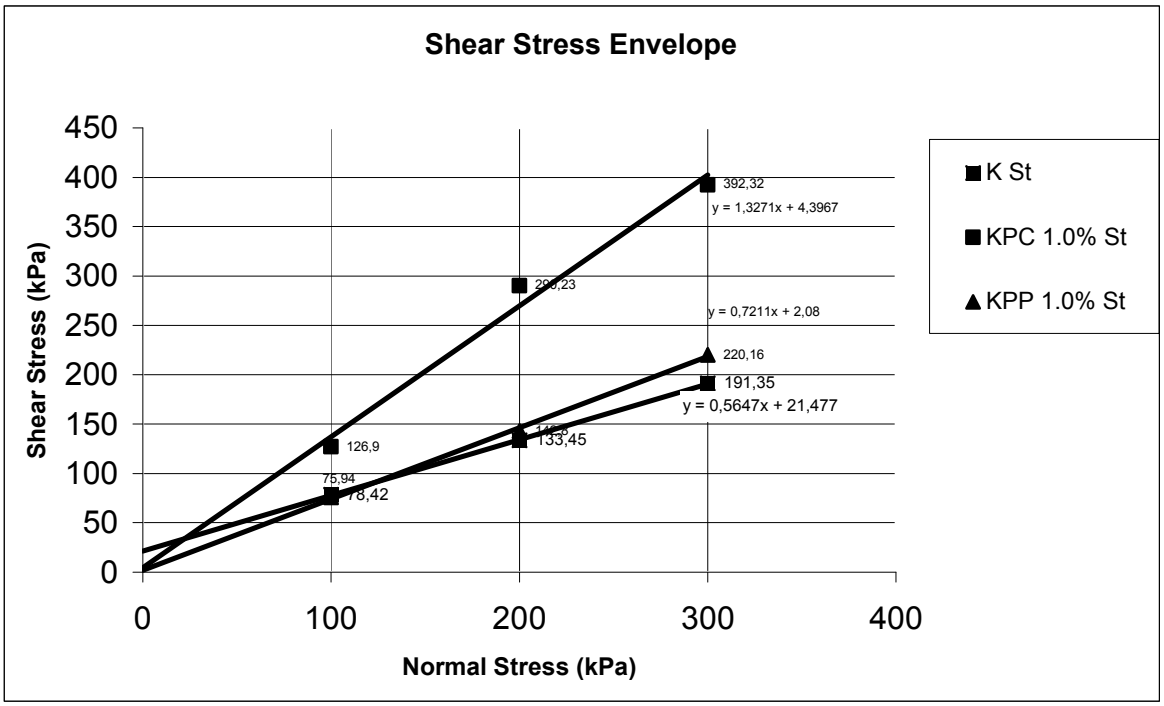

Figure 4.46. The shear stress envelope of K-St, KPC 1.00-St, KPP 1.00%-St group samples under normal stress

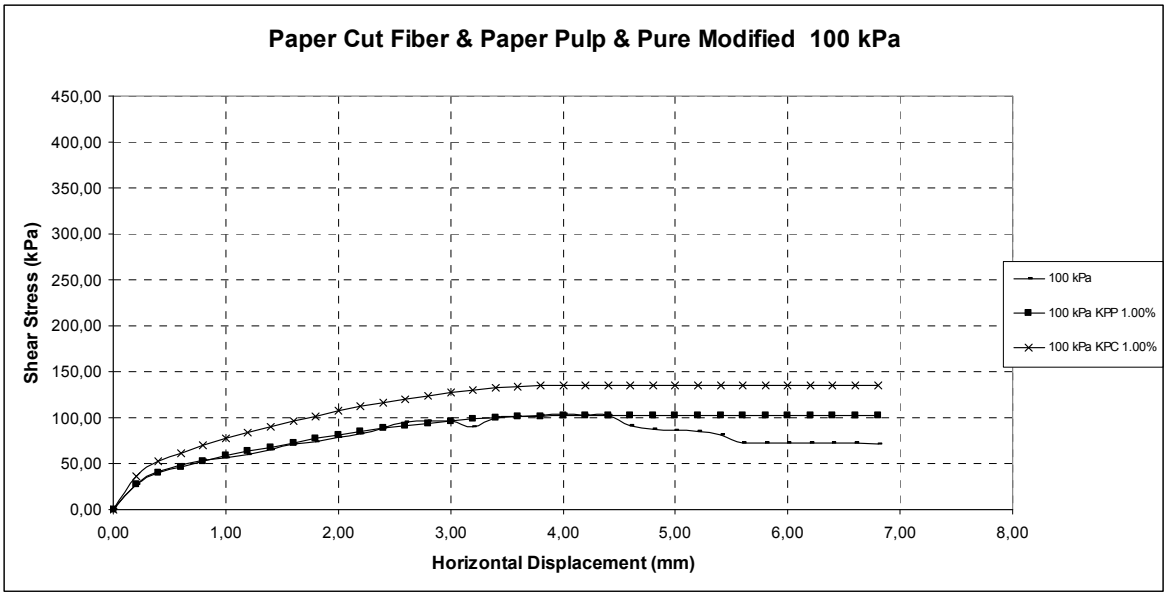

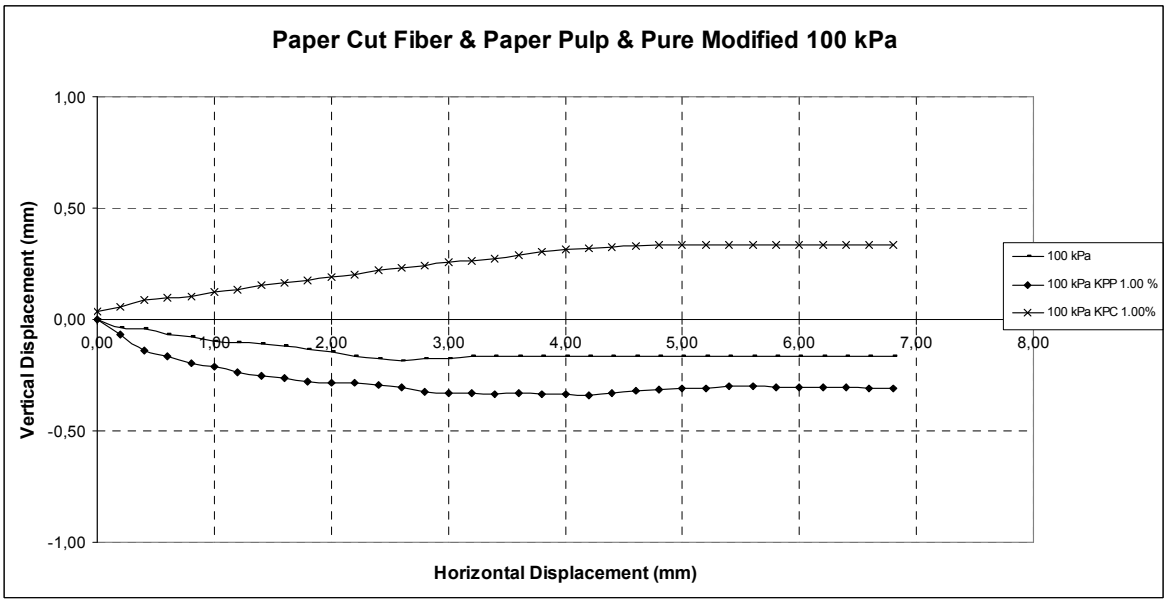

Figure 4.47. The direct shear test results of K-Md, KPC 1.00%-Md, KPP1.00%-Md group samples under 100 kPa normal stresses

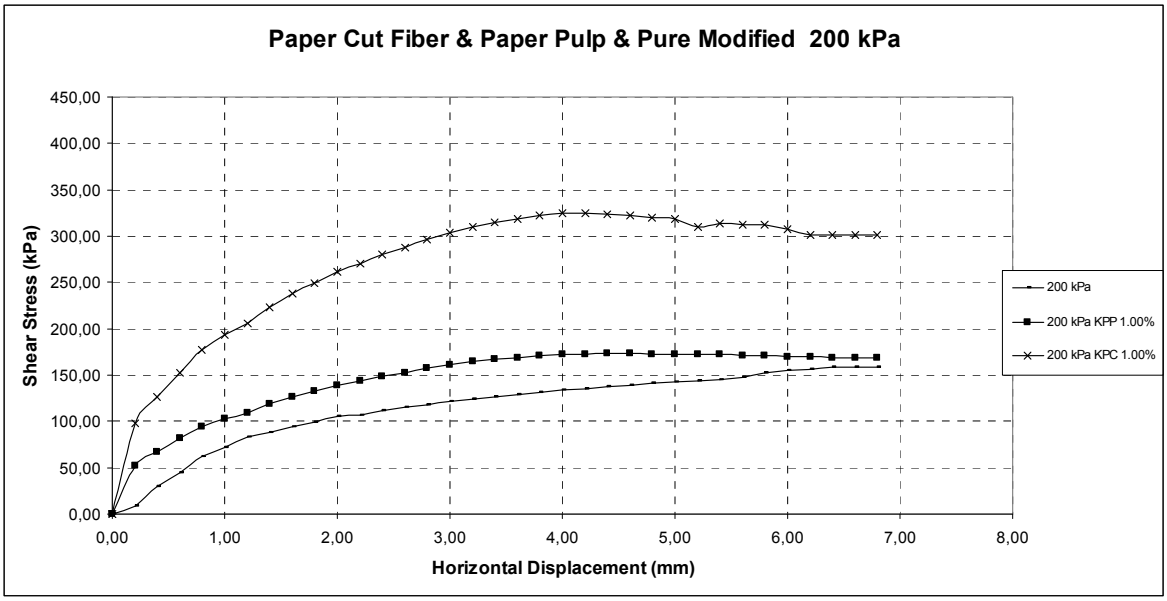

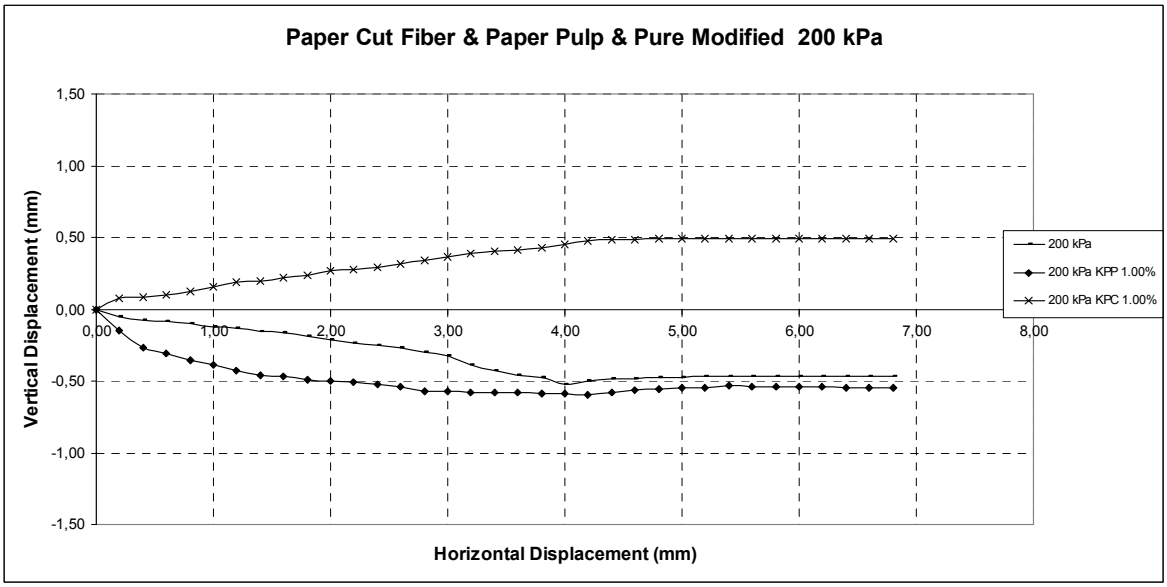

Figure 4.48. The direct shear test results of K-Md, KPC 1.00%-Md, KPP1.00%-Md group samples under 200 kPa normal stresses

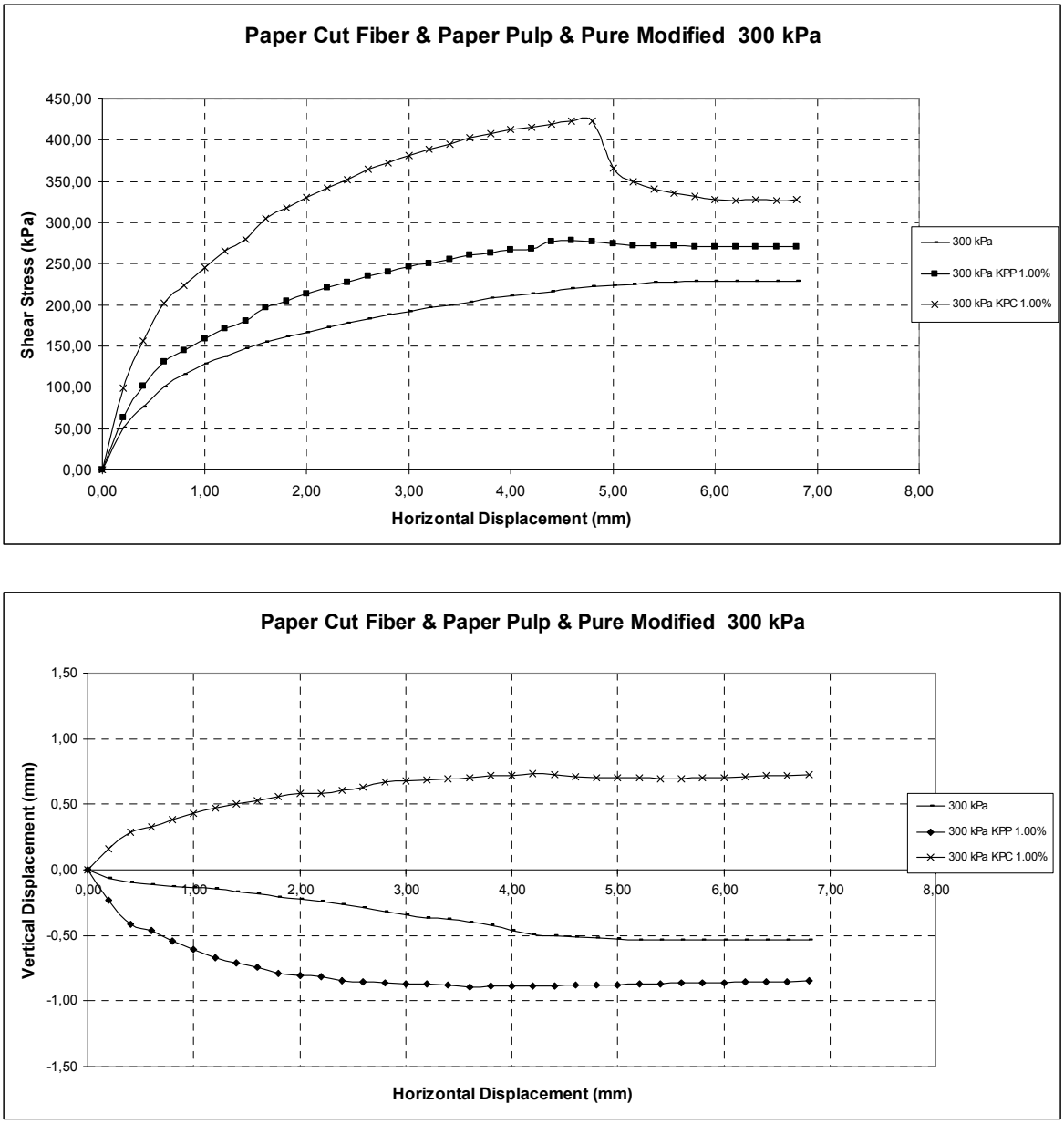

Figure 4.49. The direct shear test results of K-Md, KPC 1.00%-Md, KPP1.00%-Md group samples under 300 kPa normal stresses

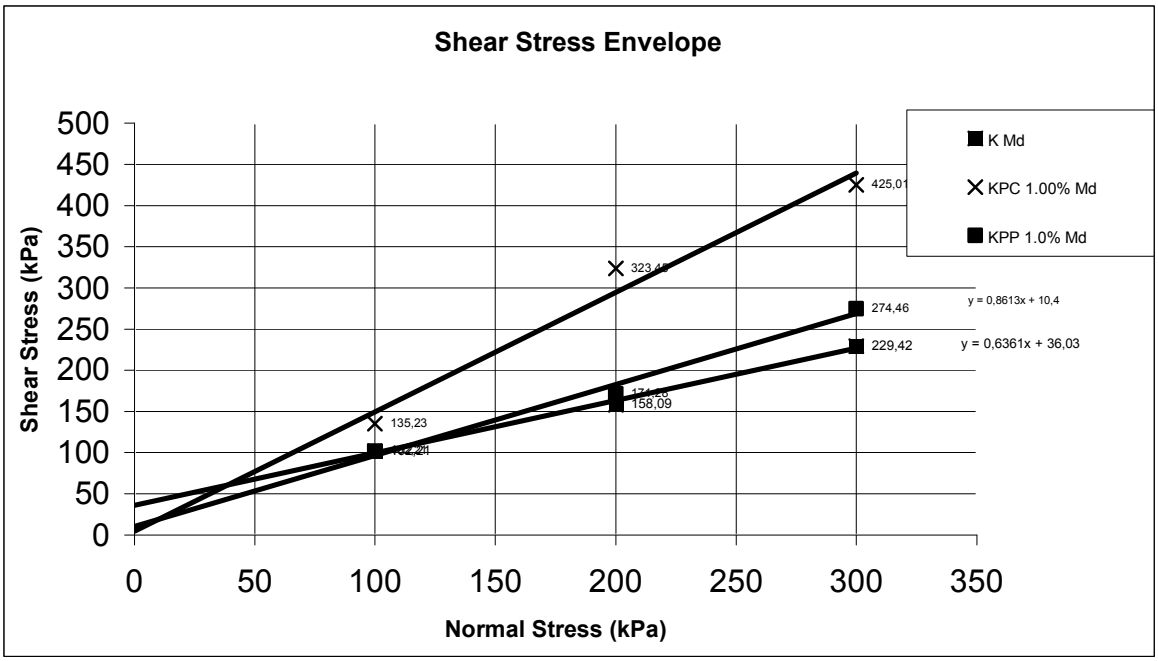

Figure 4.50. The shear stress envelope of K-Md, KPC 1.00-Md, KPP 1.00%-Md group samples under normal stress

Between figure 4.43-4.50 direct shear test results, and graphs of K, KPC 1.00 %, KPP-1.00% group samples which were compacted by standard and modified effort under 100 kPa, 200 kPa, 300 kPa normal stresses are shown. The difference between adding paper cut fibers and paper pulp as an additive to kaolinite was clearly seen from the results. Mixing paper pulp was more practical in use. Paper cut fibers and paper pulp increased shear stress.

4.3. Unconfined Compression Test Results

Unconfined compression tests were conducted on kaolinite, paper cut fibers and paper pulp reinforced clay samples. Paper cut fibers and paper pulp was added kaolinite 1.00% by weight. Specimens were prepared by using Harvard miniature compaction equipment both using spring tamper and impact hammer compaction. Kaolinite mixed with paper cut fibers 1.00 % by weight compacted with impact hammer will be referred as KPC-1%-Hm and compacted with spring tamper will be referred as KPC-1%-Sp. Kaolinite mixed with paper pulp 1% by weight compacted with impact hammer will be referred as

KPP-1%-Hm, and compacted with spring tamper will be referred as KPP-%1-Sp. Kaolinite compacted with impact hammer will be referred as K-Hm and kaolinite compacted with spring tamper will be referred as K-Sp. Corrected areas were used for calculation of unconfined compressive strength (q_u) and cohesion is found as the radius of Mohr's circle. Unconfined compression test results are shown in Table 4.2. Strain rate of 0.5 mm/min was selected in order to complete the test within 10 minutes to prevent loss of water content during test. Maximum stress value is determined at failure mode and this value is divided by corrected area to obtain unconfined compression strength (q_u). Equation 4.1 shows the computation of unconfined compressive strength of soils.

$$\sigma = \frac{P}{A'} \tag{4.1}$$

Table 4.2. Unconfined Compression Test Results

Soil Type	Final Water Content w%	Diameter (cm)	Height (cm)	Weight (gf)	Unit Weight (kN/m3)	Max.Axial Strain (%)	Corrected Area At Failure (cm2)	qu (kPa)	c (kPa)
K-Hm	16.7	3.34	7.28	95.43	16.36	2.9	9.02	126	63
KPC-1.00%-Hm	18.8	3.32	7.34	105.40	16.27	13.10	9.96	177.30	88.6
KPP-1.00%-Hm	17.9	3.32	7.19	102.55	16.42	8.70	9.61	139.7	69.9
K-Sp	16.9	3.32	7.15	93.68	15.90	6.2	9.22	140.7	70.4
KPC-1.00%-Sp	18.2	3.28	7.22	100	16.08	13.60	9.78	244.2	122.1
KPP-1.00%-Sp	18.5	3.32	7.28	93.45	15.52	7.4	9.35	148.3	74.1

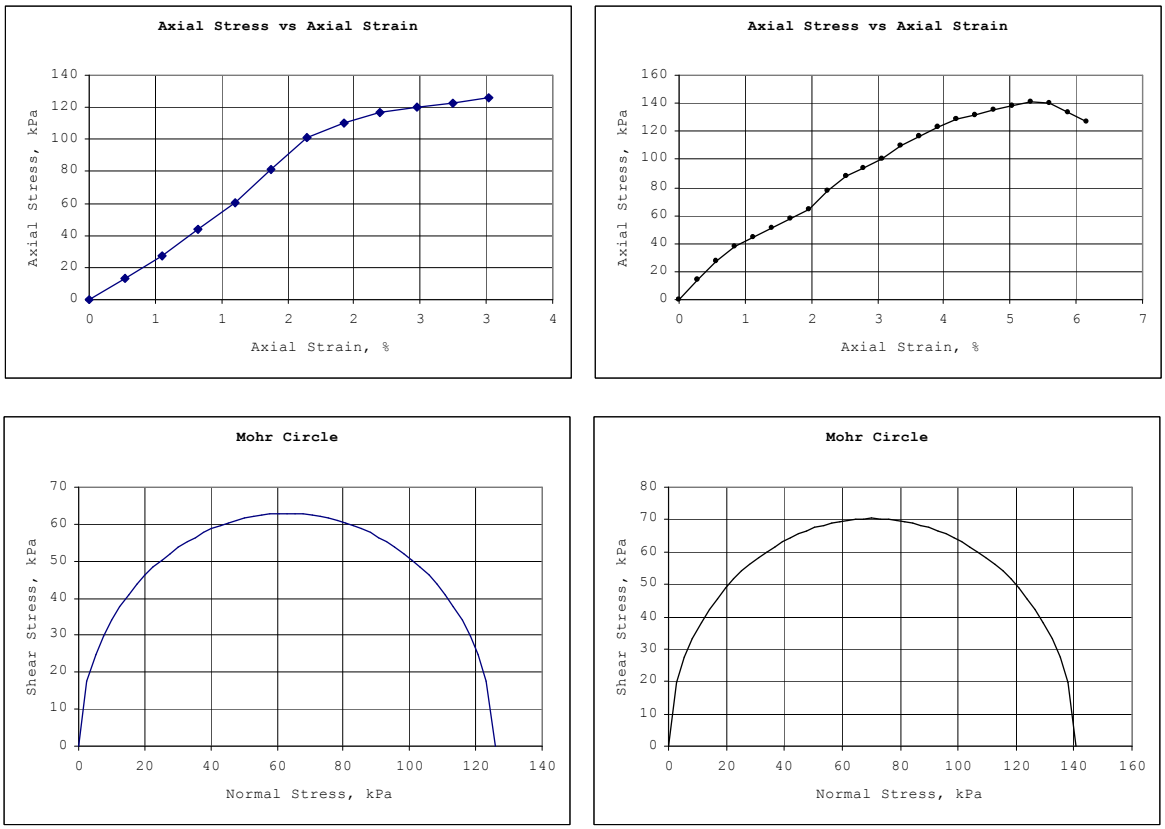

(a) **(b)**

Figure 4.51. Unconfined compression test results for K samples (a) compaction with hammer and (b) compaction with spring tamper

Figure 4.51. shows unconfined compression test results for kaolinite clay. Results for both hammer compaction and spring compaction efforts are given in the same figure in order to make clearer comparison. For samples compacted with hammer, maximum axial strain is found to be 2.9% and unconfined compressive strength is 126 kPa. Cohesion is 63 kPa. The final water content is 16.7 % and unit weight is 16.36kN/m^3. Brittle type of failure is observed at failure condition. Obvious single crack occurs at failure. For samples compacted with spring tamper maximum axial strain is found 6.2% and unconfined compressive strength of 140.7 kPa is obtained. Cohesion is 70.40 kPa. The final water content is 16.90% and unit weight is 15.90kN/m^3. The result of unconfined compressive strength for K samples changed from 126 kPa to 140 kPa between compaction efforts. Approximately all compressive strength values are same in both compaction with standard hammer and compaction with spring tamper.

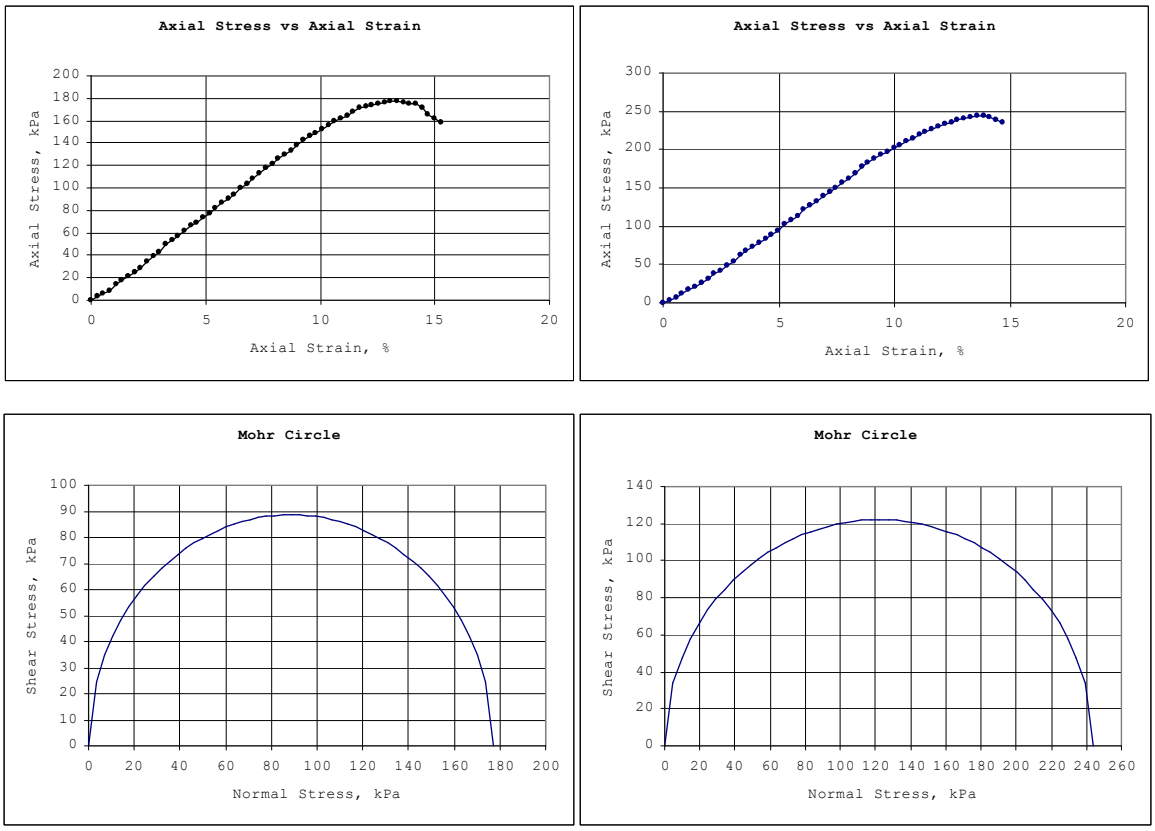

(a) **(b)**

Figure 4.52. Unconfined compression test results for KPC-1.0% samples (a) compaction with hammer and (b) compaction with spring tamper

In Figure 4.52, unconfined compressive strength test results are given for paper cut fiber reinforced kaolinite clay with 1% by weight. Results for both compaction with standard hammer and spring tamper are given in the same figure. For samples compacted with standard hammer the maximum axial strain is 13.10% and unconfined compressive strength is found to be 177.30 kPa. The final water content is 18.8% and unit weight is found to be 16.27kN/m^3. Cohesion is 88.60 kPa. The samples compacted with spring tamper have unconfined compressive strength of 244.2 kPa with a maximum axial strain of 13.60%. The final water content value is 18.2% and unit weight is 16.08kN/m^3. There is a significant difference in strength parameters between samples compacted with standard hammer and spring tamper. The unconfined compressive strength of composite compacted with spring tamper is greater than the composite compacted with standard hammer. The maximum axial strains are same for samples compacted with spring tamper. When

compared to the clay alone, the main difference observed during tests was that paper-reinforced soil composites showed ductile behavior during failure cracks occurred.

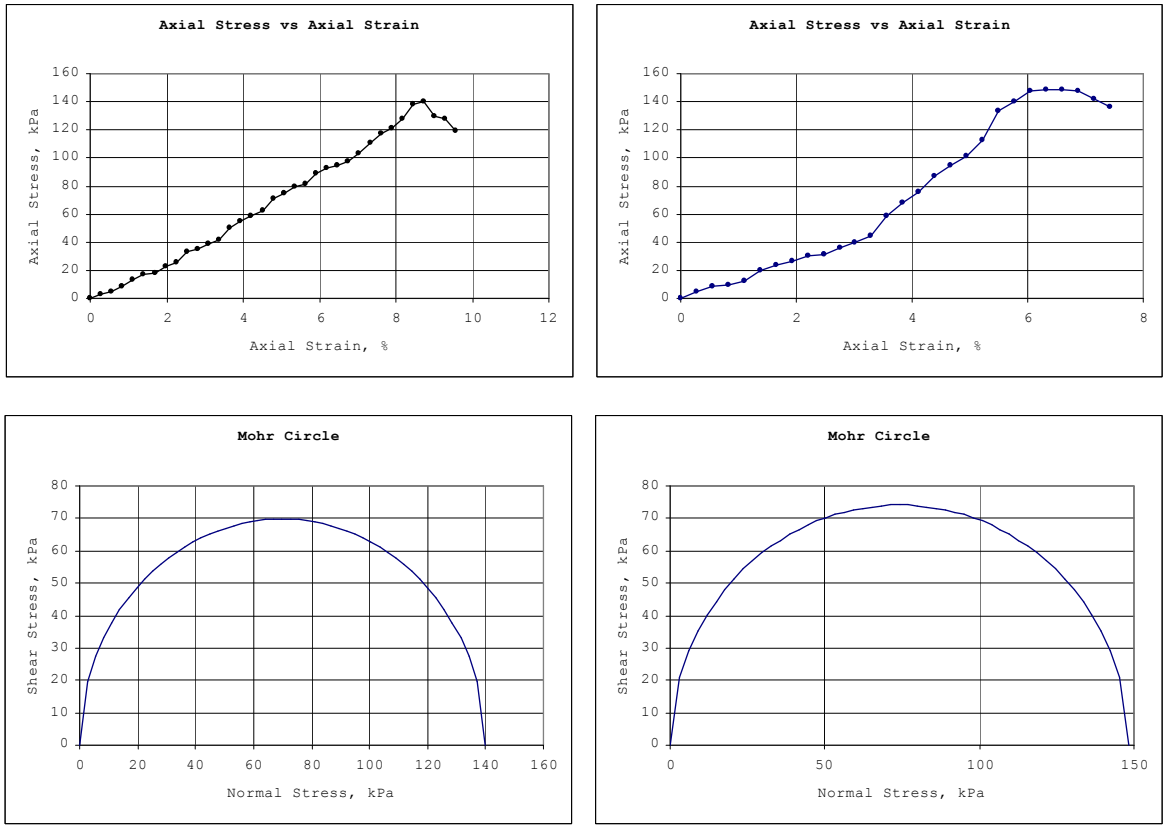

(a) **(b)**

Figure 4.53. Unconfined compression test results for KPP-1.0% samples (a) compaction with hammer and (b) compaction with spring tamper

Unconfined compression test results for kaolinite clay reinforced with paper pulp 1.00% by weight are shown in Figure 4.53. Soil composites compacted with standard hammer have unconfined compressive strength of 139.70 kPa with a maximum axial deformation of 8.70%. The final water content is 17.9 % and unit weight of soil sample is 16.42 kN/m^3. Unconfined compressive strength is 148.30 kPa for soil compacted with spring tamper with a maximum axial strain of 7.40%. The final water content is found 18.50% and unit weight is 15.52 kN/m^3. KPP samples showed plastic failure.

In all tests, the unconfined compressive strength of samples increased with addition of paper. With addition of 1.00% paper cut fibers by weight, the unconfined compressive strength increased from 126 kPa to 177 kPa for compaction with standard hammer and from 140 kPa to 244 kPa for spring tamper compaction. With addition of 1.00% paper pulp by weight, the unconfined compressive strength increased from 126 kPa to 139 kPa for compaction with standard hammer and from 140 kPa to 148 kPa for spring tamper compaction. The samples compacted with spring tamper show higher unconfined compressive strength values. This is due to the kneading effect caused by piston, which results in curved shape fiber distribution in soil matrix. The kaolinite clay alone shows brittle type of failure with obvious cracks within sample whereas the soil with paper cut fibers show ductile type of failure with multiple crack formations. Those cracks mainly occur along fibers that resist shear stresses formed within soil matrix due to compressive stress. The types of failure vary according to fiber rate and failure surfaces occur mainly where number of fibers are less or can not resist shear stresses.

4.4. Splitting Tensile Strength Test Results

Splitting tensile strength tests are conducted on both clay and paper cut fiber reinforced soil specimens, and paper pulp reinforced clay. Samples are prepared at optimum water content and compacted with standard energy. Harvard miniature compaction equipments are used to compact and obtain soil samples prior to testing. Compaction with both standard hammer and spring tamper effort is applied and results are compared. Mechanical compression device manufactured by ELE International Testing Equipments is used. The proving ring is 4.5 kN. In order to finish testing before 10 minutes to prevent loss of water content, 0.5 mm/min strain rate is selected. Table 4.3 shows general results for splitting tensile strength tests conducted on soil specimens. Determination of splitting tensile strength is given in Equation 4.2.

$$\sigma_t = \frac{2P}{\pi LD} \tag{4.2}$$

Table 4.3. Summary of Splitting Tensile Strength Tests

Compaction Type	Soil Type	Diameter of Specimen (mm)	Thickness of Specimen (mm)	Axial Deformation at Failure (%)	Maximum Applied Load (N)	Splitting Tensile Strength (kPa)
Compaction With Standard Hammer	K	33,0	21,1	9.71	15.708	**14.308**
	KPP-1.0	33,1	17,1	10.31	34.409	**38.702**
	KPC-1.0	33,2	20.0	10.24	37.654	**36.101**
Compaction With Spring Tamper	K	32,9	20,6	11.55	26.928	**25.294**
	KPP-1.0	33,2	20,2	9.04	49.070	**46.580**
	KPC-1.0	31,0	16.5	8.90	52.660	**65.541**

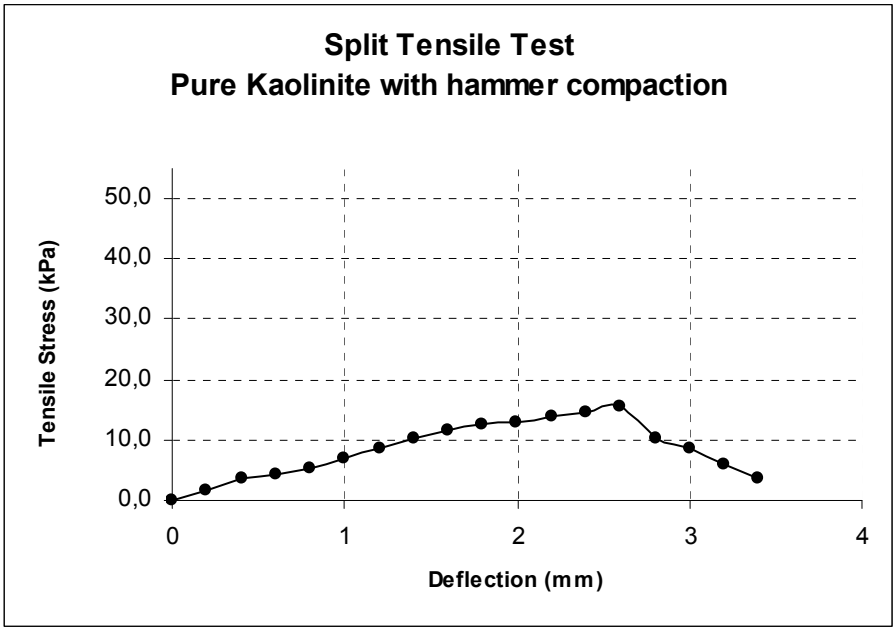

Figure 4.54a. Splitting tensile strength test results for K samples compacted with standard hammer

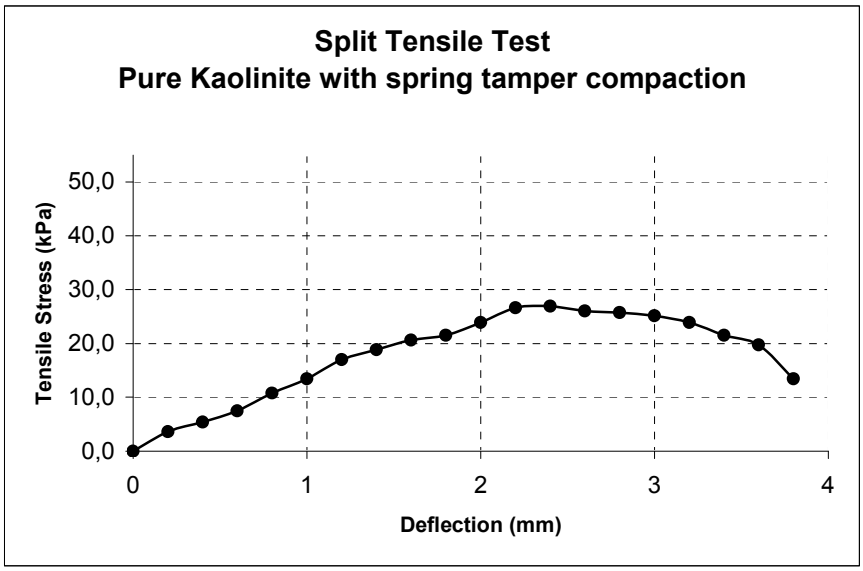

Figure 4.54b. Splitting tensile strength test results for K samples compacted with standard hammer and spring tamper

Figure 4.54 shows splitting tensile strength test results for kaolinite clay samples compacted with both standard hammer and spring tamper. The samples compacted with standard hammer had a tensile strength of 14,308 kPa. The maximum applied load is 15,708 N. The tensile strength is 25,294 kPa for samples compacted with spring tamper. The maximum applied load is 23.936 N. Single crack occurrence and brittle failure were observed in all kaolinite samples. After failure stresses, sudden decrease in applied load was observed. This is due to the lack of reinforcing materials that resist tension at failure plane. Axial strains are relatively same compared to the samples reinforced with paper cut fibers, and paper pulp. No significant variations are observed between standard hammer compaction and spring tamper compaction efforts.

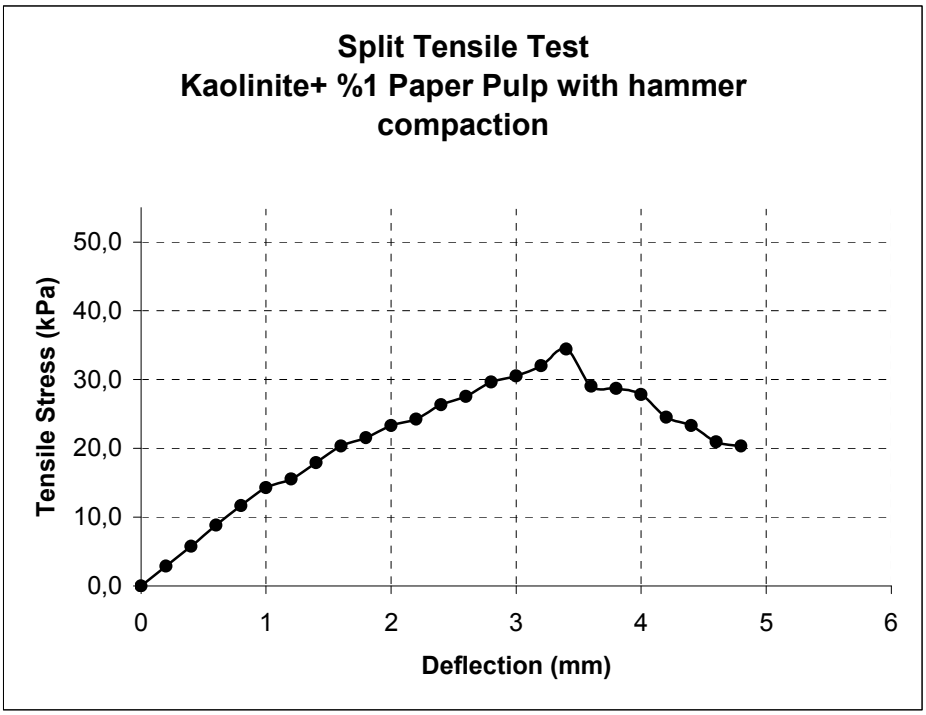

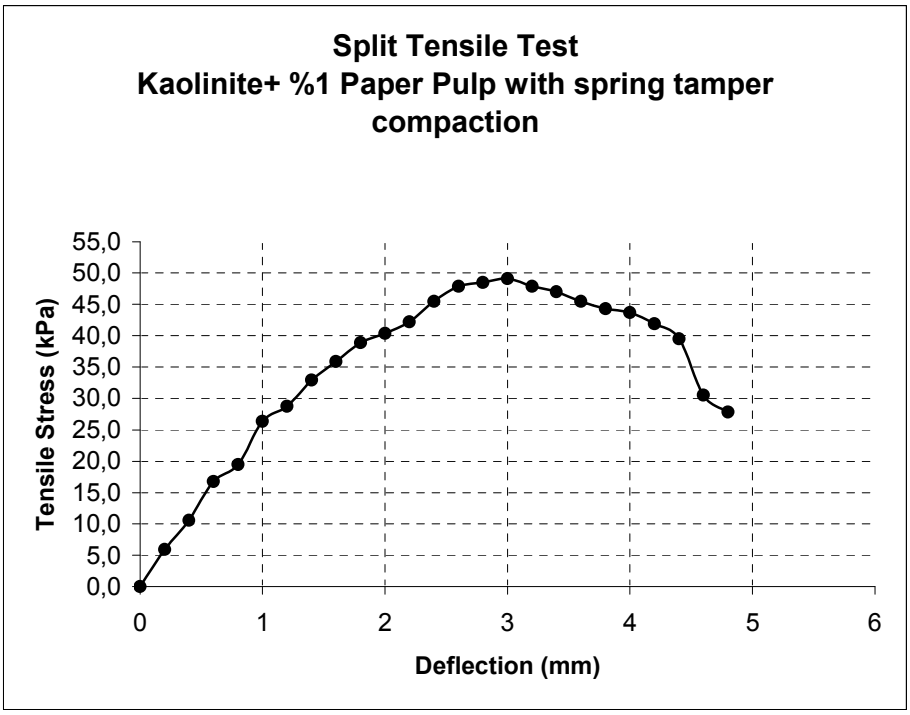

Figure 4.55. Splitting tensile strength test results for KPP-1.00% samples compacted with standard hammer and spring tamper

Figure 4.55 shows splitting tensile strength test results for kaolinite clay samples modified with paper pulp and compacted with both standard hammer and spring tamper. The samples compacted with standard hammer had a tensile strength of 38,702 kPa. The maximum applied load is 34,409 N. The tensile strength is 46,580 kPa for samples compacted with spring tamper. The maximum applied load is 49,070 N.

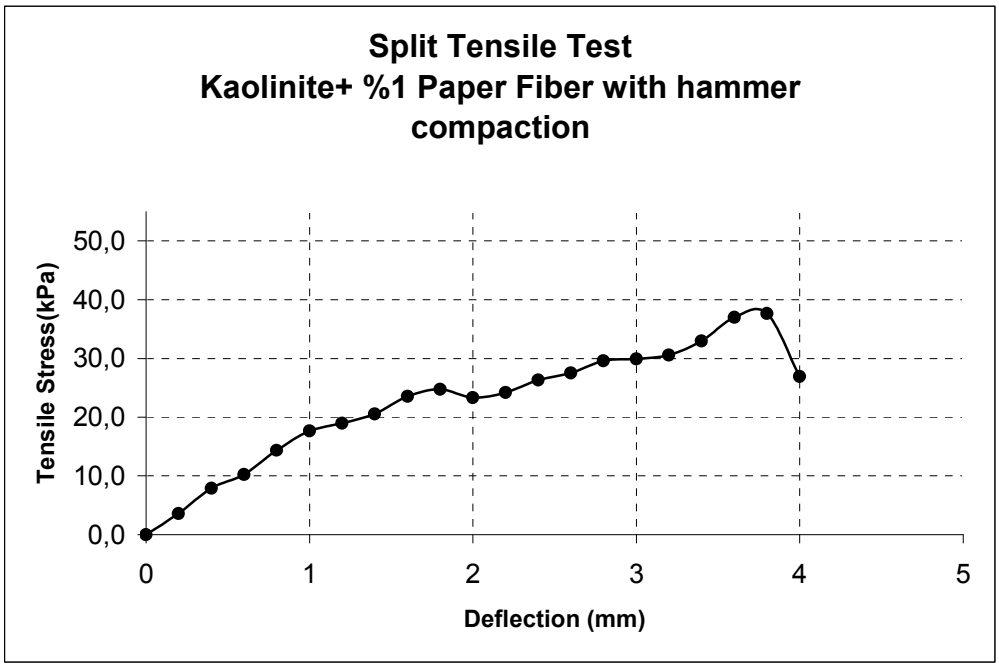

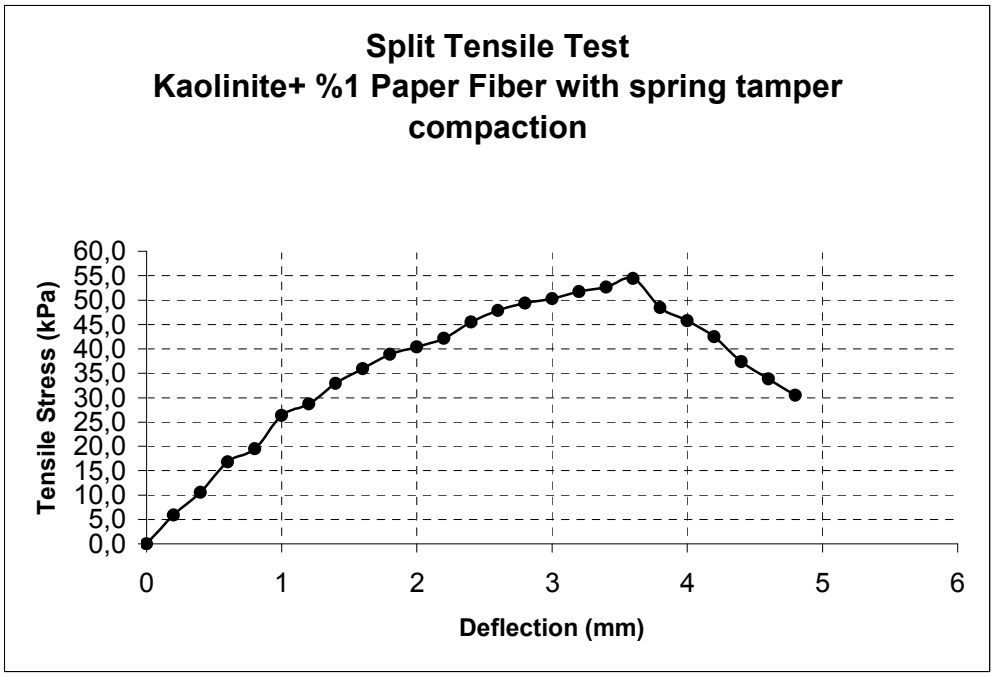

Figure 4.56. Splitting tensile strength test results for KPC 1.00% samples compacted with standard hammer and spring tamper

Figure 4.56. shows splitting tensile strength test results for kaolinite clay samples modified with paper cut fibers and compacted with both standard hammer and spring tamper. The samples compacted with standard hammer had a tensile strength of 36,101 kPa. The maximum applied load is 37,654 N. The tensile strength is 65,451 kPa for samples compacted with spring tamper. The maximum applied load is 52,660 N. When compared to K samples, KPP-1.0% samples and KPC-1.0% samples which were compacted with standard hammer and spring tamper had greater tensile strength.

4.5. Hydraulic Conductivity Test Results

Falling head tests are conducted in order to study the hydraulic conductivity behavior of clay reinforced with paper-cut fibers and paper pulp.

$$k = \frac{a.L}{A.t} \ln \frac{h_o}{h_t} \qquad (4.3)$$

k = coefficient of permeability (cm/sec)

a = area of burette standpipe (cm^2)

L = length of the specimen

A = area of specimen (cm^2)

t = elapsed time of the test (sec)

h_o = head at the beginning (time = 0) of the test

h_f = head at end (time = t) of the test (cm)

Table 4.4. Falling head test results

Soil Description	Diameter of the specimen (mm)	Area of the burette (mm2)	Area of the specimen (mm2)	Height of the specimen (mm)	Coefficient of Permeability (cm/s)
Pure Kaolinite	99	5	7697,69	130	4,62 E-06
Kaolinite + 1% Paper Cut Fiber	98	5	7542,96	128	1,54 E-07
Kaolinite + 1% Paper Pulp	98	5	7542,96	126	5,57 E-07

4.6. Linear Shrinkage Test Results

Linear shrinkage tests are conducted in order to study the shrinkage characteristics of both clay soil alone and soil reinforced with paper-cut fibers and paper pulp. Drying dish with length of 140 mm is used during testing. Test results are given in Table 4.5. The linear shrinkage of samples is calculated by using Equation 4.3. From Table 4.5., addition of paper cut fibers, paper pulp decreases linear shrinkage significantly. There is a decrease in linear shrinkage percentage from 5.00% to 1.43%. This is due to the bonding forces between fibers and soil matrix, and increased tensile strength of the soil.

$$LS = (1 - \frac{L_D}{L_0}) \times 100 \qquad (4.3)$$

Table 4.5. Linear shrinkage test results

LINEAR SHRINKAGE TEST RESULTS			
Soil Description	**Initial Length (mm)**	**Oven Dried Length (mm)**	**Linear Shrinkage (%)**
Pure Kaolinite	140	133	5.00
Kaolinite + %1 Paper Fiber	140	138	1.43
Kaolinite + %1 Paper Pulp	140	136	2.86

4.7. Microscopic Images of Samples

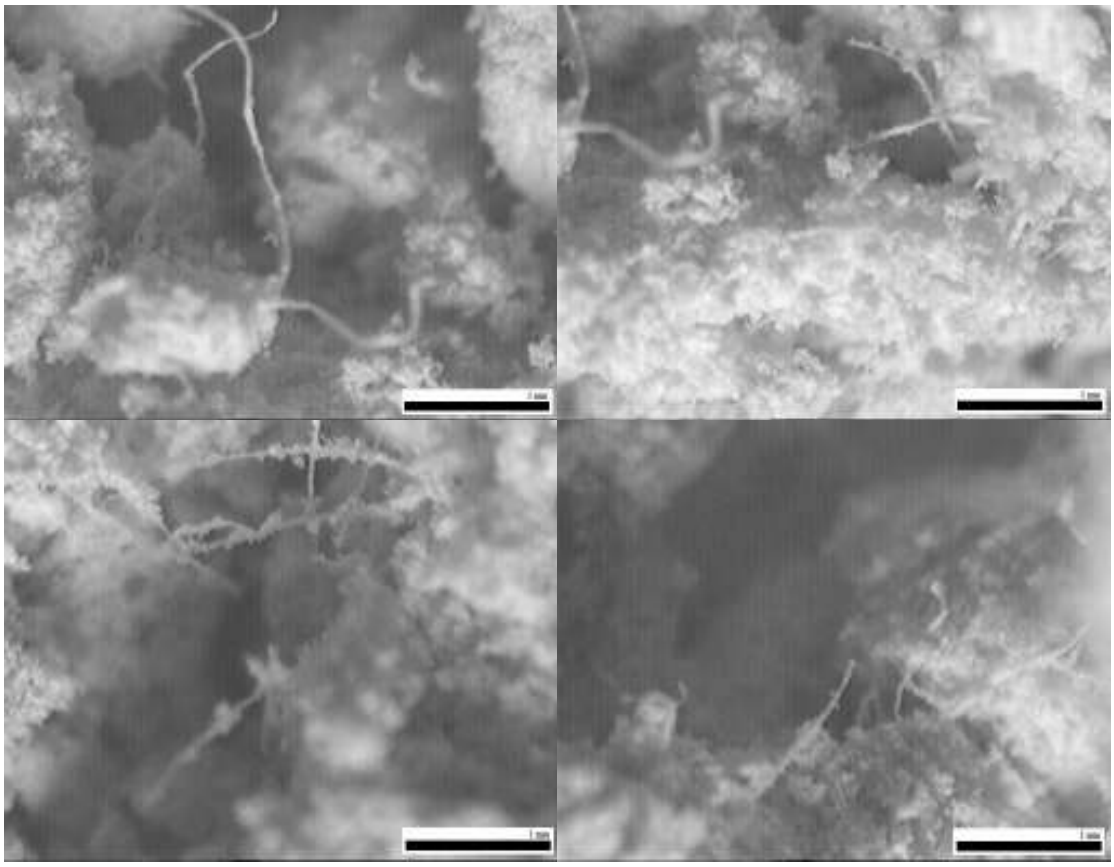

Figure 4.57. The microscopic images of compacted samples

The microscopic images of samples are shown in figure 4.57. The straw in the paper in different lengths are connected and mixed with clay particles and worked as a matrix fiber rather than individual fiber. Interparticle pores, trans assemblage pores, grain-grain contacts are easily seen from the figure. Interparticle contact orientations and their distribution are important, particularly with reference to deformation and strength properties and anisotropy.

5. CONCLUSIONS

A series of compaction tests, direct shear, unconfined compression, splitting tensile, hydraulic conductivity and linear shrinkage tests were conducted. The objective of this research is to modify the fabric of clay by mixing it with paper fibers in different forms. Fiber addition to clay is not a common procedure; however finite length fibers of tire buffings, polypropylene fibers are studied in the literature to improve the clay properties. This study investigates a different original approach in modification of clay fabric by mixing it with paper pulp fiber which acts as matrix fiber rather than individual finite length fiber.

Both paper cut fibers and paper pulp form decreased cohesion clearly, and increased internal friction angle values. Modified compaction energy causes the sharpest increase in internal friction angle for the lowest amount of paper inclusion.

Although the improvement in unconfined compressive strengths due to paper fiber inclusion was 10% to 40%, the tensile strength values increased from 100% to 250% when compared to those of control samples. This demonstrates the positive effect of introducing matrix fibers into clay fabric. The increase in soil strength parameters are also seen in unconfined compression and splitting tensile strength tests. The increase in strength also resulted in an increase in ductility with fiber inclusion. The ductility of the compacted specimens increased considerably with paper fiber inclusion.

Fiber inclusion decreased linear shrinkage to one fourth of the control samples for paper cut fibers, and to one half of the control samples for paper pulp samples.

The hydraulic conductivity values obtained from the falling head compaction permeameter test showed a one order of magnitude decrease for paper fiber inclusion when compared to that of control samples.

This study demonstrates an original technique to introduce matrix fiber into clay fabric. With very low amounts of paper additive (1% by weight) the technique proposed has economic potential for use (One ¢ per cubic meter). The improved workability, the availability, and ease of implementation make this method a good candidate for field applications.

REFERENCES

American Society for Testing Materials (ASTM), 1998, "Standard Test Method for Measurement of Hydraulic Conductivity of Saturated Porous Materials Using a Flexible Wall Permeameter", ASTM D 5084, Philadelphia.

American Society for Testing Materials (ASTM), 1998, "Standard Test Method for Unconfined Compressive Strength of Cohesive Soil", ASTM D 2166-91, Philadelphia.

American Society for Testing Materials (ASTM), 1998, "Standard Test Method for Splitting Tensile Strength" ASTM D 3967-95a, Philadelphia.

American Society for Testing Materials (ASTM), 1998, "Test Methods for Liquid Limit, Plastic Limit, and Plasticity Index of Soils", ASTM D 4318, Philadelphia.

American Society for Testing Materials (ASTM), 1998, "Test Method for Laboratory Compaction Characteristics of Soil Using Standard Effort", ASTM D 698, Philadelphia.

American Society for Testing Materials (ASTM), 1998, "Test Method for Laboratory Compaction Characteristics of Soil Using Modified Effort", ASTM D 1557, Philadelphia.

Bardet, J.P., 1997, *Experimental Soil Mechanics*, Prentice Hall Inc., New Jersey, USA.

Berilgen, S.A., M.M. Berilgen, and I.K. Ozaydin, 2006, "Compression and Permeability Relationship in High Water Content Clays", *Applied Clay Science.*, Vol. 31, pp. 249-261.

Budhu, M., 2000, *Soil Mechanics and Foundations*, John Wiley & Sons Inc., New York, USA.

Bowles, J.E., 1992, *Engineering Properties of Soils and Their Measurement*, McGraw-Hill Publishing Co., New York, USA.

Casagrande, M.D.T., M.R. Coop, and N.C. Consoli, 2006, " Behavior of Fiber-reinforced Bentonite at Large Shear Displacements", *J. Geotech. Geoenviron. Eng.*, Vol. 132(11), pp. 1505-1508.

Chew, S.H., A.H.M. Kamruzzaman, and F.H. Lee, 2004, "Physicochemical and Engineering Behavior of Cement Treated Clays", *J. Geotech. Geoenviron. Eng.*, Vol. 130(7), pp. 696-706.

Consoli, N.C., J.P. Montardo, P.D.M. Prietto, and G.S. Pasa, 2002, "Engineering Behavior of a Sand Reinforced with Plastic Waste", *J. Geotech. Geoenviron. Eng.*, Vol. 128(6), pp. 462-472.

Consoli, N.C., J.P. Montardo, P.D.M. Prietto, and L.A. Ulbrich, 1998, "Influence of Fiber and Cement Addition on Behavior of Sandy Soil", *J. Geotech. Geoenviron. Eng.*, Vol. 124, pp. 1211-1214.

Das, B.M., 2001, *Principles of Geotechnical Engineering*, Pws Pub. Co., California, USA.

Edinçliler, A., G. Baykal, and K. Dengili, 2004, "Shear Strength of Waste Materials in Embankment Construction", *7th International Symposium on Environmental Geotechnology and Global Sustainable Development*, Helsinki-Finland, pp.323-331.

Gray, D.H., and T. Al-Refeai, 1986, "Behavior of Fabric versus Fiber-reinforced Sand", *J.Geotech. Eng.*, ASCE, Vol. 112(8), pp. 804-820.

Gray, D.H., and H. Ohashi, 1983, "Mechanics of Fiber-reinforcement in Sand", *J.Geotech. Eng.*, ASCE, Vol. 109(3), pp. 335-353.

Gregory, G.H., 2006, "*Shear Strength, Creep and Stability of Fiber-reinforced Soil Slopes*", Ph.D. Thesis, Oklahoma State University, Oklahoma City, USA.

Gregory, G.H., 1999, "Theoretical Shear Strength Model of Fiber-Soil Composite" *Proceedings, ASCE Texas Section Spring Meeting*, Longview, Texas, USA, April .

Hausmann, M.R., 1990, *Engineering Principles of Ground Modifications*, McGraw-Hill Publishing Co., New York, USA.

Heineck, K.S., M.R. Coop, and N.C. Consoli, 2005, "Effect of Microreinforcement of Soils from Very Small to Large Shear Strains", *J. Geotech. Geoenviron. Eng.*, Vol. 131(8), pp. 1024-1033.

Horpibulsuk, S., N. Miura, and D.T. Bergado, 2004, "Undrained Shear Behavior of Cement Admixed Clay at High Water Content", *J. Geotech. Geoenviron. Eng.*, Vol. 130(10), pp. 1096-1105.

Hsuan, Y.G., 2002, "Approach to the Study of Durability of Reinforcement Fibers and Yarns in Geosynthetic Clay Liners", *J. Geotextiles and Geomembranes*, Vol. 20, pp. 63-76.

Köprülü, K., 1991**, "***Hydraulic Conductivity and Strength of Rubber Reinforced Fly Ash Used as Liner Material*", M.S. Thesis, Boğaziçi University.

Lekha, K.R., 2006, "Coir Geotextile Reinforced Clay Dykes for Drainage of Low-Lying Areas", *J. Geotextiles and Geomembranes*, Vol. 24, pp. 38-51.

Maher, M.H., and D.H. Gray, 1990, "Static Response of Sands Reinforced With Randomly Distributed Fibers", *J. Geotech. Eng.*, ASCE, Vol. 116(11), pp. 1661-1677.

Maher, M.H., and Y.C. Ho, 1994, "Mechanical Properties of Kaolinite/Fiber Soil Composite." *J. Geotech. Eng.*, Vol. 120(8), pp. 1381-1393.

Michalowski, R.L., and J. Cermak, 2003, "Triaxial Compression of Sand Reinforced with Fibers", *J. Geotech. Geoenviron. Eng.*, Vol. 129(2), pp. 125-135.

Michalowski, R.L., and A. Zhao, 1996, "Failure of Fiber-reinforced Granular Soils", *J. Geotech. Geoenviron. Eng.*, Vol. 122(3), pp. 226-234.

Miller, C.J., and S. Rifai, 2004, "Fiber Reinforcement for Waste Containment Soil Liners", *J. Environ. Eng.*, Vol. 130(8), pp. 891-895.

Özkul, Z.H., 2005, **"***Shear Strength and Deformation Behavior of Clay with Randomly Oriented Tire Buffing Inclusions*", Ph.D. Thesis, Boğaziçi University.

Ranjan, G., R.M. Vasan, and H.D. Charan, 1994, "Behavior of Plastic-fiber-reinforced Sand", *Geotext. Geomembr.*, Vol. 13, pp. 555-565.

Santoni, R.L., J.S. Tingle, and S.L. Webster, 2001, "Engineering Properties of Sand-fiber Mixtures for Road Construction", *J.Geotech. Geoenviron. Eng.*, Vol. 127(3), pp. 258-268.

Tingle, J.S., R.L. Santoni, and S.L. Webster, 2002, "Full-scale Field Tests of Discrete Fiber-reinforced Sand", *J. Transp. Eng.*, Vol. 128(1), pp. 9-16.

Wan, Y., J. Kwong, H.G. Brandes, and R.C. Jones, 2002, "Influence of Amorphous Clay-Size Materials on Soil Plasticity and Shrink-Swell Behavior", *J. Geotech. Geoenviron. Eng.*, Vol. 128(12), pp. 1026-1029.

Viratjandr, C., 2006, "*Fiber-reinforcement of Soils and Stability Analysis of Reinforced Foundation Soils*", Ph.D. Thesis, The University of Michigan.

Yeşiller, N., 1991, "*Hydraulic Conductivity of Waste Rubber-clay Mixtures as Earthen Liners for Petroleum Based Contaminants*", M.S. Thesis, Boğaziçi University.